TRW

(NASA-CR-143932) STUDY ON PROCESSING IMMISCIBLE MATERIALS IN ZERO GRAVITY Final Report (TRW Systems Group) 124 p HC $5.25 CSCL 11G

N75-30210

Unclas
G3/12 34316

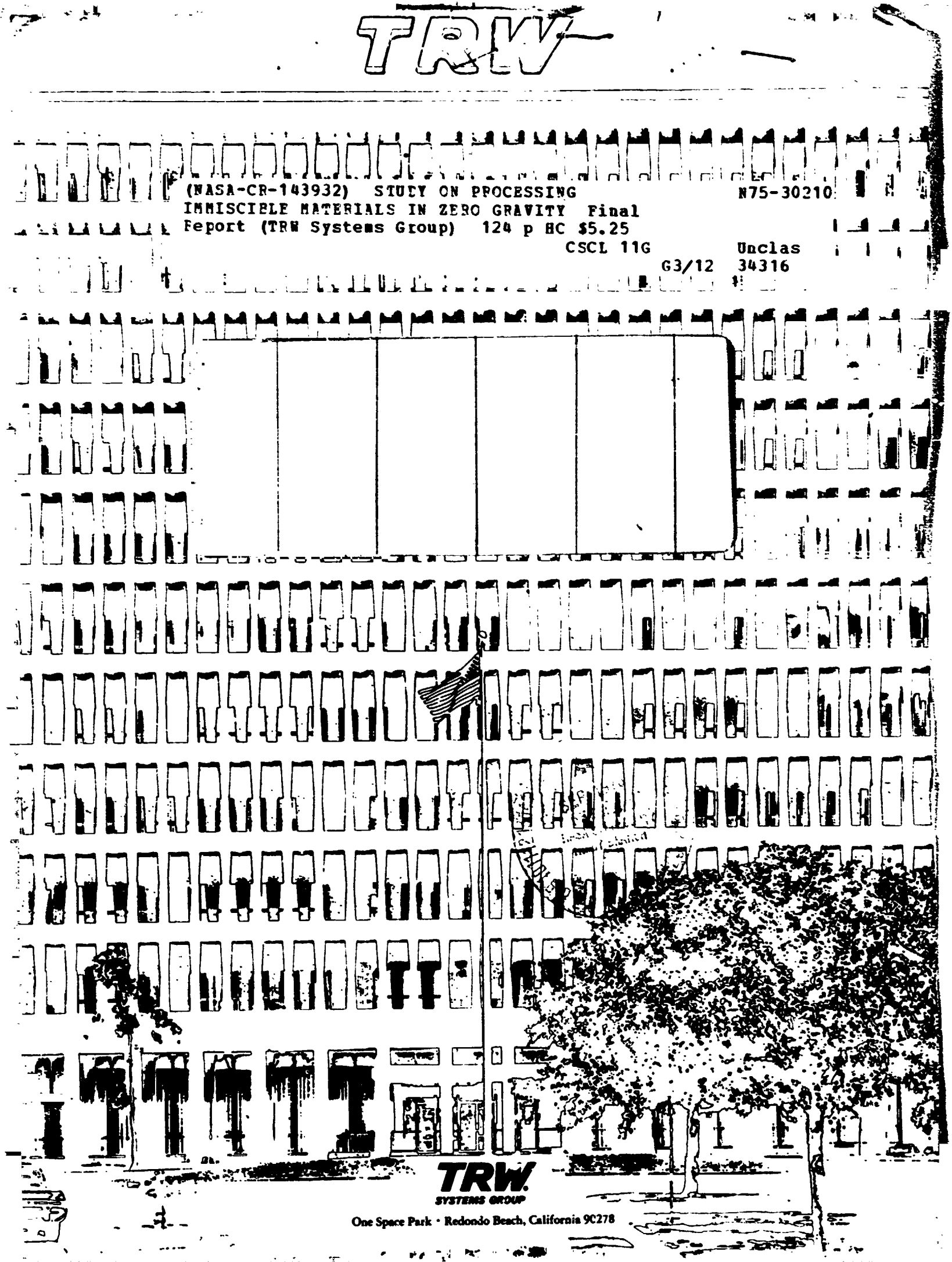

TRW
SYSTEMS GROUP
One Space Park · Redondo Beach, California 90278

14725-6028-RU-00

STUDY ON PROCESSING IMMISCIBLE MATERIALS IN ZERO GRAVITY

FINAL REPORT

June 1975

Prepared for

George C. Marshall Space Flight Center
Marshall Space Flight Center, Alabama 35812

Under

National Aeronautics and Space Administration
Contract NAS 8-28267

by

J. L. Reger and R. A. Mendelson
Materials Technology Department

TRW
SYSTEMS GROUP

FOREWORD

This report was prepared by TRW Systems Group, Redondo Beach, California and contains the final results of the work accomplished from 30 April 1973 to 6 June 1975. The total program effort was initiated on 27 April 1972 and the results accomplished from 27 April 1972 to 30 April 1973 are contained in the TRW Systems Group Interim Report No. 14725-6010-RU-00, published under the subject contract number and title. The program was originated and is managed by the George C. Marshall Space Flight Center under the technical direction of Mr. I. C. Yates, Jr.

The work performed on the program was accomplished by the Advanced Technology Division of TRW Systems Group. Technical direction of the program is provided by the Materials Technology Department. The Principal Investigator is Mr. J. L. Reger. Responsible technical personnel who supported this program are acknowledged below:

Dr. W. T. Anderson, Space Processing and Physics of Materials
Mr. L. A. Beason, Thermodynamics and Heat Pipes
Mr. W. B. Hewitt, Metals and Ceramics
Mr. R. A. Mendelson, Space Processing and Physics of Materials
Mr. E. R. Peters, Systems Group Research Staff
Mr. C. Richou, Materials and Analysis Department
Mr. C. Salts, Thermodynamics and Heat Pipes
Mr. E. K. Takaio, Mechanical Hardware Operations
Mr. E. S. Thompson, Production and Integration Staff
Mr. R. Valencia, Jr., Materials Technology Department

TABLE OF CONTENTS

TABLE OF CONTENTS (CONT.)

LIST OF TABLES

LIST OF FIGURES

LIST OF FIGURES (CONT.)

LIST OF FIGURES (CONT.)

SUMMARY

This report describes technical work accomplished in the second portion of the study work performed under Contract NAS 8-28267. The initial work is described in TRW Systems Report 14725-6010-RU-00, entitled "Study on Processing Immiscible Materials in Zero Gravity," May 1973.

An experimental investigation was conducted to evaluate mixing immiscible metal combinations under several process conditions. Under one-gravity, these included thermal processing, thermal plus electromagnetic mixing and thermal plus acoustic mixing. Subsequently, the same process methods were applied during free fall on the MSFC drop tower facility.

This phase included design of drop tower apparatus to provide the electromagnetic and acoustic mixing equipment. Also, a thermal model was prepared to design the specimen and cooling procedure.

Materials systems studied during this portion of the effort were Ca-La, Cd-Ga and Al-Bi. Evaluation of the processed samples included the morphology and electronic property measurements. The morphology was developed using optical and scanning electron microscopy and microprobe analyses. Electronic property characterization of the superconducting transition temperatures were made using an impedance change-tuned coil method.

While better dispersions were obtained under reduced gravity processing than under one gravity, a wide range of particle distribution sizes occurred, indicating further process control will be necessary to produce both increased uniformity and size control. Superconducting properties again confirmed higher transition temperatures for some immiscible compositions; however, better sample uniformity and fundamental work on a theoretical basis are essential to further this avenue.

The subsequent sections and appendices detail the experimental, materials characterization and analysis work.

1.0 INTRODUCTION

Previous investigations on processing immiscible systems in a low gravity environment have produced materials having unique structural and electronic features [References 1 and 2]. The definition of immiscible systems, as used in this report, are those combinations of materials, primarily metals, which exhibit a miscibility (two-phase) gap in the liquid regime. Processing these materials from the liquid state and allowing them to cool in the Earth's gravitational field for relatively long periods of time enhances gravity induced segregation. Other metallurgical connotations for these types of materials are monotectic or metastable alloys (or phases).

If this class of materials, which have shown unusual behavior, are to be implemented for Shuttle and the associated Space Processing Program, a large amount of additional investigation and experimentation is required to define the processing, potential applications and properties of immiscible systems. The primary purpose of this program, then, was to provide preliminary information in terms of a literature survey of immiscible systems, their potential applications, experimental processing techniques with respect to their known or surmised phase relationships and to process candidate immiscible systems in order to determine the efficacy of the processing methods. Finally, the structural and electronic properties of the processed materials were evaluated in order to assess any differences between one and low gravity processed specimens.

The investigational and experimental effort of the portion of the program covered by this report is concerned with the development and fabrication of an acoustic and an electromagnetic mixer, processing of four immiscible formulations; three in the acoustic mixer and one in the electromagnetic mixer and evaluation of their metallographic structures and electronic behavior. In addition, a computerized thermal analysis program plus a set of bismuth-gallium experimental capsules which had been thermally profiled are included in this report, as well as additional bismuth-gallium and lead-zinc capsules which were sent to MSFC.

The literature survey of immiscible systems, an analysis of their potential applications and four strictly thermally processed systems along with their metallurgical and electronic properties are contained in the Interim Report, TRW Systems Document No. 14725-6010-RU-00, dated May 1973 and published under the subject contract number and t tle.

2.0 PROCESSING METHODS

The processing methods for producing specimens materials depends upon four major aspects: (1) The type of low gravity facility to be utilized; (2) the desired thermal history, both on heating and cooling; (3) the electrical or magnetic characteristics of the system in either the solid or liquid state; and (4) processing in either a single or two-phase liquid state.

The type of low gravity facility dictates the size of the sample to be processed. For the relatively short duration facilities, such as drop towers and KC-135 research aircraft, the sample sizes will be small due to the short time available for cooling. The heating time requirement for the samples on these facilities is not particularly critical since the available power is high and they can be initially heated in a one gravity mode until the desired temperature is reached, then processed and cooled during the drop or low gravity maneuver. The sample sizes for the longer duration facilities such as sounding rockets can probably be larger, since longer cooling times are available, although total payload weight for both the sample and processing apparatus must be taken into consideration.

The desired thermal history of the materials to be processed depends on three main considerations: (1) The processing temperature, (2) reactivity of the materials and (3) cooling to the primary monotectic or other microstructural retaining temperatures. For temperatures to 1500°C, direct thermal heating is the preferred process method. For temperatures above 1500°C, electron beam, induction heating, plasma beam or an electromagnetic technique could be utilized.

These processing methods also depend upon the electrical properties of the materials to be processed. For dielectrics such as glasses or ceramics, available technology for use in low gravity facilities precludes use of methods such as direct plasma electron beam heating. A combination of thermal heating to an acceptable electrical conductivity for induction heating could be utilized, but it is felt that such equipment would be both cumbersome and complex. Electrically conducting materials such as the semi-metals and metals do not have such restrictions.

Processing above the consolute temperature, all other parameters satisfied, poses no problems in terms of processing techniques. This has been the primary method utilized on previous programs [References 2 and 3] except for the original Apollo 14 experiments [Reference 1] where mechanical agitation was utilized to obtain dispersion of the immiscible system. However, when excessive processing temperatures, compatibility and unknown consolute temperatures may pose problems, other processing methods must be considered.

During the course of this program, four processing methods were identified and used. The processing methods were: (1) Thermal heating above the consolute temperature, (2) electron beam melting and (3) acoustic agitation and (4) electromagnetic stirring. Thermal processing was performed on drop tower samples and the electron beam melting used on the KC 135 flights. The main thrust of this portion of the program was to design, build, debug and demonstrate acoustic agitation and electromagnetic stirring.

2.1 ACOUSTIC PROCESSING

2.1.1 Preliminary Experiments

In order to determine the effects of various acoustic mixing processes which could be utilized in dispersing immiscible liquid mixtures, a neutral bouyancy tank was constructed using Freon TF-hexane as the neutral bouyancy medium with water as the neutrally bouyant material. Three processing methods were tried: bulk ultrasonic agitation, focused ultrasonic agitation and mechanical agitation. Considerable difficulty was encountered in obtaining the correct operating conditions. Reproducible results were finally obtained by baking silicone grease on the vessel interior, and by maintaining constant temperature with an air bath surrounding the container.

Only the focused ultrasonic agitation successfully dispersed the water. Bulk ultrasonic agitation coalesced the water droplets, and mechanical agitation was successful only when an air gap was left in the system so that both fluids could move. Figures 2-1 through 2-4 show the dispersion obtained from a parabolically focused ultrasonic irradiation unit operating at 40 watts, 26.5 kHz in the neutrally bouyant tank. Figures 2-2

and 2-3 were taken approximately 0.25 seconds apart. Figure 2-4 was taken approximately one minute after ultrasonic irradiation was stopped to illustrate the stability of the emulsion formed. The primary feature of this experiment was to show that ultrasonic agitation could produce extremely fine dispersions of immiscible materials in a two phase regime, which would be encountered with ceramics/glasses and metallic systems having consolute temperatures difficult to achieve by thermal processes alone. One feature found was that the parabolic horn and the material to be dispersed must be closely coupled. Figures 2-2 and 2-3 show the extraneous dissipated energy dispersed from the horn due to inefficient coupling. There are focusing systems which can overcome this difficulty, but this requires examination of the system to be processed [Reference 5]. Thus by proper mechanical and acoustic coupling, this method could prove a valuable adjunct to processing electrically inert materials in their two phase liquid region.

2.1.2 Acoustic Mixer Design

Based upon the preliminary experiment described in 2.1.1, a design for a mixer for immiscible systems was prepared. Figure 2-5 is an engineering drawing of the mixer and Figure 2-6 shows the experimental setup and an enlarged view of the mixer and an experimental glass cartridge. Appendix A presents a more detailed analysis of the acoustic mixer in its drop tower configuration as well as the instructions provided for its operation.

The mixer was designed for 27 kHz for a variable cartridge weight of between 3 to 10 grams approximately. The most efficient mixing frequency, however, was found to be 31 to 32 kHz. It was found that the mixing frequency was cartridge size rather than weight dependent.

2.1.3 Design Demonstration

Using the acoustic mixer, a series of tests were conducted with a variety of glass cartridges containing different gallium-mercury mixtures in order to determine optimum mixing frequency, coupling efficiency, sonoration or mixing time, the effect of cartridge (sample) size and the effect of sample composition and weight.

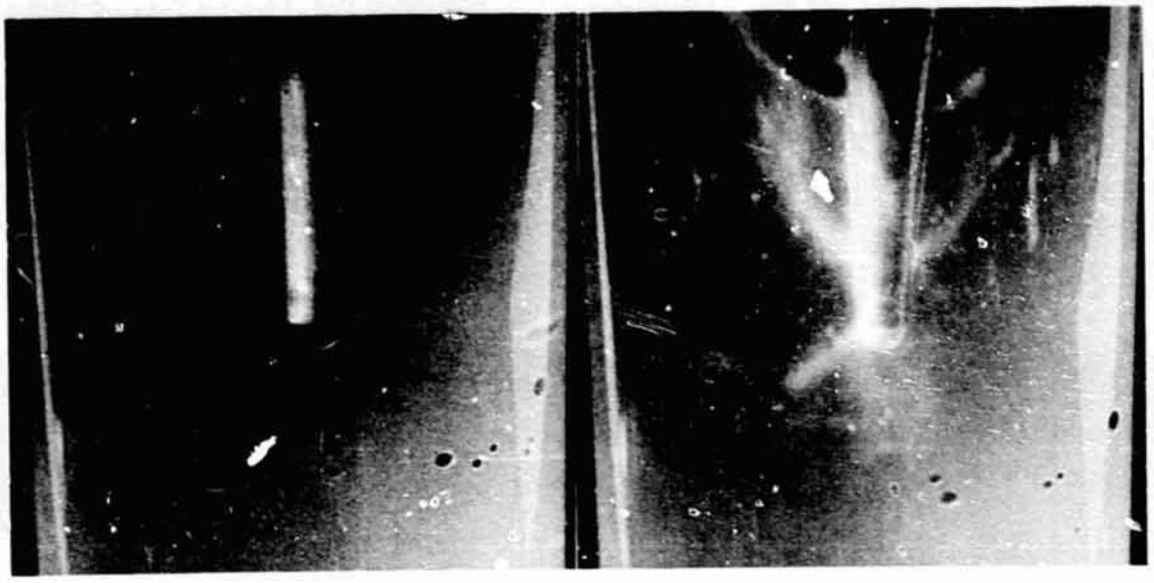

Figure 2-1. Quiescent Droplet in Neutral Bouyant Tank

Figure 2-2. Agitation after 0.25 Seconds, 40 Watts at 26.5 KHz.

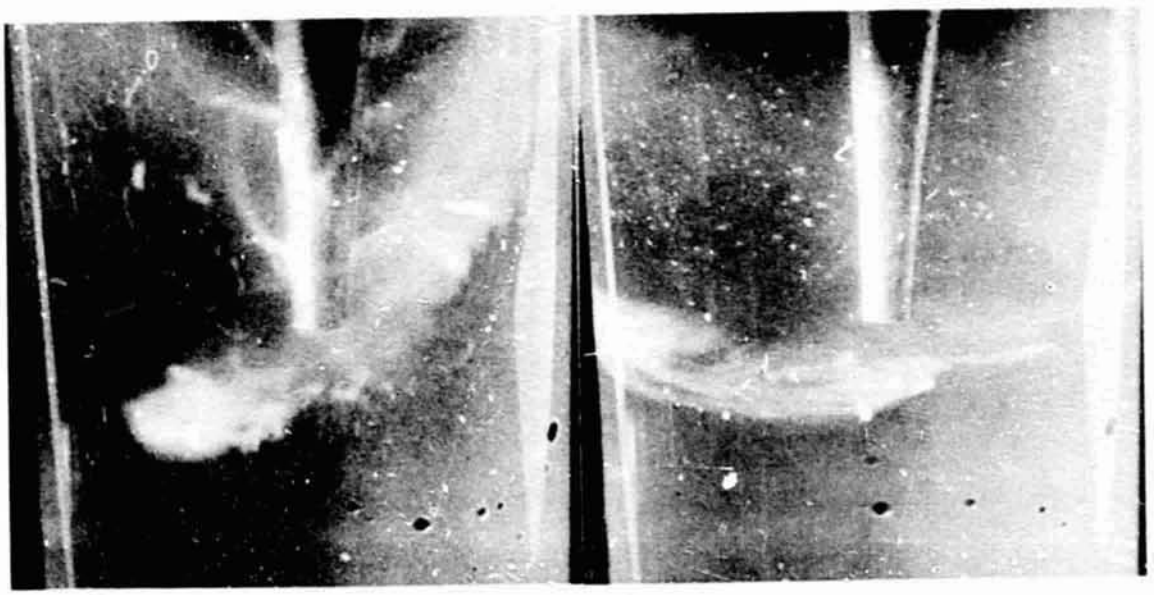

Figure 2-3. Droplet Dispersal after 0.5 Seconds.

Figure 2-4. Emulsion Stability after Cessation of Ultrasonic Agitation.

Figures 2-1 through 2-4. Ultrasonic Processing of Immiscible Water-Freon TF/Hexane Mixture.

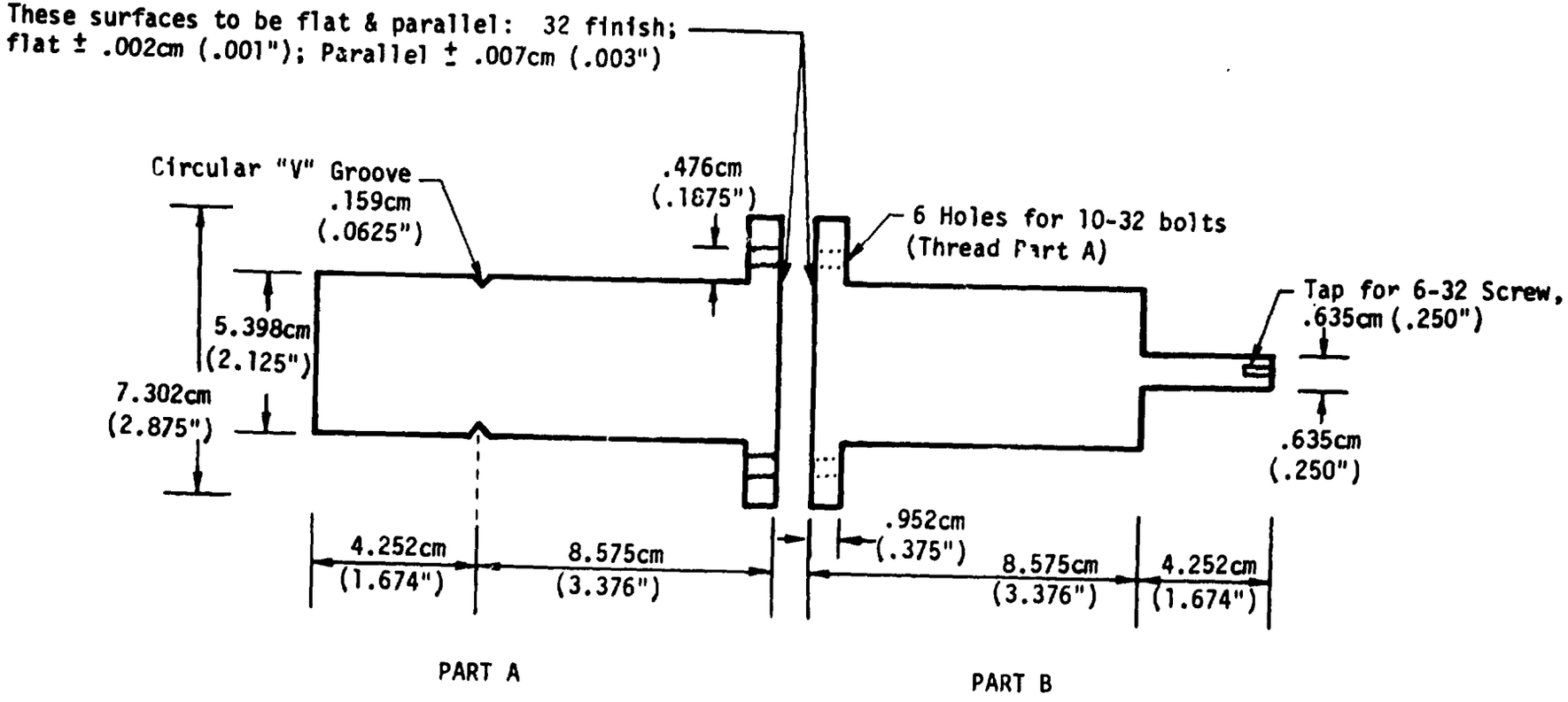

(All Dimensions are ± .002cm (.001") - Break all edges & corners
Material: Stainless 304)

Figure 2-5. Schematic Diagram of Acoustic Mixer

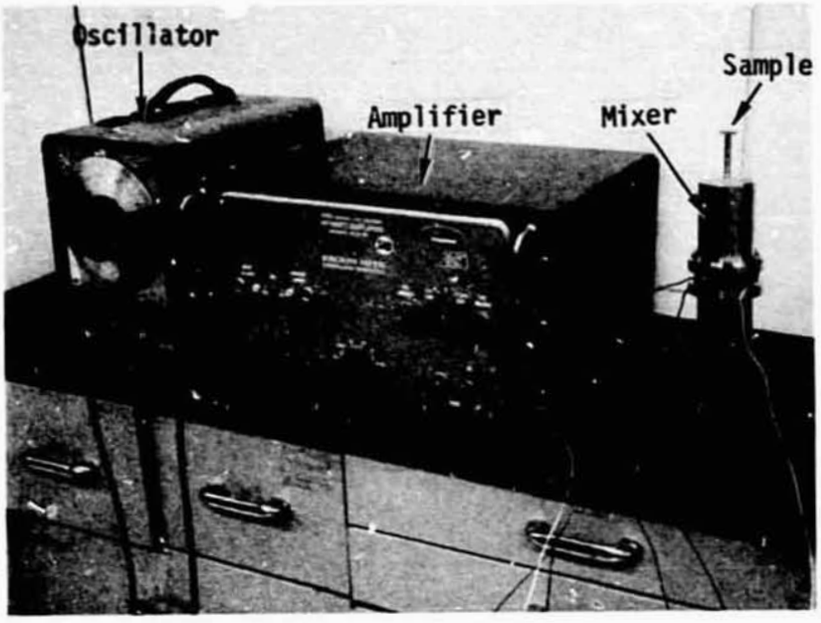

a. Experimental Apparatus Arrangement

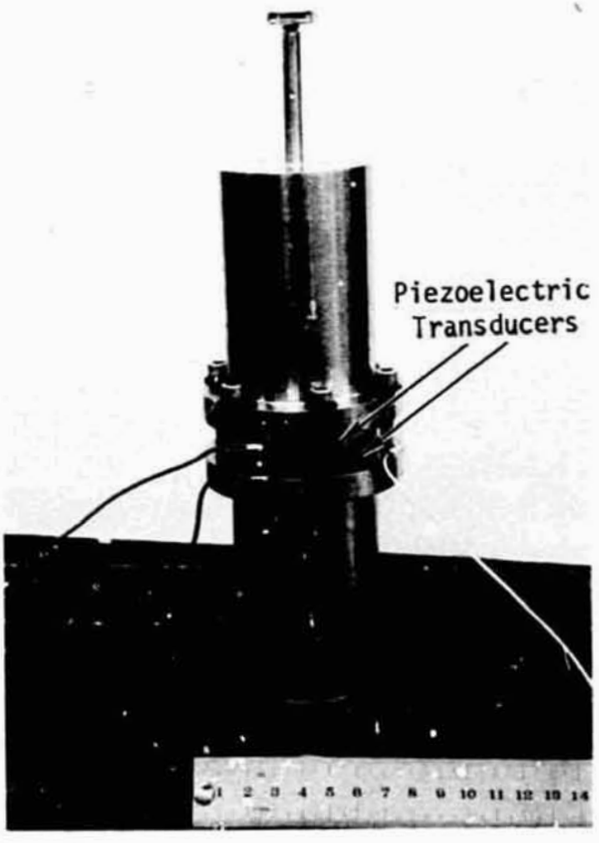

b. Transducer Arrangement within Mixer

Figure 2-6. Acoustic Mixer

The sonoration or mixing action was visibly noticeable in the glass cartridge end, after approximately 10 seconds, the mixing was essentially complete and no further mixing was noted after 30 seconds. It was noted that the coupling between the cartridge and the mixer was critical and, since the experimental glass cartridges were connected to the horn by a screw which was epoxy bonded, little torque could be applied. Thus, on several occasions during testing, the capsule loosened and the mixing was noticeably reduced or, in some cases, ceased completely.

Figure 2-7 presents photomicrographs of an 80/20 a/o Ga-Hg mixture which was mixed for 30 seconds and cooled with ice while being mixed. From the photomicrographs it may be seen that this immiscible couple is reasonably well dispersed with the majority of the mercury present being in the form of spheres 1 to 2 μm in diameter.

After successful testing and rework of the acoustic mixer, the package was reinforced for integration into the drop tower package, using the associated components detailed in Appendix A.

A description of the materials selected and the drop tower testing and analyses are presented in Section 3.0 below.

2.2 ELECTROMAGNETIC MIXER

2.2.1 Background

Originally, the concept of electromagnetic processing was involved in inducing eddy currents in the molten metal, similar to one of the processes used by the AEC [Reference 4]. Examination of the total process requirement, however, leads to the following analysis. The model system chosen was lead-gallium, since it has a wide miscibility gap and represents relatively widely divergent physical properties. The system properties to be known are: physical properties of the system, magnetic field, current density and experiment container.

Then:

$$\vec{F} = I\vec{\ell} \times \vec{B}$$

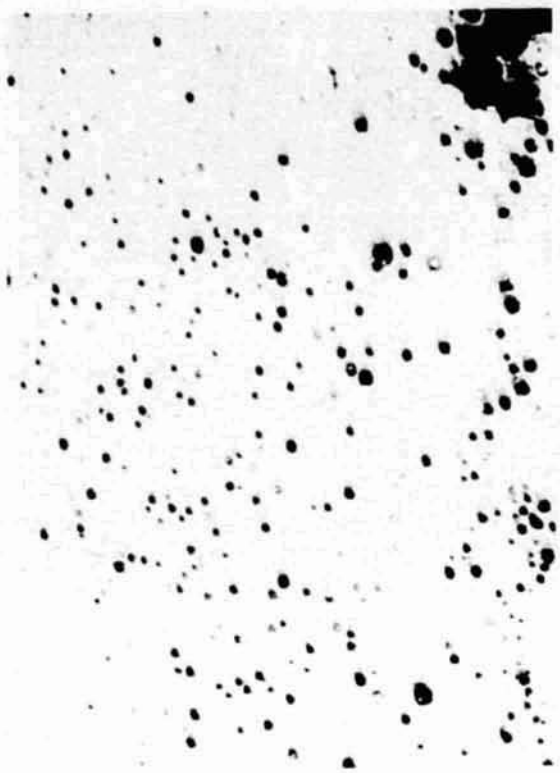

Magnification: 50X

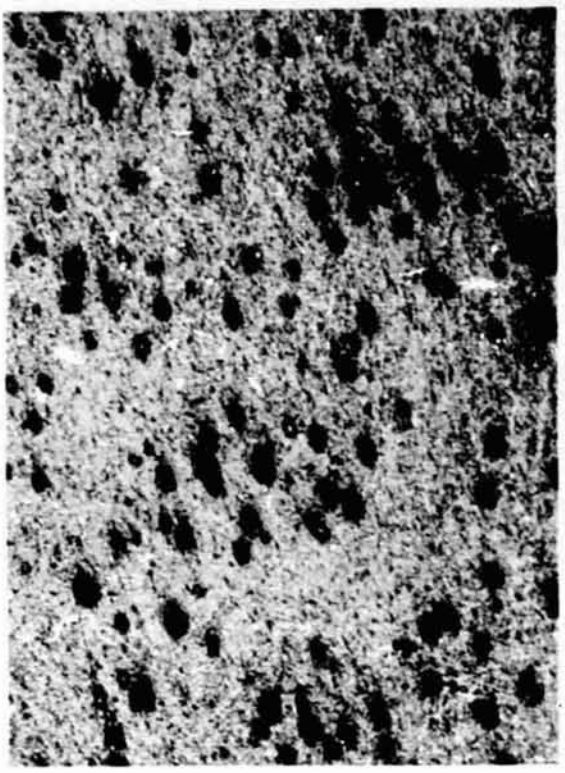

Magnification: 100X

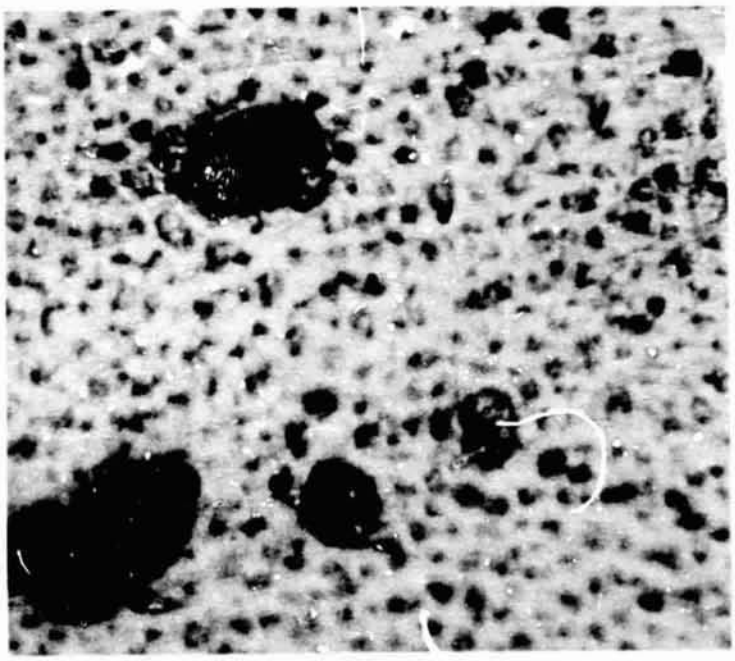

Magnification: 100X

Figure 2-7. Photomicrographs of Ultrasonically Dispersed Gallium-Mercury Immiscible System

where:

$\vec{F}$ = force in dynes

$\vec{I}$ = current in abamperes

$\vec{B}$ = magnetic field strength in gauss (for nonmagnetic materials)

ℓ = length in centimeters

Assume a one cm cube of material at rest carrying a current density of 1A cm^{-2} in a magnetic field of one gauss. Then $\vec{F} = \vec{I} \times \vec{B}$ = 0.1 dyne.

For a current density of 10^2 A cm^{-2} and a magnetic field strength of B = 2 KG, F = 2 x 10^4 dynes. For an alloy of 50 a/o Ga-Pb,

Ga = 69.7 atomic weight
density ρ = 5.7 g cm^{-3} (molten)
Pb = 207.2 atomic weight
density ρ = 10.6 g cm^{-3} (molten)
ρ alloy = 8.15 g cm^{-3}

Then the acceleration of a cubic centimeter of alloy in a magnetic field normal to the electric field is a $\frac{F}{m}$ = 2.45 x 10^3 cm/sec^{-2} or about 2.5 gravities. This should be enough acceleration for rapid mixing.

Ignoring viscous drag, the velocity of the alloy after undergoing 5 cm of $\vec{I} \times \vec{B}$ acceleration will be:

D (distance) = 1/2 A (acceleration) T^2 (time)

so v (velocity) = $(2DA)^{1/2}$

v = $(2 \times 5 \times 2.45 \times 10^3)^{1/2}$ = 1.56 x 10^2 cm/sec^{-1}

This velocity, near 1.6 meters sec^{-1}, should be adequate for mixing.

Consider the power consumption of an alloy accelerator channel 5 cm long with a cross section of 1 cm x 1 cm:

I total - 500 amps

The resistivity of gallium is 25.8 $\mu\Omega$ cm. The resistivity of lead is 95 $\mu\Omega$. Ignoring interfacial problems, the resistivity of the alloy should be about 60.4 $\mu\Omega$ cm.

The voltage drop across the channel E = 6.04 x 10^{-5} x 10^2 = 6.04 x 10^{-3} volts.

The total resistive power dissipated in the channel is about

$$5 \times 10^2 \times 6.04 \times 10^{-3} = 3.2 \text{ watts}$$

Both the voltage drop E and the power consumption will be much higher in practice because large amounts of power will be converted to fluid motion and this motion degraded to heat. The above figures show that this is a very efficient mixing scheme, electrical resistive losses being small.

It is readily seen that the current density can be increased to 10^3 amp cm^{-2} without overheating since the resistive electrical heating in the 5 cm long channel would then total only 320 watts. With a KG field, the velocity (without viscous drag) would be about 32 meters per second at the exit end of the channel.

The above calculations are based on a channel of constant 1 cm^2 cross section. In practice, a great deal of arcing will occur in a channel of this design since the fluid enters at a low velocity, leaves at a high velocity and cannot expand in volume.

To minimize arcing, with its attendant electrode erosion and alloy contamination, the channel should be of variable cross section, the cross being varied inversely with the velocity.

Another solution to this problem is to design the alloy pump/mixing unit to operate at a constant fluid velocity, the pump imparting a pressure head rather than a velocity head.

In summary, very reasonable current densities, accelerator channel lengths and magnetic fields yield ample alloy fluid velocities (or pressure heads) for mixing with good conversion efficiency of electrical power input into fluid motion.

This process method also has the advantage of applying the I^2R heating to the alloy for initial melting of the alloy as well as supplying the current component of the $\vec{B} \times \vec{I}$ force field. In addition, after the current is removed, the static magnetic field effectively "freezes" the molten dispersion and suppresses thermal motion during cooling.

2.2.2 Preliminary Electromagnetic Mixing Demonstration

Using a previously developed low melting alloy (12.3 w/o Ga, 45.2 w/o Bi, 35.2 w/o Pb, 7.1 w/o Cd)[Reference 5], a series of preliminary

experiments were performed using a simple rectangular capsule design. Glass spheres were mixed into the alloy to observe the mixing. The alloy was heated above its melting point (~100°C) before application of the current. The sample was then placed in a magnetic field of 2400 gauss, with a DC current of 30 amps. Figure 2-8 through 2-11 show the processing sequence. After application of the current, the alloy was observed to be violently agitated in the container. As was predicted by the mathematical analysis, the alloy separated from one of the electrodes and arcing occurred. Examination of the contents of the capsule indicated that this method is suitable for mixing, particularly for metals in the 2-phase liquid regime.

2.2.3 Electromagnetic Mixer Design

Based on the preliminary experiments, it became obvious that an annular test chamber would reduce arcing and should provide an optimum design.

A very simple constant velocity system is shown in Figure 2-12 below:

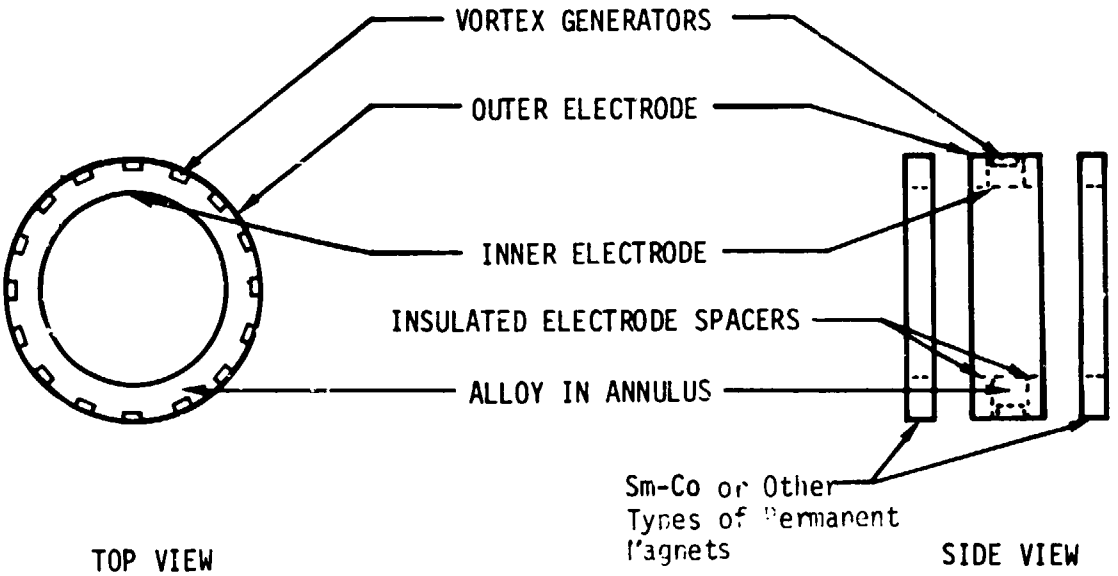

Figure 2-12. Schematic View of Electromagnetic Mixing Device

Sm-Co or other permanent magnets could be used above and below the alloy chamber. A U-shaped piece of sheet iron (not shown) would provide a flux return path for the two magnets. Cooling after processing would be accomplished by directing a water flow across the inner and outer electrodes.

Figure 2-8. Initial Set-up of Electromagnetic Stirring Apparatus.

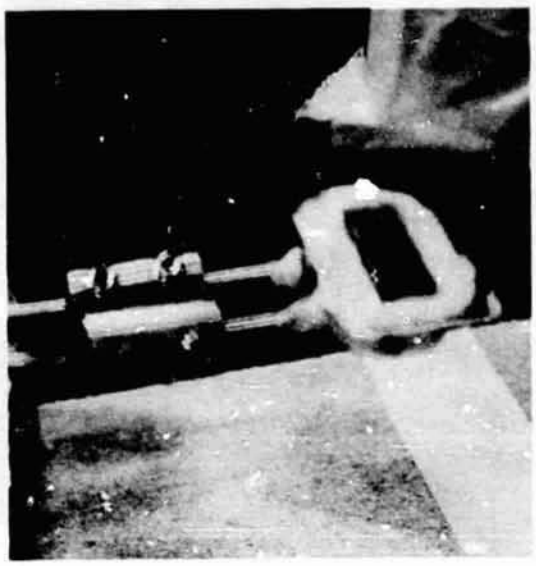

Figure 2-9. 0.2 Second After DC Current Energized.

Figure 2-10. Approximately One Second During Processing.

Figure 2-11. Approximately 5 Seconds After Initiation of Experiment

Figures 2-8 through 2-11. Electromagnetic Stirring Experiment.

Materials of construction of the test capsules were Kovar inner and outer electrodes separated by low expansion Pyrex, a 316 SS fill tube and nickel vortex generators.

The fabrication sequence used was (1) rounding of the Kovar electrodes to minimize the occurrence of stress risers which would effect the glass, (2) the 316 SS fill tube was brazed to the outer electrode using a 1200°C braze, (3) nickel vortex generators were then spot welded to the outer electrode, (4) the entire assembly was then wet hydrogen fired at 1100°C to form the nickel oxide required to form the glass seal. The final step was to seal the inner and outer electrodes together using the low expansion pyrex. The test capsules were leak checked and repaired as necessary. Figure 2-13 presents a photograph of a completed capsule.

A detailed discussion of the test capsules, the experimental package and the operation of the electromagnetic mixer is presented in Appendix B.

After substantial testing and rework of the electromagnetic mixer, the system was built into a drop tower package. A description of the materials selected for the low gravity tests and the test results are presented in Section 3.0 of this report.

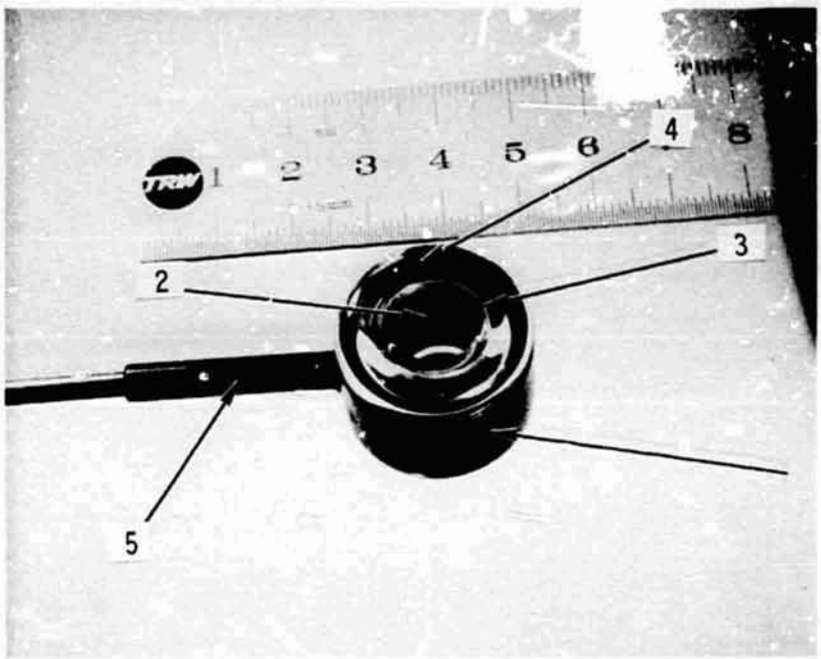

Figure 2-13 . Completed Electromagnetic Mixer Capsule Showing Component Parts (Approx. 1X)

1) Outer electrode
2) Inner electrode
3) Pyrex glass
4) Nickel vortex generator
5) 316 SS fill tube

3.0 SELECTION, PROCESSING AND EVALUATION OF IMMISCIBLE BINARY ALLOY COMPOSITIONS

3.1 SELECTION BASIS

The selection of systems containing an immiscibility gap in the liquid state was based on three main considerations: (1) process temperature, (2) process apparatus (acoustic or electromagnetic) and (3) potential application of the system.

Both the acoustic and electromagnetic mixers are limited to process temperatures achievable either by the clad heating elements or container/experiment compatibility considerations. With the present designs, this temperature limitation is approximately 1000 C, and the containers for the electromagnetic mixer are further limited to approximately 500 C due to the Kovar-Corning 7052 glass construction. Table 3-1 lists the binary couples which appeared to satisfy the above criterion.

3.2 SELECTED SYSTEMS

The couples identified in Table 3-1 were categorized initially in terms of process method as a function of temperature; thus, the primary candidates for the electromagnetic mixer were Cd/Ga and Ga/Pb, although they could just as easily be processed acoustically. Initial laboratory experiments indicated that the 80/20 a/o Ga/Pb system would be extremely difficult to handle; therefore, the system Cd/Ga was chosen for the electromagnetic mixer experiment. The system aluminum-indium was not considered further since it is being investigated elsewhere. Thus, the three couples, aluminum-bismuth, calcium-lanthanum and cadmium-gallium, were investigated in further detail.

The original investigation of the cadmium-gallium couple was performed on a 50/50 a/o composition, but, as with the gallium-lead couple, the gallium concentration was too high for convenient handling. Inasmuch as the primary purpose of selecting this couple was to compare the behavior of the gallium with that of the previously processed bismuth-gallium couple [Reference 2], a compromise composition of 65/35 a/o Cd/Ga was chosen. The same rationale was applied to the 50/50 a/o Al/Bi in that bismuth should also be the matrix metal as with the Bi/Ga couple. In this manner, a correlation between bismuth and gallium may be made from three

Table 3-1. List of Candidate Immiscible Binary Couples for Processing

Couple	Consolute Temp., °C[a]	Suggested Process Temp., °C	Suggested Elemental Ratio, a/o	Suggested of Type Processing
Al/In	875	800	80/20	Acoustic
Al/Bi	1220	850	50/50	Acoustic
Al/Bi	1050	850	25/75	Acoustic
Ca/La	880	850	80/20	Acoustic
Cd/Ga	290	285	65/35	Electromagnetic or acoustic
Ga/Pb	570	370	80/20	Electromagnetic or acoustic

[a]Consolute temperature at suggested elemental ratio. This temperature varies with composition.

separate immiscible binary systems.

Assuming that extremely fine (approaching atomic) dispersions can be obtained with the acoustic mixer, then a 25/75 a/o Al/Bi mixture would have an electron to atom ratio (e/a) of 4.5, which corresponds to one of the empirical e/a ratios that has shown an enhancement of the superconducting transition temperature [Reference 6].

The calcium-lanthanum was chosen because lanthanum is the only rare earth element that superconducts without applied pressure [Reference 7], has two transition temperatures depending on the crystallographic habit [Reference 6] and it has been postulated that the superconducting behavior arises from the f-band arrangement of the element [Reference 8]. Thus, it was a logical candidate for processing to determine if its superconducting behavior could be altered by processing in a low gravity environment. Figures 3-1, 3-2 and 3-3 show the phase diagrams of the three couples chosen.

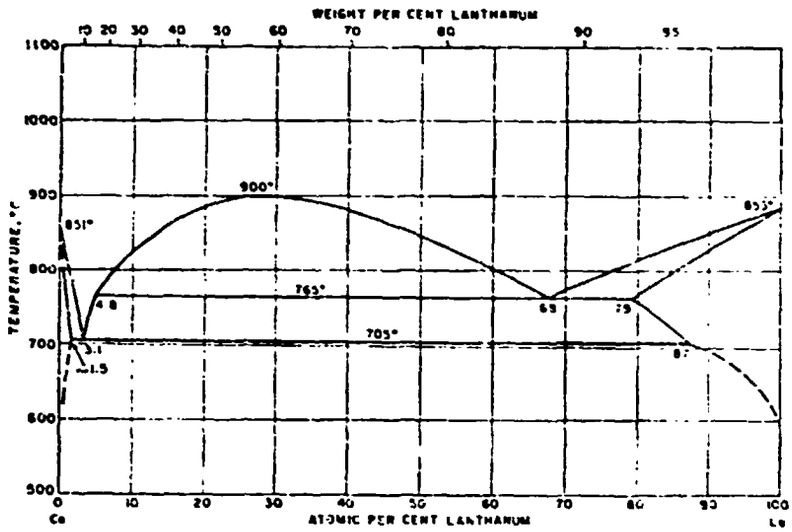

Figure 3-1. Phase Diagram of the Calcium-Lanthanum System

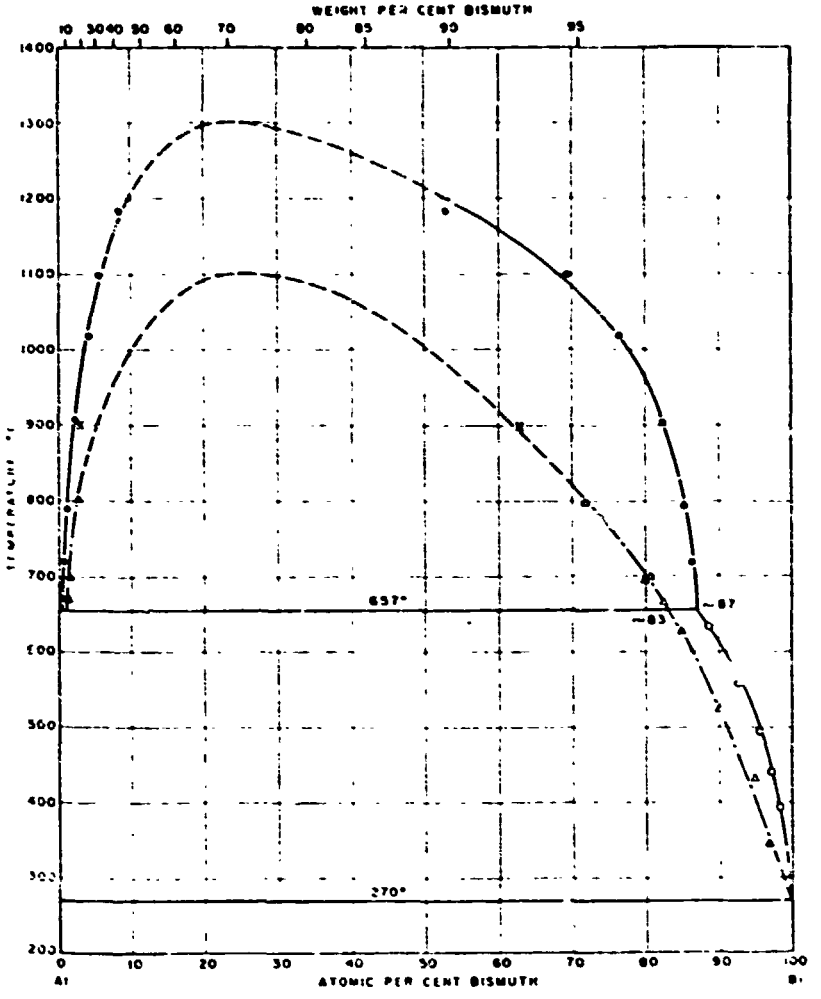

Figure 3-2. Phase Diagram of the Aluminum-Bismuth System

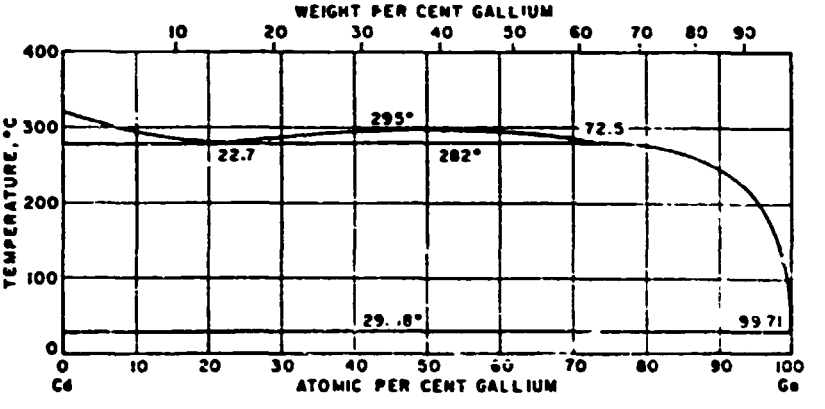

Figure 3-3. Phase Diagram of the Cadmium-Gallium System

3.3 FABRICATION AND PROCESSING OF THE SELECTED SYSTEMS

3.3.1 Fabrication

As mentioned previously, the aluminum-bismuth and calcium-lanthanum systems were chosen to be processed acoustically and the cadmium-gallium system to be processed in the electromagnetic mixer. The electromagnetic experimental cartridge was shown in Section 2. Inasmuch as the acoustic mixer will accept a variety of cartridge shapes, provided they conform within the weight/volume constraints of the acoustic horn, a final decision was made to fabricate right circular cylindrical cartridges.

Since aluminum is relatively agressive with respect to materials compatibility at elevated temperatures, a two-part cartridge was fabricated. The outer container was 316 stainless steel, with an inner container of ATJ Star graphite, which is compatible with aluminum. Figure 3-4 illustrates the cartridge configuration.

Fabrication of the experimental cartridges was fairly straightforward. Weighed amounts of the elements were placed in the precleaned, vacuum fired (1000°C) graphite containers and melted under argon by induction heating. The higher melting element was melted initially, followed by the lower melting component. The experiment volume was approximately 0.2 cm^3, of which 80 percent was utilized to allow for thermal expansion at the process temperature. After filling, the graphite container was capped, placed in the stainless outer container and the end cap containing the fill tube was TIG welded in place. The entire unit was then helium leak checked and while under vacuum, the fill tube was crimped and spot welded in place.

The electromagnetic mixer experiment cartridges were processed somewhat differently. Both the container and the cadmium were mated in an oven inside of a dry box. When the cadmium was melted, it was poured into a funnel containing a ball and socket joint and the molten cadmium forced into the cartridge with an overpressure of argon. The cartridges were then cooled and weighed to determine that the correct amount of cadmium had been transferred. The weights were correct to within $\pm$ one percent. Since gallium is a low melter, the cartridges were not heated but otherwise the same procedure was followed. In spite of precautions (e.g. shak-

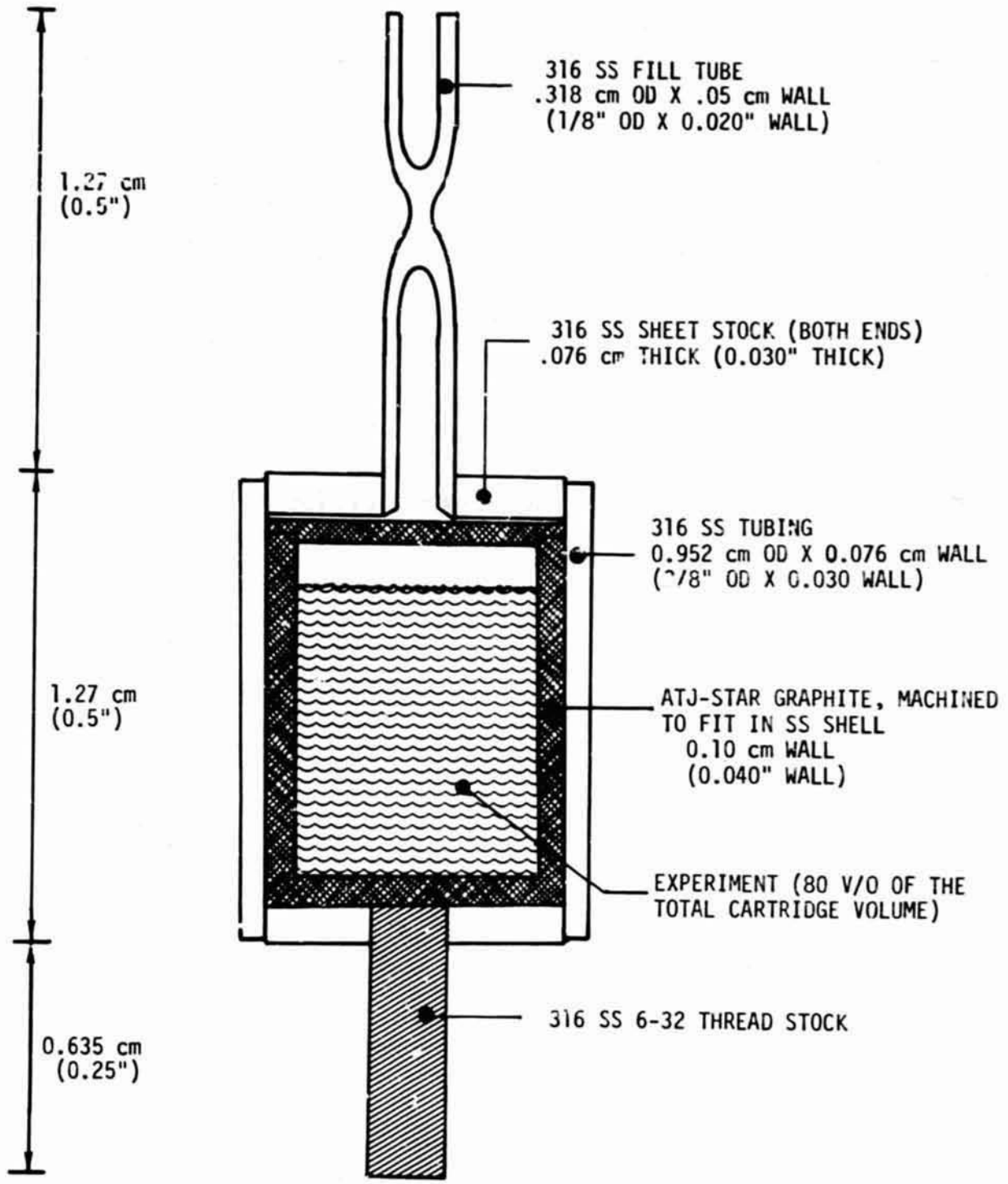

NOTE: ALL METAL EDGES AND INSERTS TIG-WELDED
FILL TUBE IS CRIMPED AND SPOT WELDED

15-89

FIGURE 3-4. Schematic Drawing of Experiment Cartridge for Acoustic Processor.

ing while cooling), the Pyrex cracked slightly when the gallium solidified and expanded. These cracks were repaired with Autostick, an alumina-based ceramic cement, and were leak tight. The same closure procedure as used with the acoustic cartridges was employed.

3.3.2 Processing

The cartridges were processed at the MSFC drop tower in accordance with the sequences delineated in Appendices A and B. Tables 3-2 through 3-5 list the telemetered data as received from MSFC.

The telemetered data traces for the cadmium-gallium showed anomalous behavior which prevented extensive data reduction. It appears that when the current relay was activated to start the mixing, the drain on the batteries was so large that the telemetry output was offset. As an example, there appears to be an immediate 100°C temperature drop, and a shift in the low-g accelerometer output. Conversations with the MSFC data acquisition personnel tend to corroborate this hypothesis; thus, about 2 seconds of data during mixing are suspect, as is the data just prior to the mixing since it does not correlate with the measurements made at the drop tower blockhouse, independent of the telemetered data. However, the data is very consistent between the three runs (a one-g and two low-g experiments); thus it is presented as received from MSFC.

3.4 EVALUATION OF PROCESSED SPECIMENS

3.4.1 Metallurgical Evaluation

The three immiscible systems, comprising four formulations, were examined metallurgically in order to determine the degree of morphological similitude with respect to previous experiments and also to evaluate the efficacy of the two types of mixing processes utilized in this portion of the program.

After receipt of the specimens from MSFC and removal from the experimental cartridges, it was discovered that, in the case of the acoustically mixed samples, the majority of the specimens were distorted and/or disintegrated to the extent that meaningful analyses could not be obtained. A very slight correlation might exist between the initial degree of cooling and specimen integrity. This correlation could not be carried further since both the sample population and telemetry accuracy were limited in

Table 3-2. Telemetered Drop Tower Results for the 50/50 a/o Al/Bi Experiment

	AB-5	AB-4	AB-1	AB-3
Initial Drop Temperature, °C	885	900	885	875
Final Drop Temperature, °C[a]	310	300	305	300
Indicated Initial Temperature Rate of Change, °C/Sec	7000	1750	7750	6300
Indicated Total Temperature Rate of Change, °C/Sec	669	882	1115	1045
Gravity Level During Drop, G_e	1	-.005	-.005	-.001

[a] Bottom calibration curve for telemetry data.

Table 3-3. Telemetered Drop Tower Results for the 25/75 a/o Al/Bi Experiment

	AB-6	AB-7	AB-8	AB-10
Initial Drop Temp., °C	870	900	880	875
Final Drop Temp., °C[a]	300	300	300	300
Indicated Initial Temperature Ratio of Change, °C/Sec	4214	350	1450	531
Indicated Total Temperature Rate of Change, °C/Sec	1676	233	203	240
Gravity Level During Drop, G_e	1	-.008	+.003	-.003

[a] Bottom calibration curve for telemetry data.

Table 3-4. Telemetered Drop Tower Results for the 80/20 a/o Ca/La Experiment

	CL-1	CL-4	CL-2	CL-5	CL-3
Initial Drop Temp., °C	910	865	850	840	870
Final Drop Temp., °C [a]	300	300	300	300	320
Indicated Initial Temperature Rate of Change, °C/Sec	483	444	525	1265	2000
Indicated Total Temperature Rate of Change, °C/Sec	117	233	184	540	275
Gravity Level During Drop, G_e	1	(0)	-.005	.005	-.05

[a] Bottom calibration curve for telemetry data.

Table 3-5. Telemetered Drop Tower Results for the 65/35 a/o Cd/Ga Experiment[a]

	CG-2	CG-3	CG-4
Initial Drop Temp., °C	375	375	375
Final Drop Temp., °C	200	200	220
Indicated Total Temperature Rate of Change, °C/Sec	53	53	47
Gravity Level at End of Drop, G_e	1	-.005	-.005

[a] Assuming minimal calibration shift.

scope. Thus, only the ground (one-g) specimen and a low gravity specimen from the acoustically processed specimen were analyzed in depth to determine morphological characteristics. All of the electromagnetically mixed specimens were analyzed in that two independent data samples were obtained and the variations (either from telemetry or from personal observation) tended to be reconciled within the data base utilized.

3.4.1.1 50/50 a/o Al/Bi Specimens

Figures 3-5 through 3-10 are scanning electron and electron microprobe photomicrographs of the one and low gravity processed specimens. As can be seen, a more uniform dispersion of aluminum in bismuth is evident in the low gravity specimen than in the one gravity control, although some dispersion of bismuth in aluminum and vice-versa occurs near the interface of the specimen. The rosette-like feature of a relatively large amount of the dispersed aluminum is present in both specimens, although to a greater extent in the low gravity processed one. If the aluminum is solidifying dendritically, then as the bismuth solidus line is approached, the energy imparted to the system from the acoustic mixture could cause dendrite arm breakage and distortion, which could explain the irregular shapes within the matrix. This is relatively clearly shown in Figure 3-7 of the one gravity control specimen.

3.4.1.2 25/75 a/o Al/Bi Specimens

Figures 3-11 through 3-14 are the scanning electron and electron microprobe photomicrographs of these specimens. In contrast to the 50/50 a/o Al/Bi specimens, both the one and low gravity processed specimens are relatively well dispersed. In addition, the rosette-like structure is much more prevalent in the one gravity control specimen than in the low gravity processed one in contrast to the 50/50 a/o Al/Bi specimens. There may have been a more extensive breakup and dispersion of dendritically solidified aluminum in the low gravity specimen, as evidenced by the irregular shapes of the aluminum in the bismuth matrix.

3.4.1.3 80/20 a/o Ca/La Specimens

Figures 3-15 through 3-19 show the scanning electron and electron microprobe photomicrographs of the one and low gravity processed calcium-lanthanum specimens. Due to the reactivity of these elements, the speci-

Segregation - 100X

300X

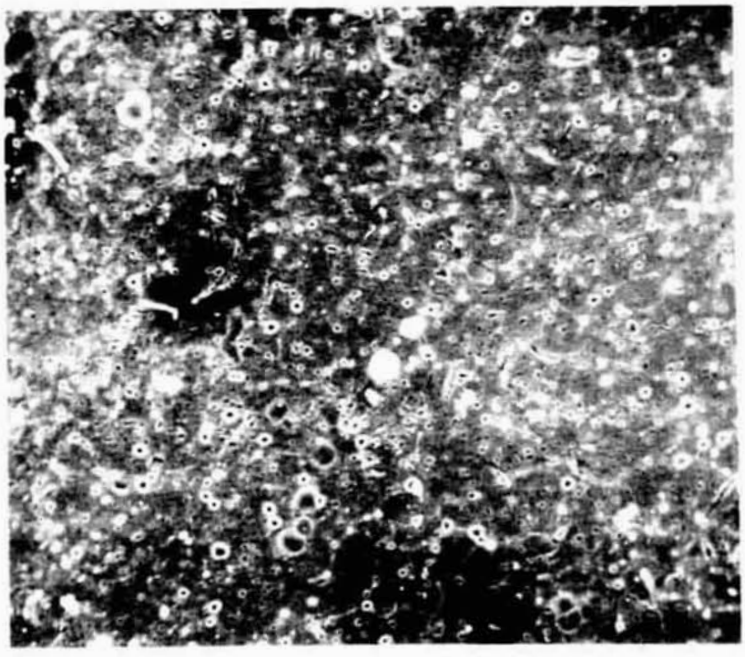

Aluminum-Rich Area - 300X

Figure 3-5. Scanning Electron Photomicrographs of 50/50 a/o Al/Bi Specimen No. AB-5 (1-g)

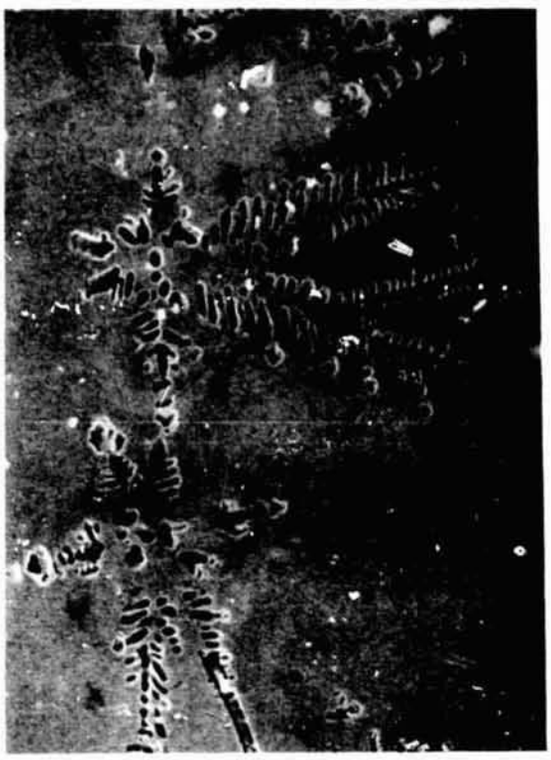

500X

2000X

4000X

Figure 3-6. Scanning Electron Photomicrographs of 50/50 a/o Al/Bi Specimen No. AB-5 (1-g)

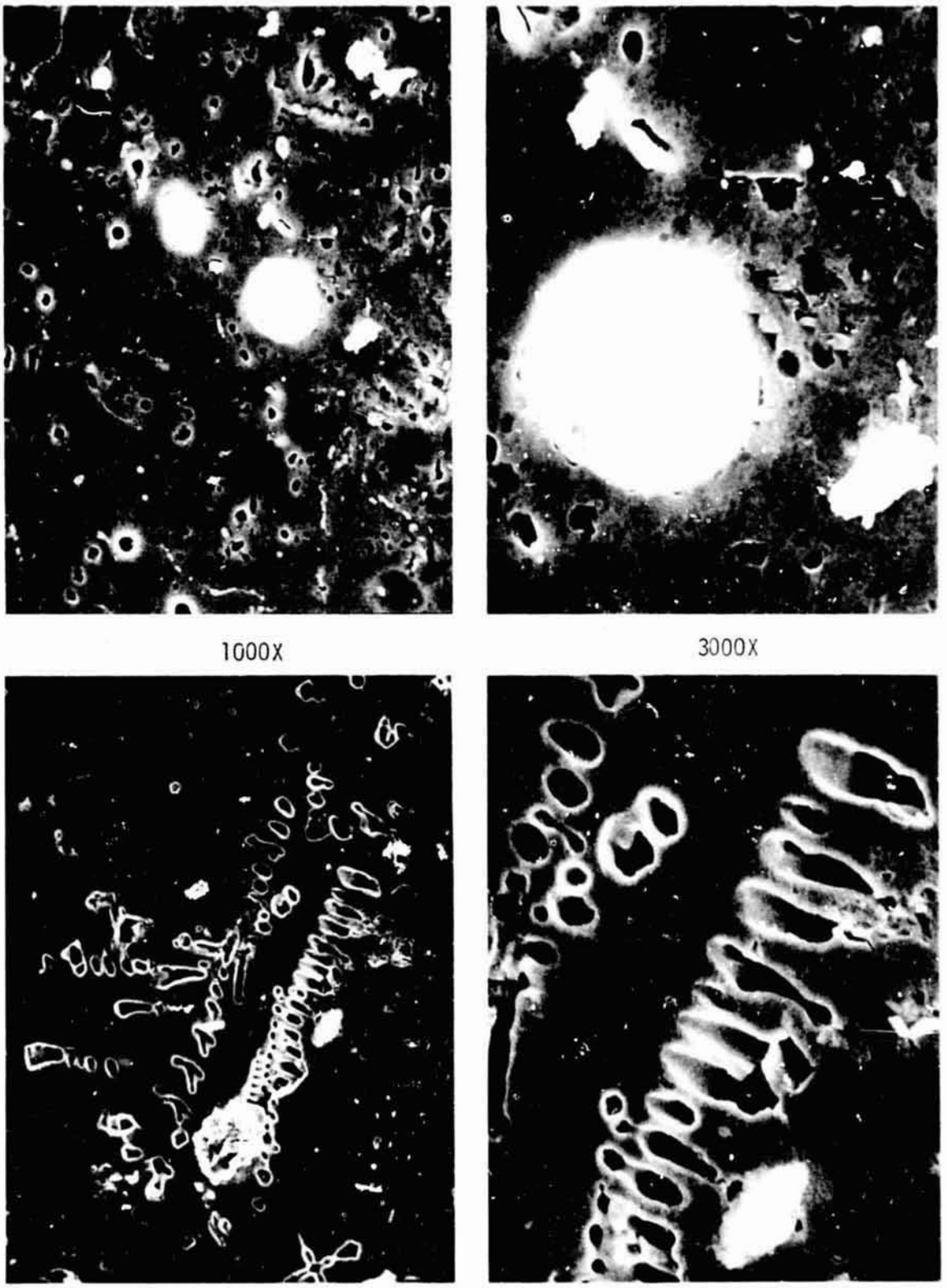

1000X 3000X

1000X 3000X

Figure 3-7. Scanning Electron Photomicrographs of 50/50 a/o Al/Bi Specimen No. AB-5 (1-g)

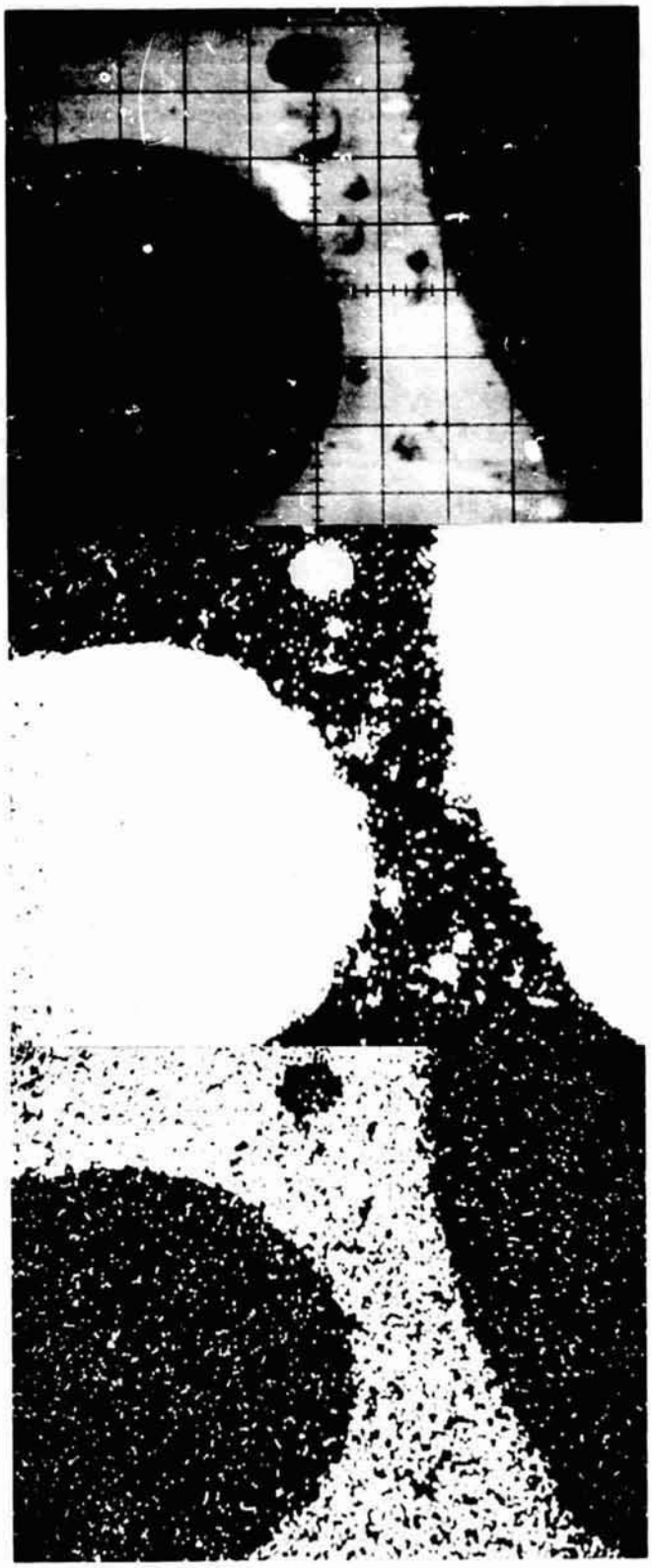

Figure 3-8. Electron Microprobe Photomicrographs of 50/50 a/o Al/Bi Specimen No. AB-5 (1-g) Magnification: 300X

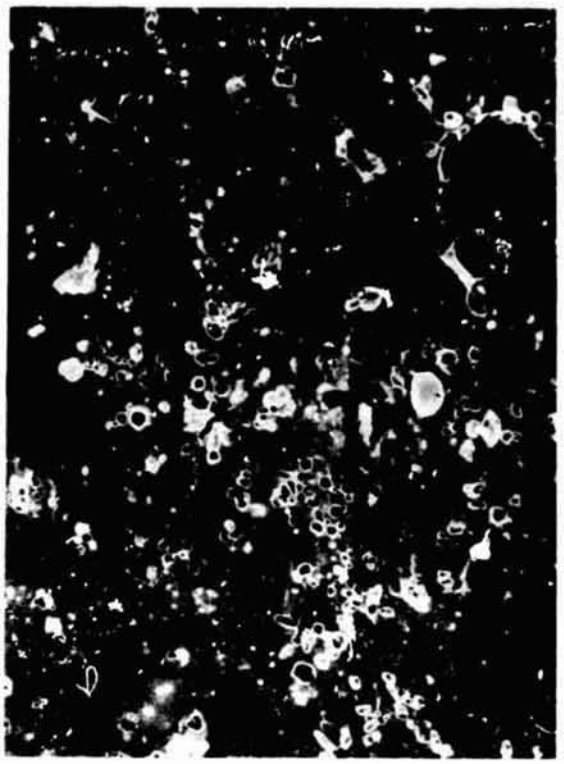

3000X

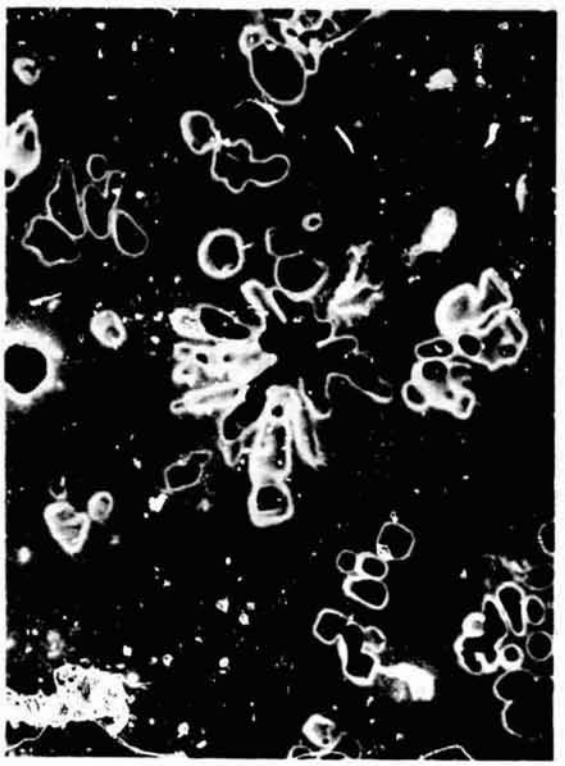

1000X

3000X

Figure 3-9. Scanning Electron Photomicrographs of 50/50 a/o Al/Bi Specimen No. AB-1 (0-g)

Figure 3-10. Electron Microprobe Photomicrographs of 50/50 a/o Al/Bi Specimen No. AB-1 (0-g) Magnification: 300X

500X

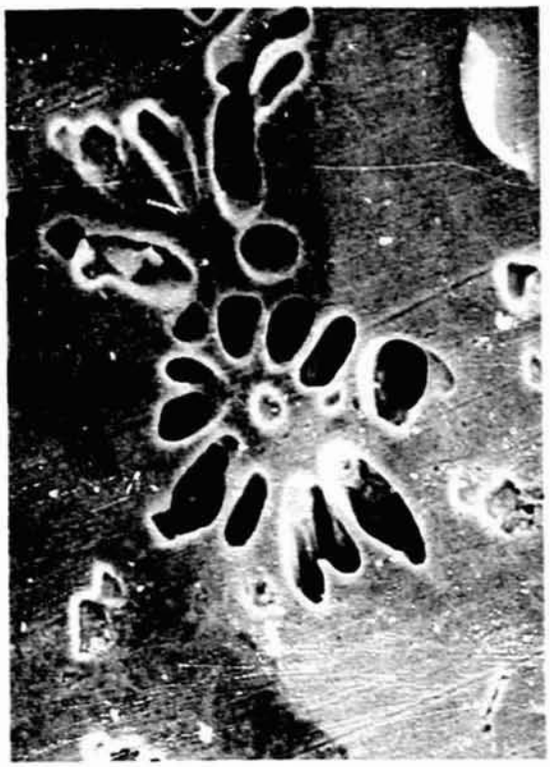

2000X

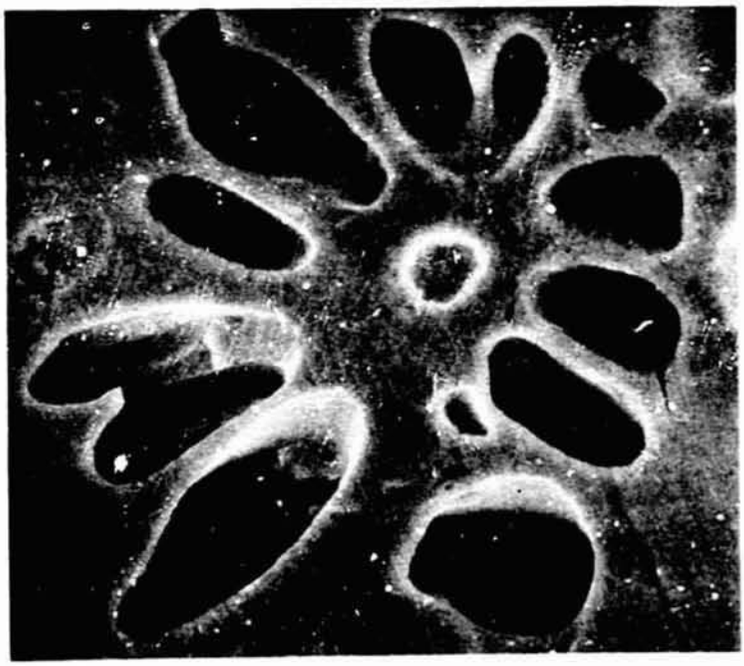

4000X

Figure 3-11. Scanning Electron Photomicrographs of 25/75 a/o Al/Bi Specimen No. AB-6 (.-g)

Figure 3-12. Electron Microprobe Photomicrographs of 25/75 a/o Al/Bi Specimen No. AB-6 (1-g) Magnification: 300X

500X

Rosette Area - 500X

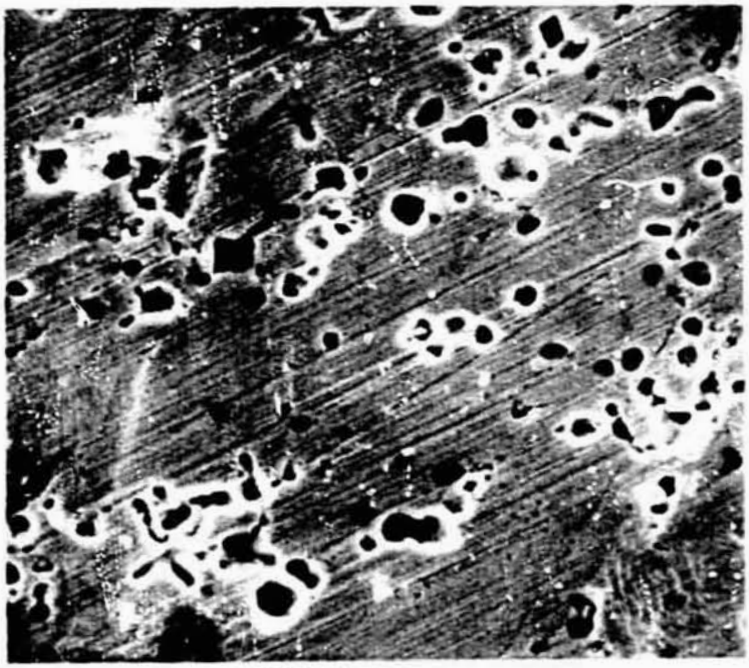

2000X

Figure 3-13. Scanning Electron Photomicrographs of 25/75 a/o Al/Bi Specimen No. AB-7 (0-g)

Figure 3-14. Electron Microprobe Photomicrographs of 25/75 a/o Al/Bi Specimen No. A3-7 (0-g) Magnification: 300X

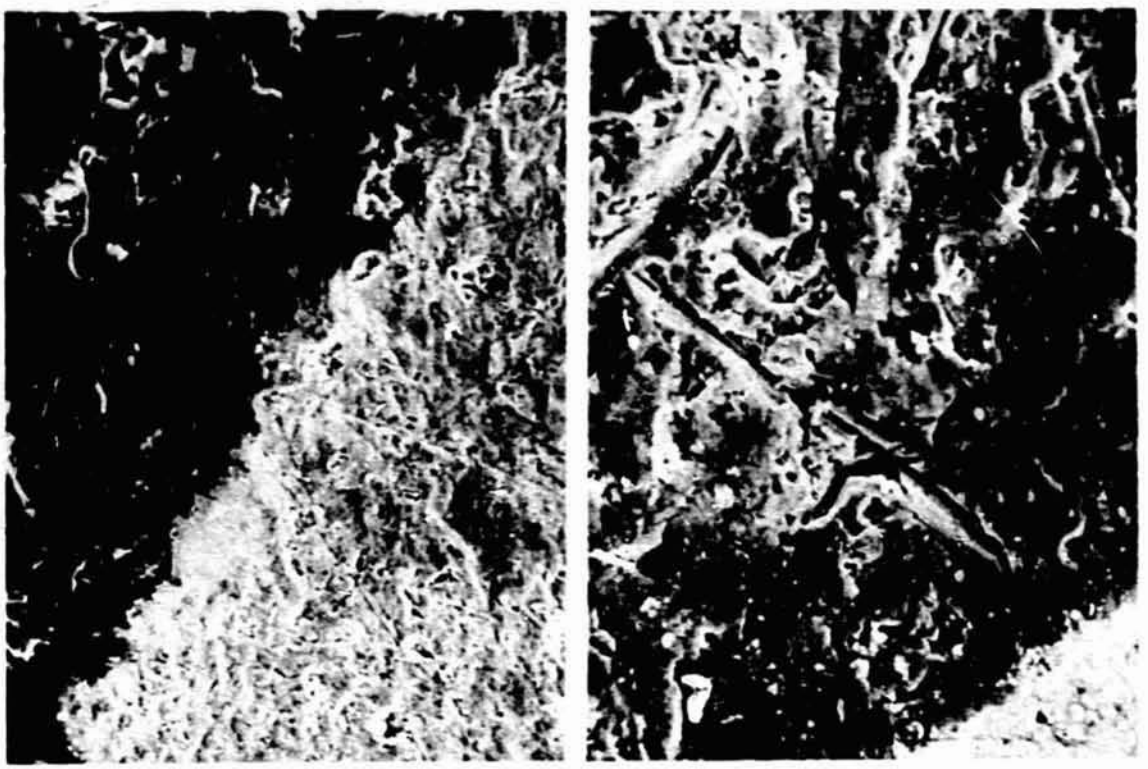

Segregation

Calcium-Rich Side

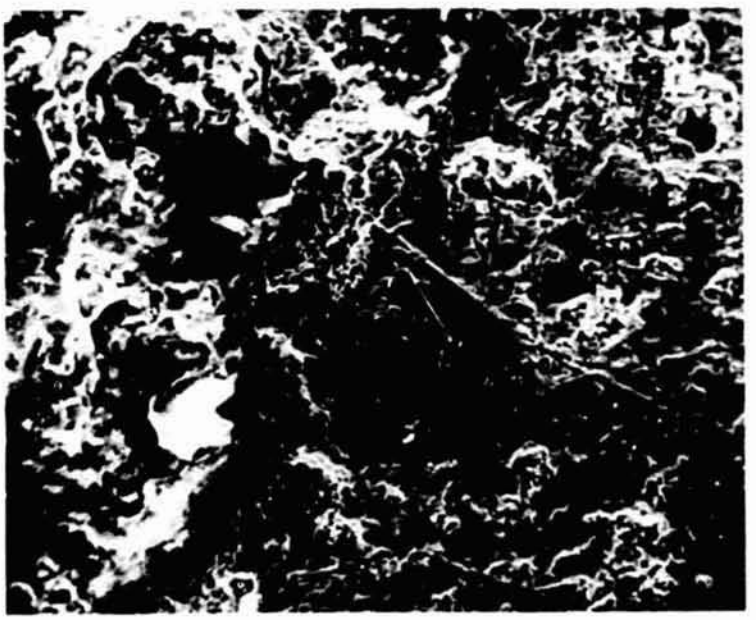

Lanthanum-Rich Side

Figure 3-15. Scanning Electron Photomicrographs of Calcium-Lanthanum Specimen No. CL-1 (1-g) Magnification: 300X

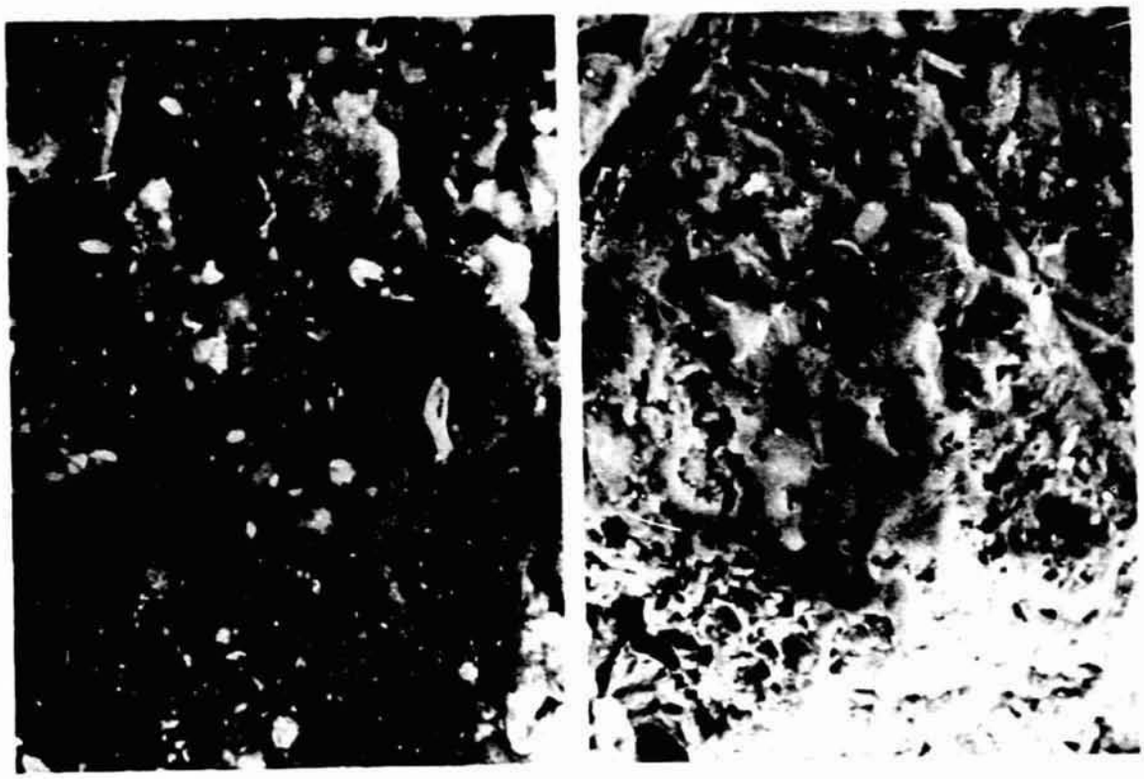

Calcium-Rich - 1000X

Lanthanum-Rich - 1000X

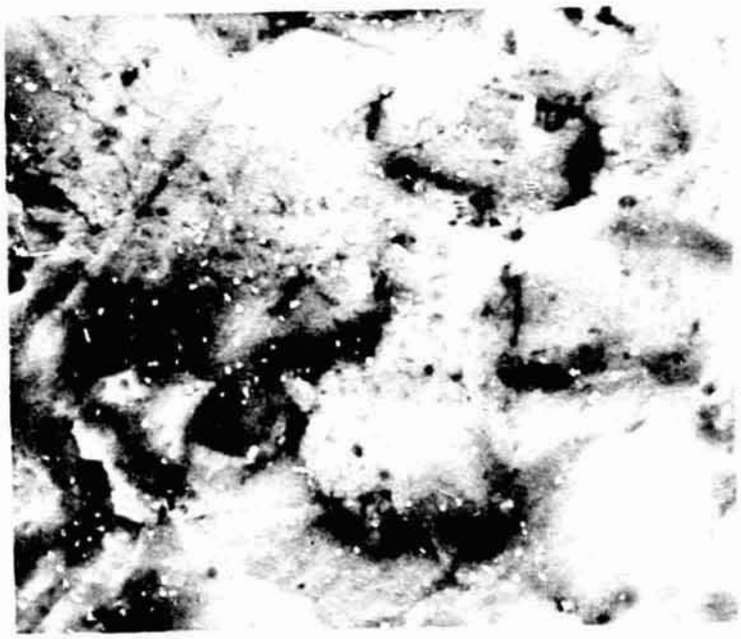

Lanthanum-Rich - 3000X

Figure 3-16. Scanning Electron Photomicrographs of Calcium-Lanthanum Specimen No. CL-1 (1-g) Magnification: 300X

Backscatter Electrons

La L-α

Ca K-α

Figure 3-17. Electron Microprobe Photomicrographs of Calcium-Lanthanum Specimen No. CL-1 (1-g) Magnification: 300X

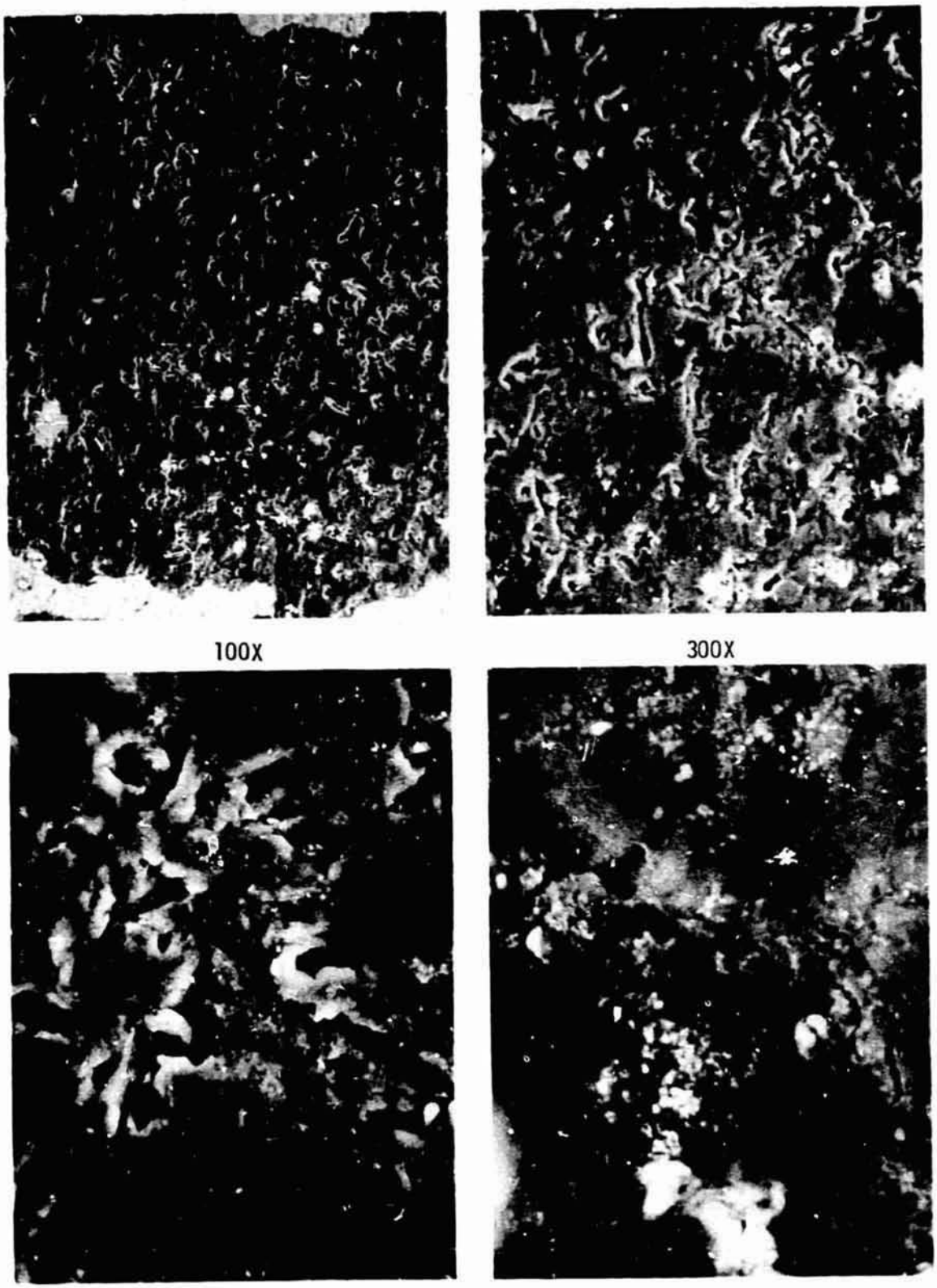

Figure 3-18. Scanning Electron Photomicrographs of Calcium-Lanthanum Specimen No. CL-3 (0-g)

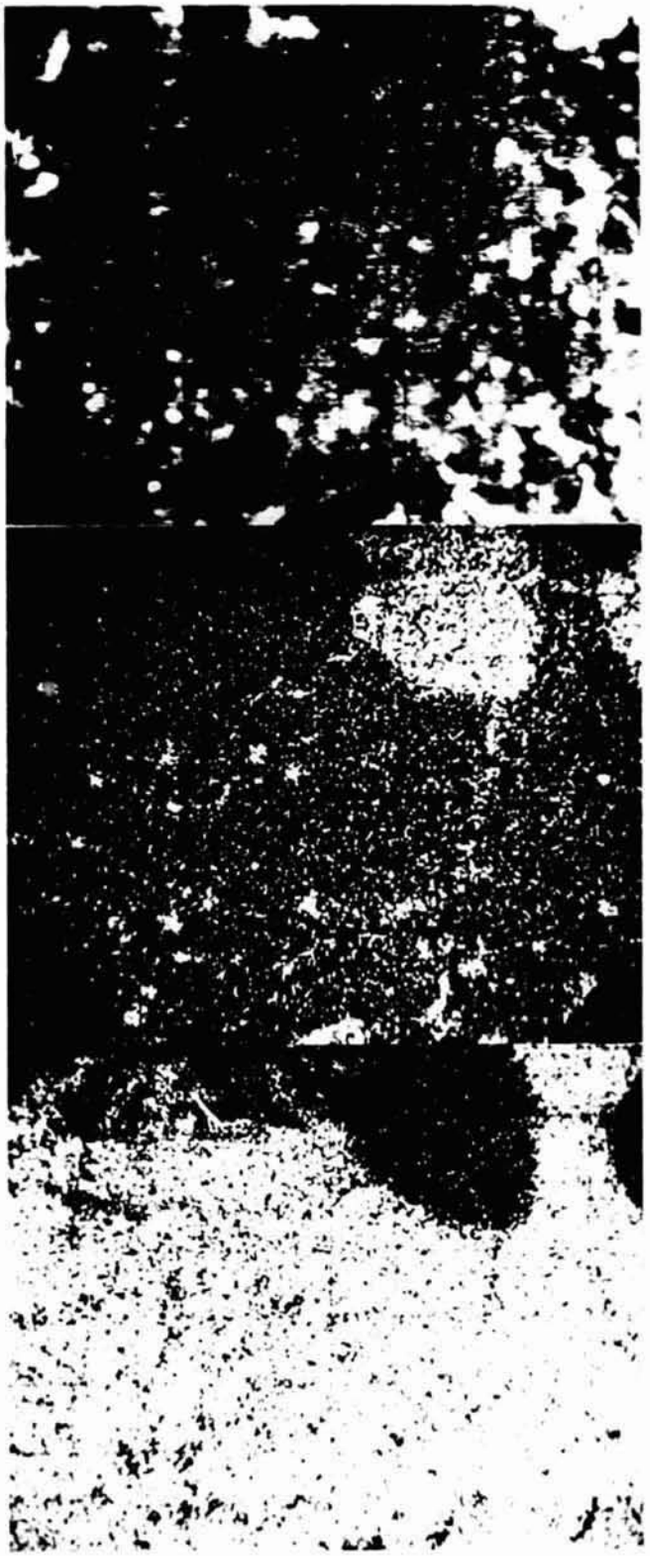

Figure 3-19. Electron Microprobe Photomicrographs of Calcium-Lanthanum Specimen No. CL-3 (0-g) Magnification: 300X

mens were stored under oil between analyses; however, there still was some surface reaction as is evident from the scanning electron photomicrographs. The one gravity control specimen exhibited a fair amount of segregation, although there was some dispersion of the elements. The low gravity processed specimen was well dispersed except for one small area (Figure 3-18) near the cylindrical wall of the specimen. Some agglomeration had been noticed from time to time during the fabrication and testing of the acoustic unit using glass cartridges and mercury-gallium mixtures, but it was not consistent and has not been evident in the other specimens.

3.4.1.4 65/35 a/o Cd/Ga Specimens

The electromagnetically mixed cadmium-gallium specimens exhibited some of the most interesting metallurgical features of all of the processed immiscible couples. Both the one gravity and the two low gravity processed specimens were dispersed, although the dispersion in the one gravity control specimen was coarser than that of the low gravity processed specimens, as shown in the scanning electron and electron microprobe photomicrographs, Figures 3-20 through 3-25. In addition, specimen CG-4 shows the duplex dispersion which has been evidenced in low gravity processed specimens of paraffin-sodium acetate trihydrate [Reference 1] and 50/50 a/o Pb/Zn [Reference 2]. The cause of this type of structure is as yet not understood, although this phenomenon has been demonstrated on Earth with oil-water emulsions during reversion [Reference 9].

3.4.2 Electronic Examination

Superconductivity measurements were made on all of the specimens. Because of the large number of specimens of different sizes that were measured, a method similar to that of Merriam and Von Herzen [Reference 10] was utilized in that each specimen was individually placed in a tuned (16 kH_z) induction coil and a 33 ohm carbon resistor mounted in thermal contact with the coil. Figure 3-26 schematically illustrates the instrumentation utilized. Each resistor was individually calibrated using a Scientific Instruments' Model 2D germanium thermometer and verified by using lead and tantalum standards within the cryostat during the test. When the specimen becomes superconducting, the rejection of the magnetic field changes the impedance of the coil which is detected by the vector

500X

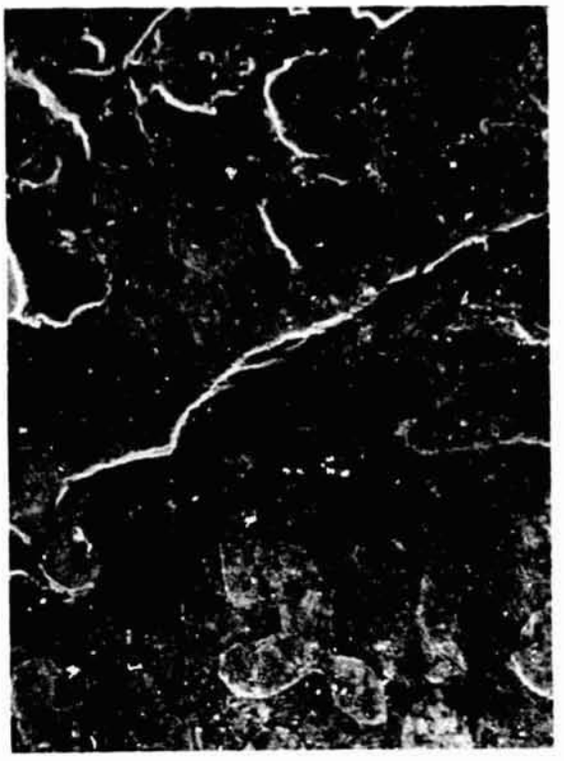

1000X

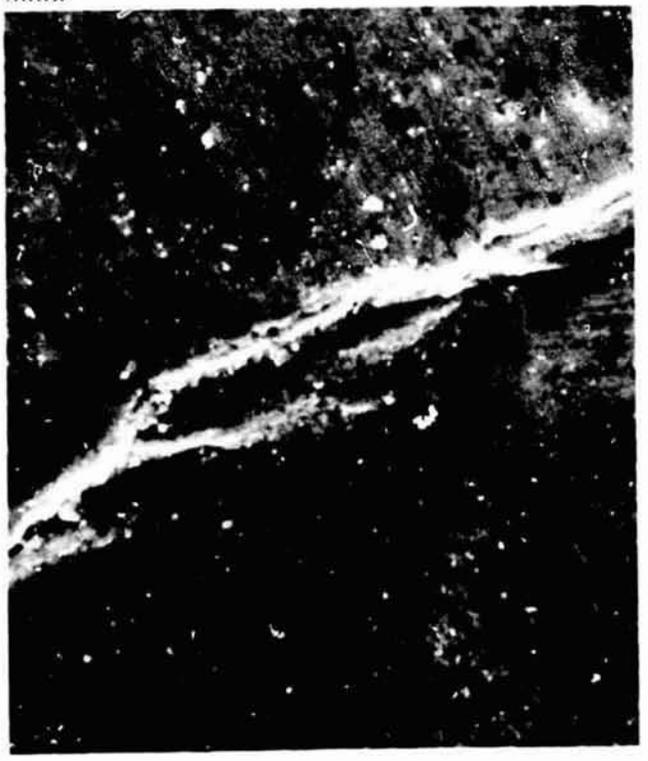

5000X

Figure 3-20. Scanning Electron Photomicrographs of Cadmium-Gallium Specimen No. CG-2 (1-g)

Backscatter Electrons

Ga K-α

Cd L-α

Figure 3-21. Electron Microprobe Photomicrographs of Cadmium-Gallium Specimen No. CG-2 (1-g) Magnification: 800X

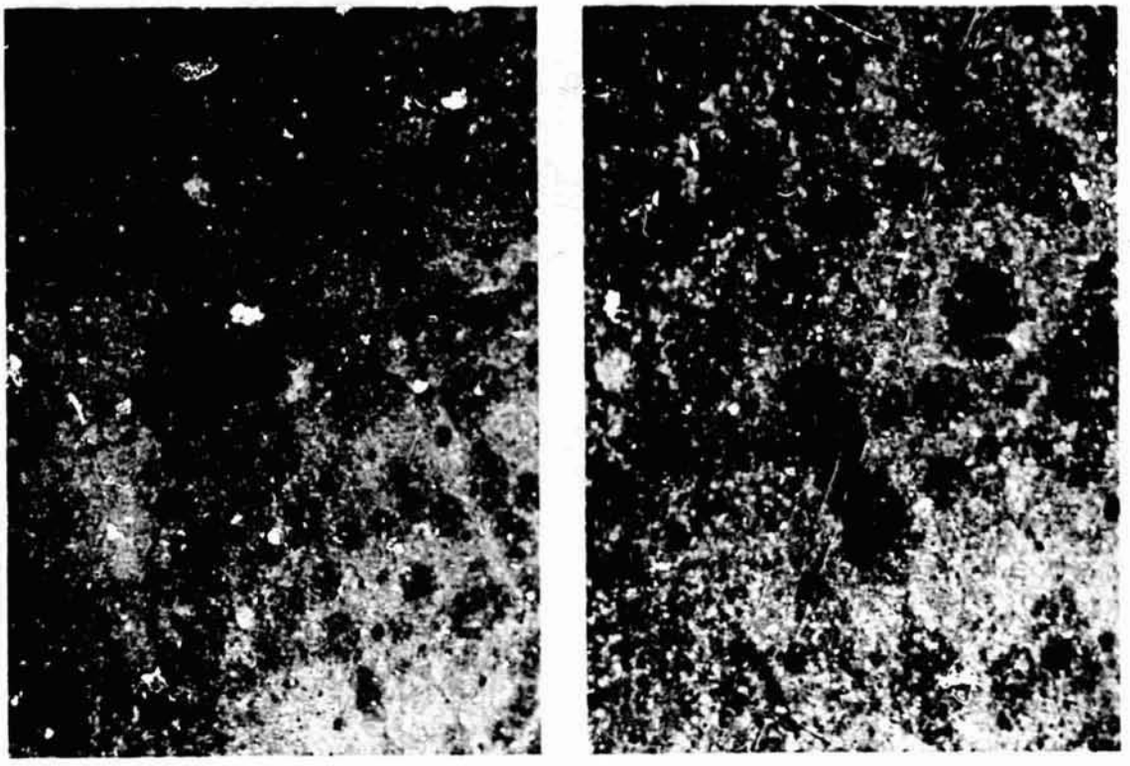

500X 1000X

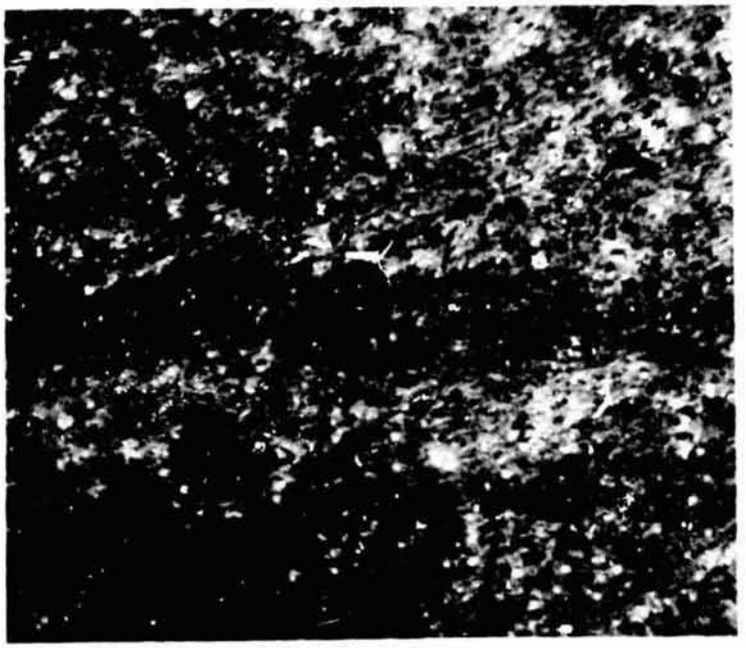

5000X

Figure 3-22. Scanning Electron Photomicrographs of Cadmium-Gallium Specimen No. CG-3 (0-g)

Figure 3-23. Electron Microprobe Photomicrographs of Cadmium-Gallium Specimen No. CG-3 (0-g) Magnification: 800X

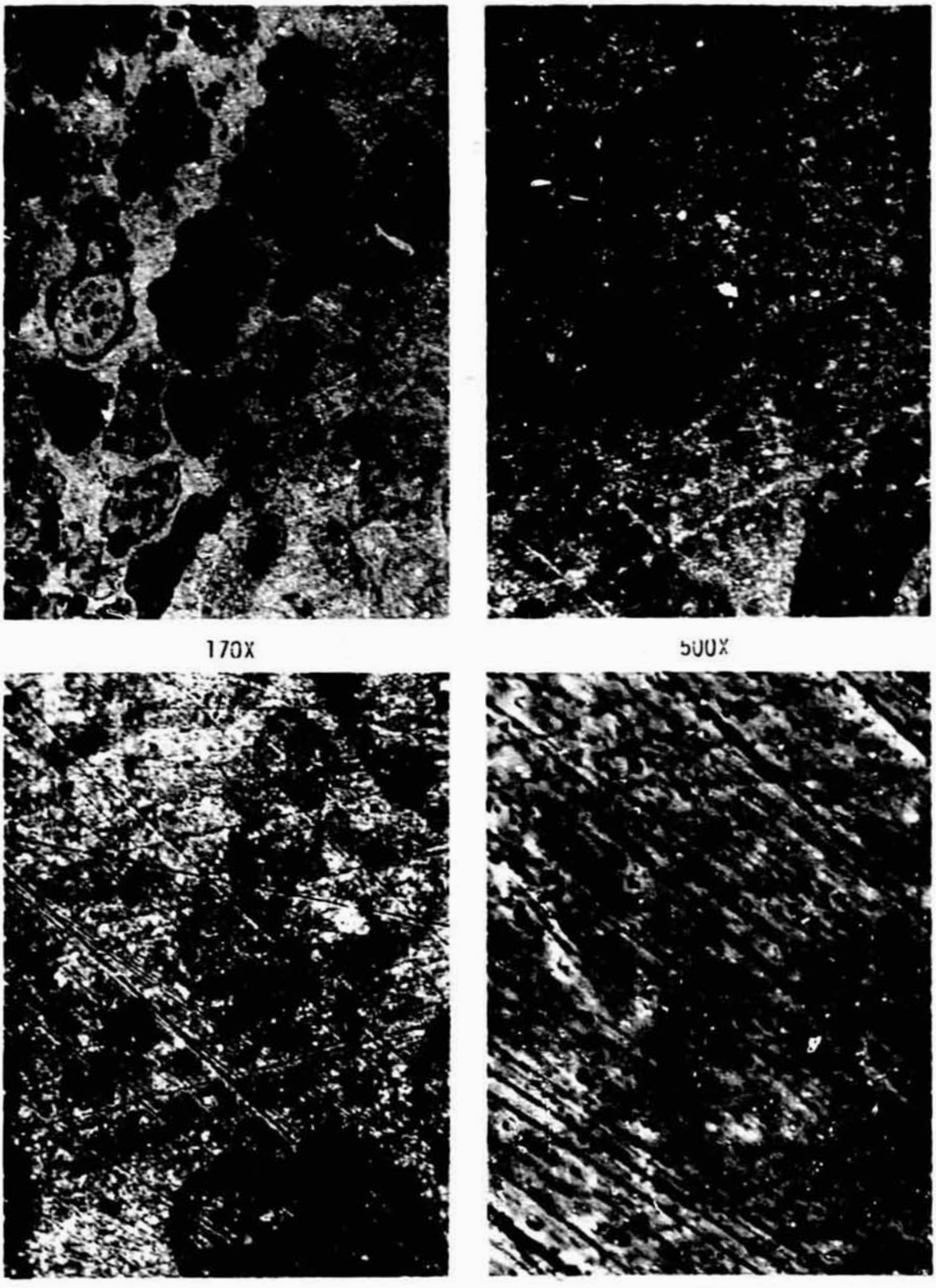

170X 500X

1000X 5000X

Figure 3-24. Scanning Electron Photomicrographs of Cadmium-Gallium Specimen No. CG-4 (0-g)

Figure 3-25. Electron Microprobe Photomicrographs of Cadmium-Gallium Specimen No. CG-4 (0-g) Magnification: 800X

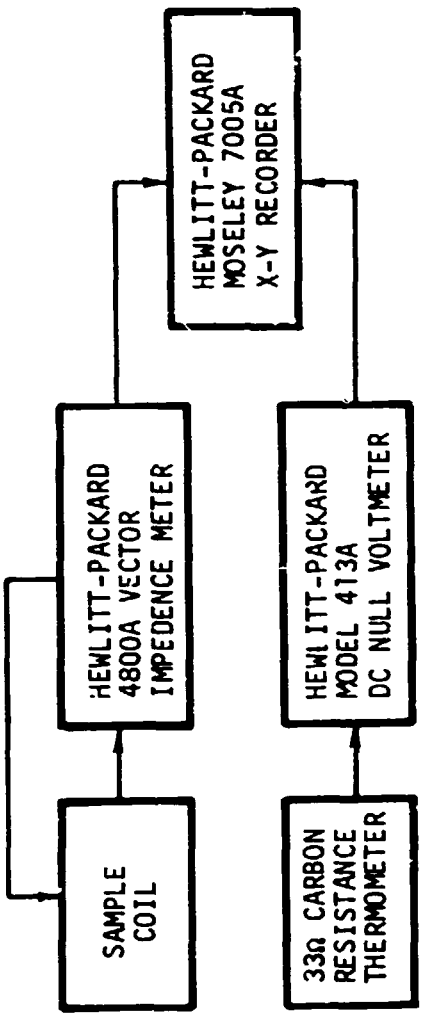

Figure 3-26 . Schematic Representation of Superconductivity Measuring Apparatus.

impedance bridge and the output voltage shift is plotted on an X-Y recorder along with the temperature. The temperature of each specimen was measured by recording the voltage drop across the resistor, generated by a constant current through the resistor. The average transition temperatures are considered to be accurate to ± 0.2K.

The temperature sweep from 4.2K and above was obtained by raising and lowering the sample platform containing the samples in the coils through the temperature gradient above the helium level, in a MVE model HLSM-60 cryostat. The results are shown in Table 3-6 and are discussed below.

3.4.2.1 Calcium-Lanthanum

As mentioned previously, lanthanum has two superconducting transition temperatures; 5.0K for the low temperature hexagonal structure and 6.3K for the higher temperature cubic structure [Reference 6]. Both of these transitions were detected, as well as a higher transition at 7.2K. The inductance change (i.e. T_c) versus temperature plot was very broad, resembling the broad-downward shift observed previously for lead [Reference 2]. Due to this phenomenon, the calculated volume percent of the superconducting portion is considered to have an accuracy of only ± 25%.

It is felt that all of the superconductivity is derived from the lanthanum since the two lower transition temperatures correspond to lanthanum. The high temperature β-La phase could have been frozen in by quenching and the higher than "normal" transition temperature measured has been accomplished previously in certain immiscible metal systems having at least one superconducting element present [References 2 and 3].

3.4.2.2 Cadmium-Gallium

The high (7.8K) T_c of this couple as contrasted to the low T_c's of the separate elements (0.56K for Cd, 1.09K for normal Ga) corroborate the findings for the Bi-Ga couple [Reference 2]. It would now appear to be conclusive that the gallium plays the dominating role in raising the transition temperature, although the ameliorating effect of the second element as mentioned in the Interim Report may play an important role. Due to the irregular shapes of the Cd-Ga specimens, again the calculated volume percent change is considered to be accurate only to ± 25%.

3.4.2.3 Aluminum-Bismuth

Neither the 50/50 or the 25/75 a/o Al/Bi specimens superconducted down to 3.0K. This corroborates at least partially that the matrix metal does not appear to play a dominating factor in enhancement of the superconducting transition temperature, although the processing parameters may have an effect on the electronic behavior of immiscible systems as mentioned in Reference 3 for the gold-germanium system.

Table 3-6. Superconducting Transition Temperatures of the Processed Specimens and the Volume Percent of the Superconducting Phase

Couple	Specimen No.	T_c, K	v/o Superconducting Phase	v/o Superconducting [a]
Ca-La (80/20 a/o)	CL-1 (1 g)	5.1 6.3 7.2	18 (La)	16 1.1 .2
Ca-La (80/20 a/o)	CL-3 (0 g)	5.1 6.3 7.2	18 (La)	17 1.0 .2
Cd-Ga (65/35 a/o)	CG-2 (1 g)	7.8	36 (Ga)	4
Cd-Ga (65/35 a/o)	CG-3 (0 g)	7.8	36 (Ga)	4
Cd-Ga (65/35 a/o)	CG-4 (0 g)	7.8	36 (Ga)	4
Al-Bi (50/50 a/o)	All	- [b]	- [c]	0
Al-Bi (25/75 a/o)	All	- [b]	- [c]	0

[a] Based on lead at 7.2K.
[b] Did not superconduct.
[c] Not calculated.

4.0 COOLING EXPERIMENTS

As a portion of this program, an attempt was made to measure the cooling rate of the drop tower tests samples and to create a universal computer program which could be used to compute and compare heat transfer rates.

4.1 EXPERIMENTAL SETUP FOR BI-GA CAPSULES

Cooling experiments on an instrumented Bi-Ga cartridge were conducted using the simulated drop tower quench apparatus. Actual processing and sequencing conditions utilized at MSFC were duplicated as closely as possible. Three channels of information were recorded during each test: inner cartridge temperature, outer cartridge temperature and valve actuation/deactuation times. The data acquisition system enables raw analog data from the thermocouples and valve to be recorded simultaneously on the same record in both analog and digital form. This system was developed for high temperature transient thermal shock testing and, consequently, has more than adequate response characteristics for the flow apparatus. Figure 4-1 is a functional block diagram of the data acquisition system and test configuration. All inputs to the system are fed through an input board, with up to eight input amplifiers utilized as required. The analog signals are routed directly to the multiplexer which commulates the signals, synchronized by the numeric function generator, which are then fed to the analog-to-digital (A/D), binary-coded decimal (BCD) converted for processing. The A/D converter is triggered by the multiplexer with a synchronizing pulse when a conversion is to be made. Multiplexer output channel 1 is a "clock read command" signal which causes the elapsed time digital clock to furnish time signals to the BCD-to-decimal converter and gates off the A/D converter output. The A/D converter output is fed through the clock circuitry at all other times. The timekeeping cycle is continuous even during actual clock readout so that no elapsed test time is lost on the oscillograph printout.

The test sequence was as follows: (1) The test temperature is dialed in on the thermal controller regulating the heater power supply (12 VDC at 6A maximum), (2) after reaching the test temperature and stabilization, a 15-minute soak time is initiated, (3) ice water is pumped into the water

tank 3 minutes prior to flow, (4) the water tank is then pressurized to 2.4 M Pa (350 psig) with argon, (5) the pilot valve is pressurized to 689 k Pa (100 psig) with air, (6) the test is then initiated by manually turning on the chart (1.62 m/sec [64 in/sec]), (7) one second later the delay circuit is initiated, (8) the heaters are turned off and the valve solenoid power activated ~ 160 msec later and (9) the test manually terminated 6 seconds later. For the very low flow rates, re-thermalization after test termination was monitored for 400 seconds to determine if any problems would exist during retrieval of the package from the catch tube at MSFC.

The results of nine out of twelve runs are presented in Table 4-1 and the reduced data is shown in Figures 4-2 through 4-6. Except for run 1, the data for runs 2 through 4 correlate relatively well with the previous results from the drop tests at MSFC. The flow rates on the simulated test apparatus are higher (~ 25%) than the drop apparatus at MSFC and the indicated cooling rates are lower, probably due to taking 100°C as the lower temperature in order to include runs 11 and 12. The anomalies in run 1 may be due to the method of supplying valve power; this was subsequently changed so as to eliminate inductive surges on the valve open signal (VOS) which may have impacted the water flow (WF) time for that run. Examination of the time-temperature run profiles, however, show that the shape of the curve is essentially the same within each orifice run.

Runs 5 through 7 were made with a 50 percent flow area reduction. These runs were virtually identical with runs 1 through 4, including the flow rate. Discussions with various fluid mechanics specialists indicated that these inserts were probably decreasing turbulence and flow restrictions in the experiment inlet and thus increasing the efficiency of the apparatus even though the flow area was reduced.

The figures have the consolute, the first monotectic (Bi solidification) and the Ga solidification temperatures indicated. As can be seen, the solidification halts correspond closely to the Bi and Ga halts. The temperatures are estimated to be accurate to ± 2°C from calibration tests. The apparent temperature excursions are probably caused by local convection cells set up by the temperature differentials and indicate unequal

cooling in the cartridge. Since this is gravity dependent, it was felt that an orifice restriction which gave a temperature reduction to 200°C at two seconds would be within the test design goal that the first monotectic temperature (220°C) would be reached throughout the sample at 3.5 seconds and that re-thermalization would not be a problem. Thus the 0.12 cm (.046 in) orifice size is considered to be optimal if the predicted slower cooling rate during a low gravity drop is correct. A set of six heater/experimental cartridge packages with the orifice inserts were fabricated and delivered to MSFC.

4.2 THERMAL ANALYSIS

A generalized time-share computer program was written in order to calculate the heat transfer coefficient and cooling times for different sample materials, geometrics and heat transfer modes. Figure 4-7 is a flow diagram sequence of the computer program. The only required manual input is for Biot numbers greater than 0.05, in which case the Fourier number must be obtained from Heisler charts [Reference 11]. It is estimated that at least a five-fold reduction in thermal computation time is achieved by using this program. The complete computer program, required inputs and assumptions and solved heat transfer examples for every mode within the program are given in Appendix C. A punched tape of the program (which is programmed in Basic) has been delivered to MSFC.

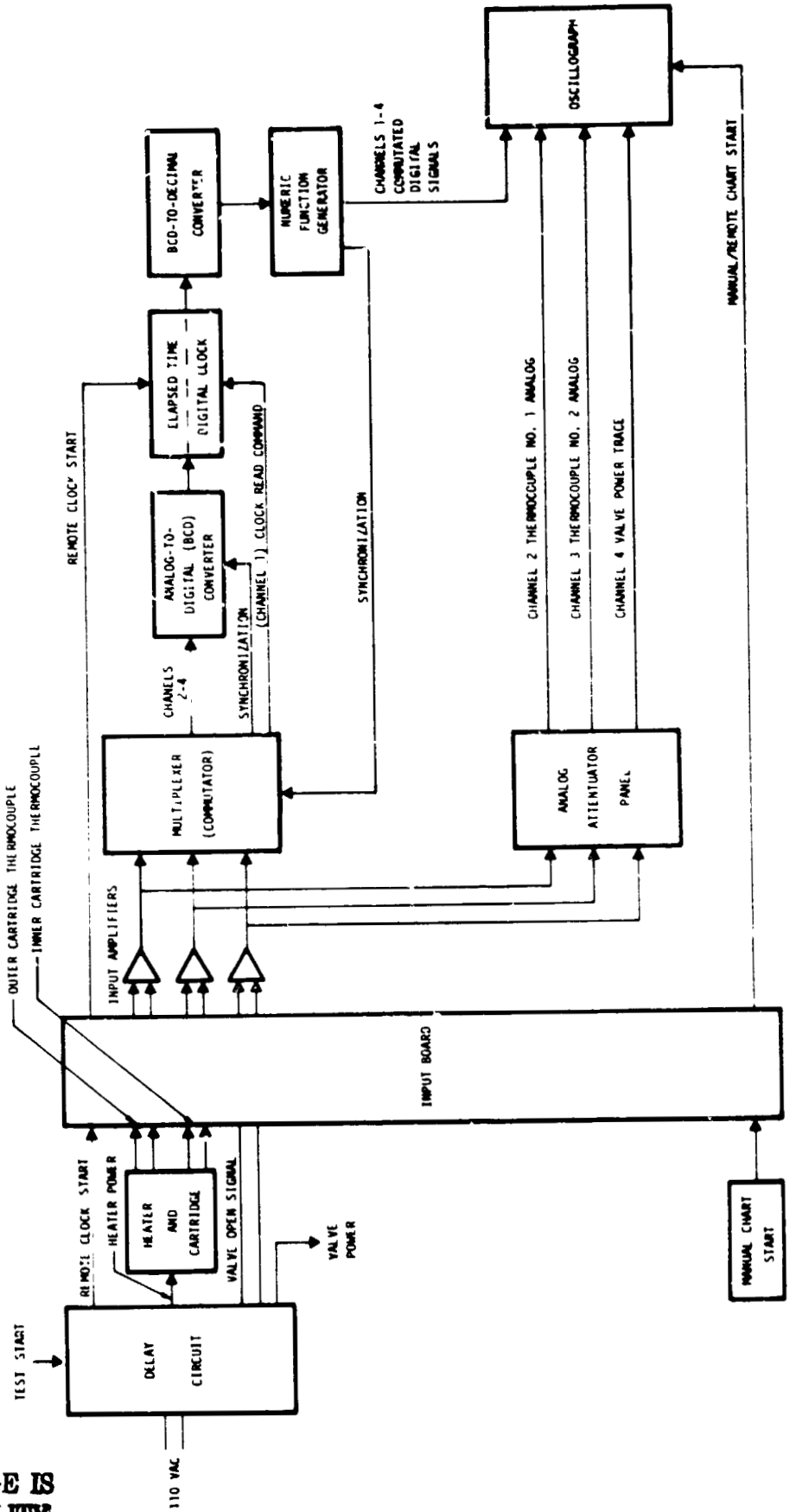

Figure 4-1. Block Diagram of Data Acquisition System and Test Configuration

ORIGINAL PAGE IS
OF POOR QUALITY

Table 4.1. Test Data from S ~ulated Flow Runs

RUN NO.	ORIFICE SIZE CM	ORIFICE SIZE IN.	INITIAL TEMPERATURE, °C OUTER	INITIAL TEMPERATURE, °C INNER	FINAL [a] TEMPERATURE, °C OUTER	FINAL [a] TEMPERATURE, °C INNER	FLOW RATE mℓ/sec	TEMPERATURE RATE [b] OF CHANGE, °C/sec INDICATED	TEMPERATURE RATE [b] OF CHANGE, °C/sec ACTUAL
1	1.27	0.5	276	275	14	26	1132	4400	188
2	1.27	0.5	307	302	10	26	1282	4640	326
3	1.27	0.5	351	351	7	21	1248	5100	323
4	1.27	0.5	404	400	9	17	1295	6080	375
8	0.32	0.125	350	349	5	21	303	2800	156
9	0.17	0.0675	349	345	5	17	87	792	160
10	0.17	0.0675	405	400	16	18	89	503	173
11	0.12	0.046	358	352	29	48	44	206	112
12	0.12	0.046	409	404	26	34	45	352	149

[a] At 3.5 seconds

[b] To 100°C

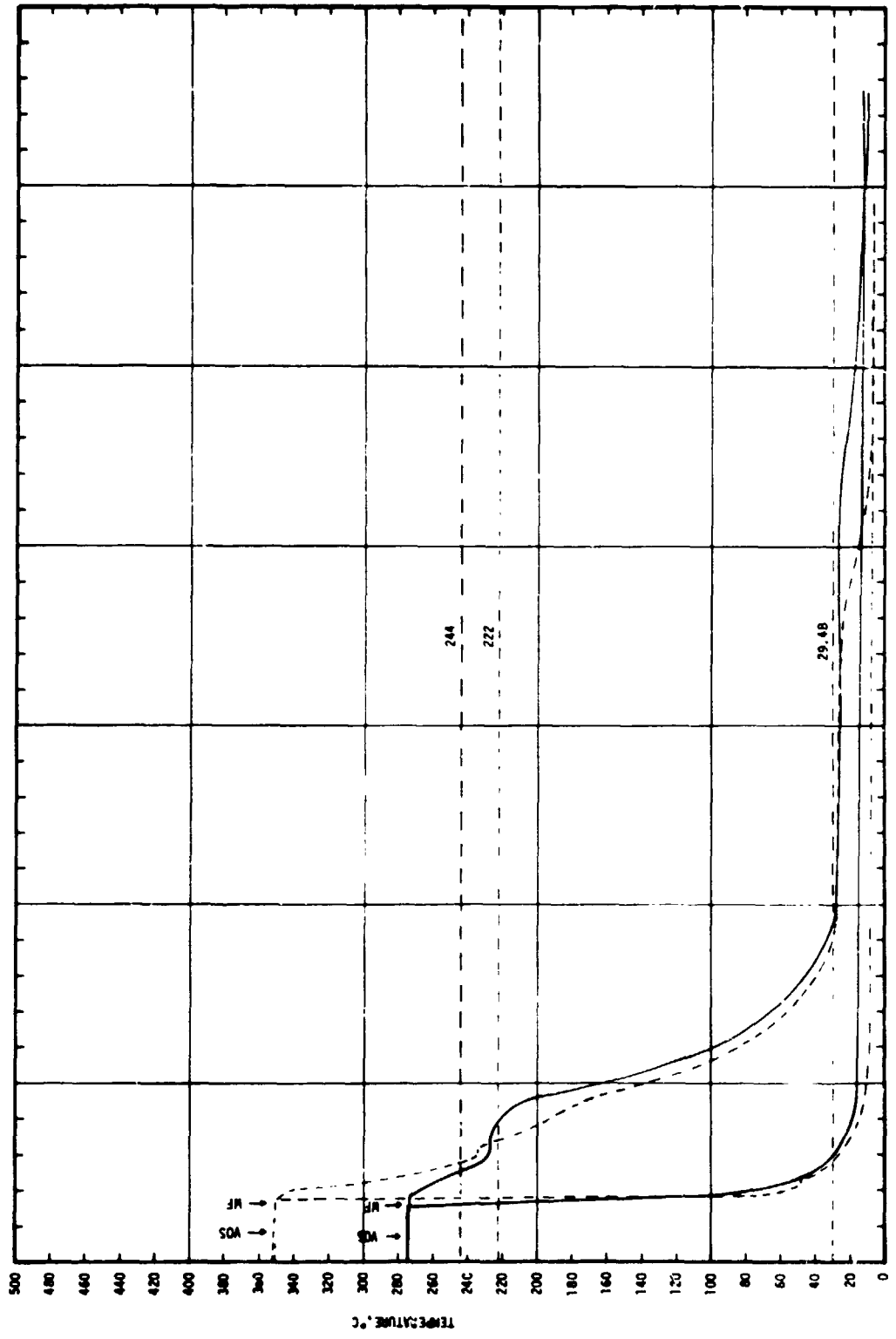

Figure 4-2. Time - Temperature Profiles for Runs 1 and 3.
(VOS = Valve open signal, WF - water flow)

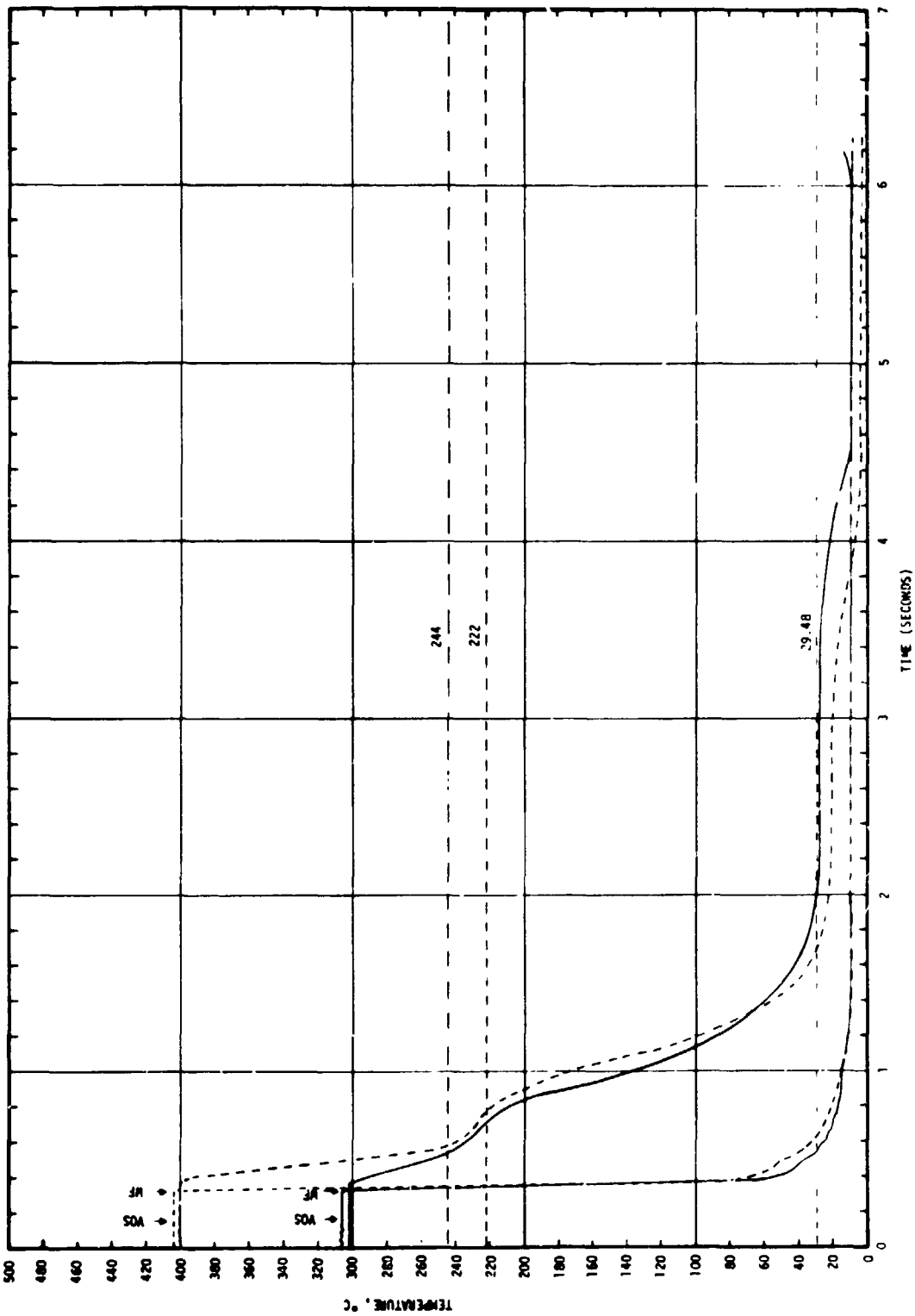

Figure 4-3. Time - Temperature Profiles for Runs 2 and 4.
(VOS = Valve open signal, WF = water flow)

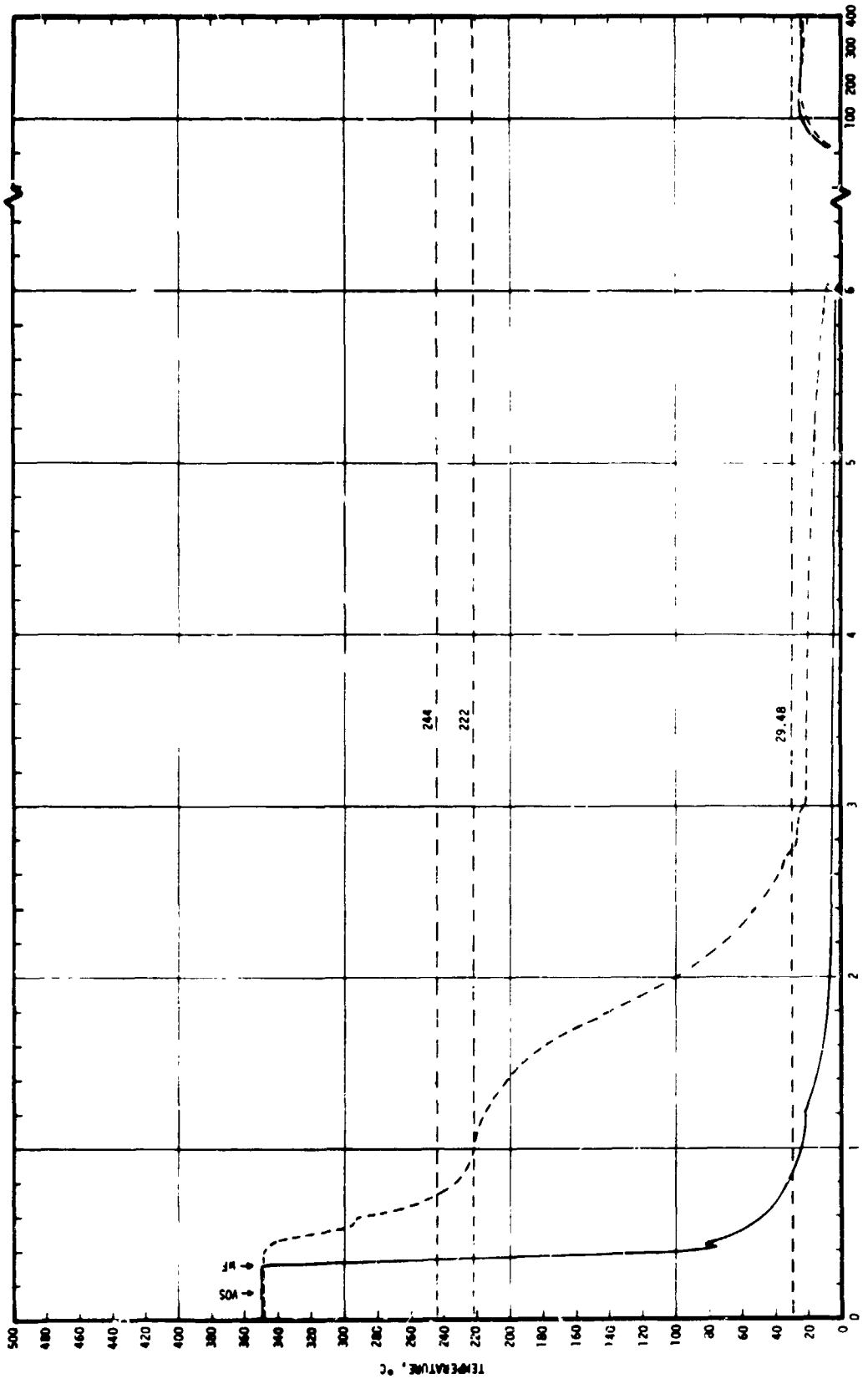

Figure 4-4. Time - Temperature Profiles for Run 8.
(VOS = Valve open signal, WF = water flow)

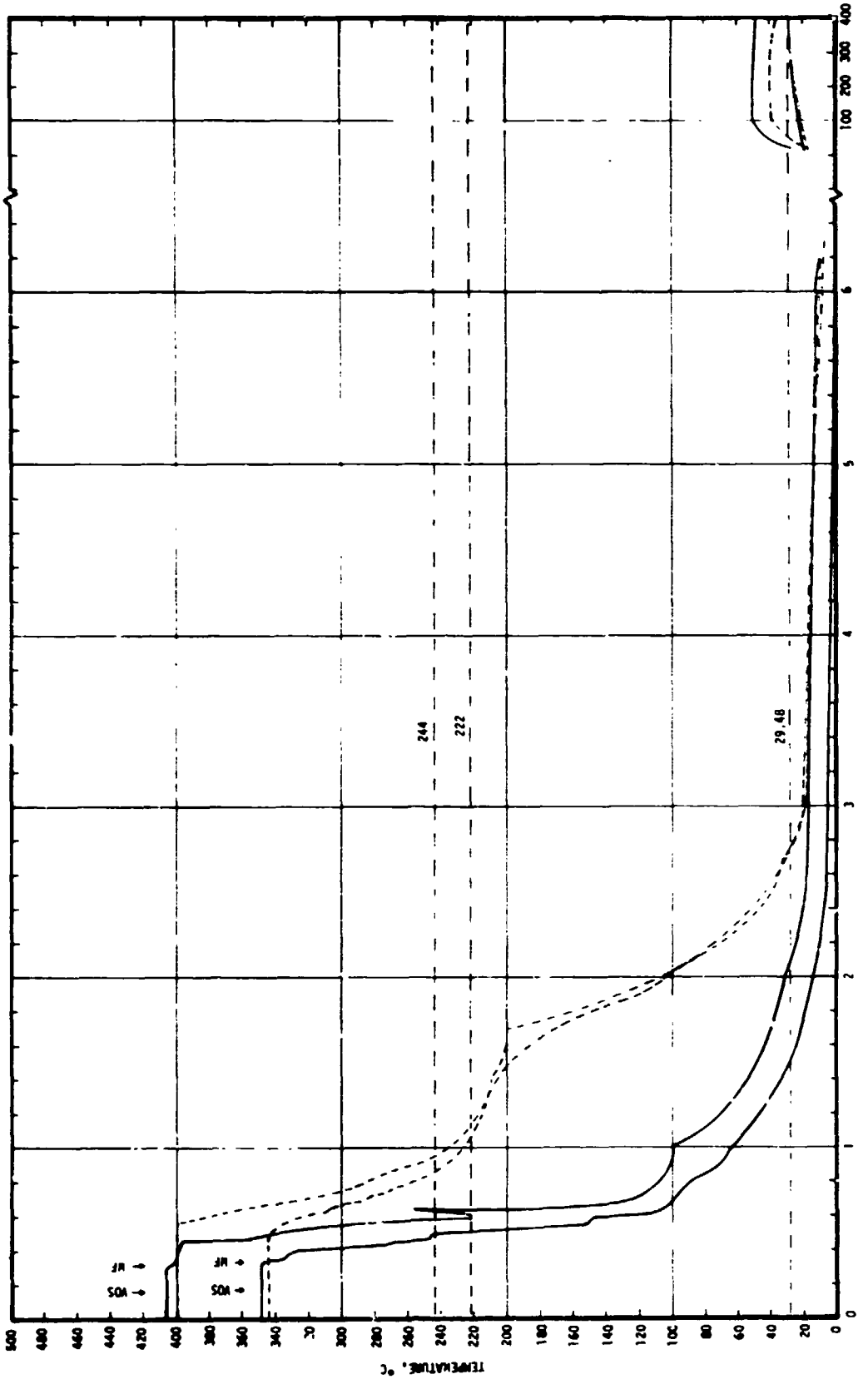

Figure 4-5. Time - Temperature Profiles for Runs 9 and 10.
(VOS = Valve open signal, WF = water flow)

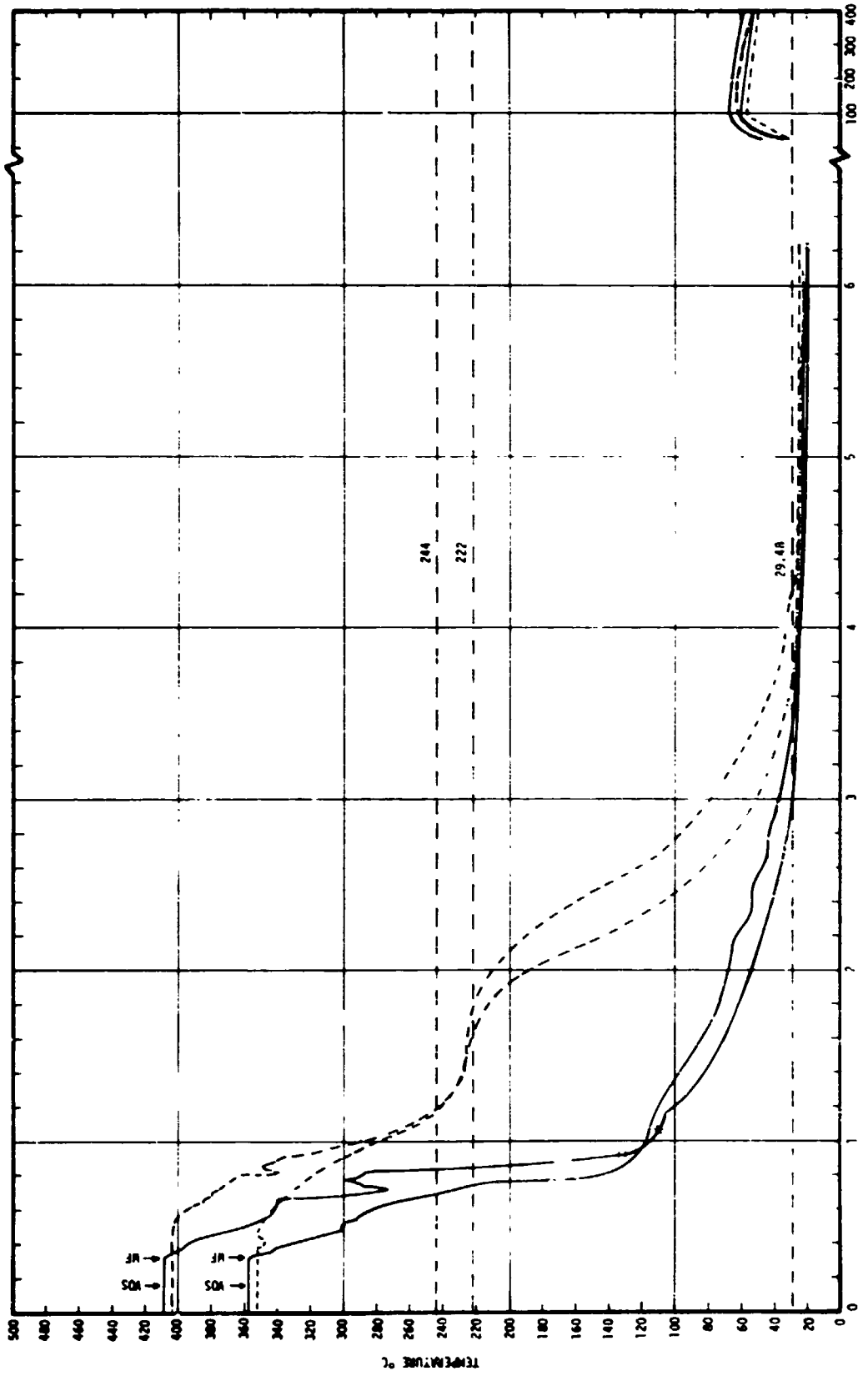

Figure 4-6. Time - Temperature Profiles for Runs 11 and 12.
(VOS = Valve open signal, WF = water flow)

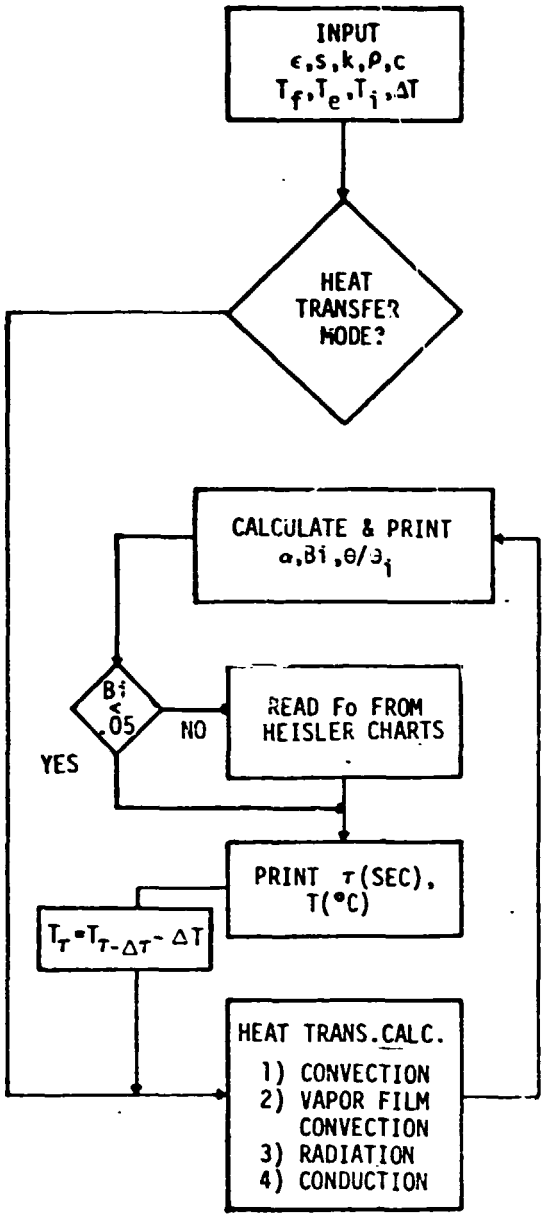

SYMBOL EXPLANATION

ϵ = EFFECTIVE SAMPLE EMISSIVITY

T = TEMPERATURE OF SAMPLE AT TIME τ

T_i = INITIAL TEMPERATURE

T_e = ENVIRONMENT TEMPERATURE

T_f = FINAL TEMPERATURE

s = SAMPLE GEOMETRY AND DIMENSIONS

k = EFFECTIVE SAMPLE THERMAL CONDUCTIVITY

ρ = EFFECTIVE SAMPLE DENSITY

c = EFFECTIVE SAMPLE SPECIFIC HEAT

α = EFFECTIVE THERMAL DIFFUSIVITY = $\frac{k}{\rho c}$

Bi = BIOT NUMBER = $\frac{Hs}{k}$

$\frac{\theta}{\theta_i} = \frac{T-T_e}{T_i-T_e}$

Fo = FOURIER NUMBER = $\frac{\alpha\tau}{s^2}$

τ = TIME

H = h_o = EQUIVALENT HEAT TRANSFER COEFFICIENT

FIGURE 4-7. Flow Chart for Computing Equivalent Heat Transfer Coefficient and Cooling Times for Various Heat Transfer Modes.

5.0 ADDITIONAL EXPERIMENTAL TASKS

At the request of NASA/MSFC, additional experiments not explicit in the work statement of the subject contract but within the general scope of immiscible materials were performed.

5.1 COPPER-LEAD ALLOYS

A series of copper-lead alloys (minimum purity: 99.99 w/o parent metal) utilizing the method as outlined by the patent issued to Carl E. Bazley [Reference 12] were prepared. Eight sets of copper-lead alloys were prepared; four with and four without the additive. In addition, one extra alloy with additive was made and recast in quartz container surrounded by sand.

The alloy compositions were (in weight percent ratios): 80/20, 70/30, 60/40 and 50/50 Cu/Pb, respectively. The recast specimen was 80/20 Cu/Pb. The method outlined in the patent was followed in general: (1) The copper was induction melted and heated to 1260°C (2300°F) in a carbon crucible with a borax protective covering under argon, (2) at this point, the melt temperature was lowered slightly and the lead added, (3) the melt reheated to 1260°C and (4) the lead sheathed additive added (to the indicated samples). The temperature was held at 1260°C and except for one sample, the melt allowed to cool under argon until solidification occurred. The one sample was reheated to 1260°C and immediately cast. Except for step (4), the same procedures were followed for the samples without the additive.

All eight samples were broken out of the mold and cut axially (parallel to the gravity gradient). One side was mounted and polished and the other reserved for shipment to MSFC.

The additive comprised aproximately one percent of the total copper-lead weight. One potential deviation from the patent was the use of copper pyrophosphate [$Cu_2 P_2O_7 .3H_2O$] instead of copper phosphate [$Cu_3 (PO_4)_2.3H_2O$] in the additive. Thus, the equal weight of each part of the additive (NaCl + copper phosphate) was recalculated on the equivalent molar basis of sodium and copper.

Figures 5-1 through 5-11 show the macro and microstructure of each of

the TRW prepared samples, as well as a sample received from MSFC which had been prepared by the corporation holding the patent. Inasmuch as the majority of the samples contained inhomogeneities, general area photomicroscopy was employed, i.e. the trend toward segregation or other anomalies were noted. Considerable difficulty was encountered in obtaining standard lighting for all specimens due to the polished condition of the copper.

Several tentative conclusions were noted:

1. All of the specimens containing the additive tended toward a more uniform structure than the "pure" alloy compositions.
2. Remelt seems to improve the homogeneity of the dispersion -- Figure 5-2 presents fewer photomicrographs because the microstructure was relatively uniform throughout the sample (gravity down on flat surface of the 2.5X magnified photomacrograph of the sample facing the bottom of page).
3. Free convection cooling was somewhat faster than anticipated; thus, the "pure" alloys did not totally segregate. The patent states that slower cooling rates improves the homogeneity of the alloys with additives.
4. The NASA supplied sample appears to be within the 60/40 w/o Cu/Pb compositional range in comparison with the TRW processed specimens.
5. Based on microscopic examination, the NASA supplied specimen exhibited more coring than the TRW specimens. It is not known if the casting size, the pour or mold temperature or other factors, significantly contribute to this phenomena.
6. It would appear that, as the amount of lead in the specimen is increased, the amount of additive should be proportionately larger. The patent gives a range of one to four weight percent for alloys containing from one to not more than fifty weight percent of lead.

In an effort to determine the dispersing mechanism of the additive, the specimens were examined by scanning electron microscopy and electron microprobe analyses. The scanning electron microscope did not show any anomalies other than those noted optically. By setting the electron microprobe detectors on phosphorus and sodium excitation wavelengths, very faint (just above the threshold level) sodium signals were detected in the lead at the lead-copper interface. No phosphorus or sodium was detected in

the copper. Thus, the mechanism of the additive appears to be similar to a surfactant: The additive "emulsifies" the copper-lead and stabilizes the mixture. This assumption is corroborated somewhat by the tendency of the lead to spheroidize in the 60/40 and 50/50 w/o Cu-Pb alloys and the interesting duplex structures found in the 50/50 w/o Cu/Pb alloy (Figure 5-12). This, of course, raises the interesting speculation that other immiscible systems may be capable of being dispersed by the addition of inorganic "surfactants." Semenchenko [Reference 13] describes the action of impurity metals on other metals with respect to their surface tension in terms of "active" or "inactive" influence: For lead, sodium is active (p. 414). Although investigations of this type are outside the scope of this contract, it is suggested that some attention be paid to this type of experimental and/or theoretical aspect on the behavior of immiscible sytems.

5.2 LEAD-ZINC

TRW fabricated five 20/80 a/o Pb/Zn cartridges for processing in the MSFC drop tower. These cartridges were produced to augment the ASTP Pb/Zn experiment in terms of microstructure, process temperatures and initial property data on the system. The cartridge containers were identical to those manufactured for the acoustic mixer, discussed in Section 3.0, and were processed using the acoustic heater without energizing the acoustic mixer.

5.3 BISMUTH-GALLIUM

From the previous work and with concurrence with NASA/MSFC, six experimental cartridges containing 50/50 a/o Bi-Ga and heater packages were fabricated and shipped to MSFC for processing in the drop tower. These cartridges are identical in composition and fabrication to the Bi-Ga experiments processed previously and the experiment is to determine if aging affects the superconducting transition temperature or amount of superconducting material present. In addition, experiments were conducted using 50/50 a/o Bi-Ga cartridges and longer cooling times as discussed in Section 4.0. Using the data obtained from the cooling experiments, six additional heater/experimental cartridge packages with 0.12 cm (.046 in) orifice openings were fabricated and sent to MSFC. After processing, the

capsules were returned to TRW for sectioning and scanning electron microscope photomicrographs of the dispersion of gallium in bismuth. After the sectioning and photography were complete, the specimens were returned to MSFC for analysis. Table 5-1 shows the time-temperature-gravity telemetry data obtained for these specimens and also submitted to MSFC.

Table 5-1. Telemetered Drop Tower Results from Bismuth-Gallium Cooling Experiment

	B-5[a]	C-6[a]	E-4[a]	F-9[a]	D-2[a]	J-12[b]	K-13[b]	G-10[b]	H-11[b]	L-14[b]
Initial Drop Temp. °C	325	328	336	313	324	316	320	318	315	349
Final Drop Temp. °C	43	38	34	32	33	48	40	36	36	37
Initial Temp. Indicated Rate of Change, °C/Sec	2950	954	3371	1920	2550	219	209	452	236	279
Indicated Total Temp. Rate of Change, °C/Sec	240	217	667	187	181	107	88	140	78	109
Gravity Level During Drop	1	-.005	-.005	-.002	-.003	1	-.005	-.005	-.004	-.004

[a] Unrestricted flow

[b] Restricted flow (0.12 cm orifice)

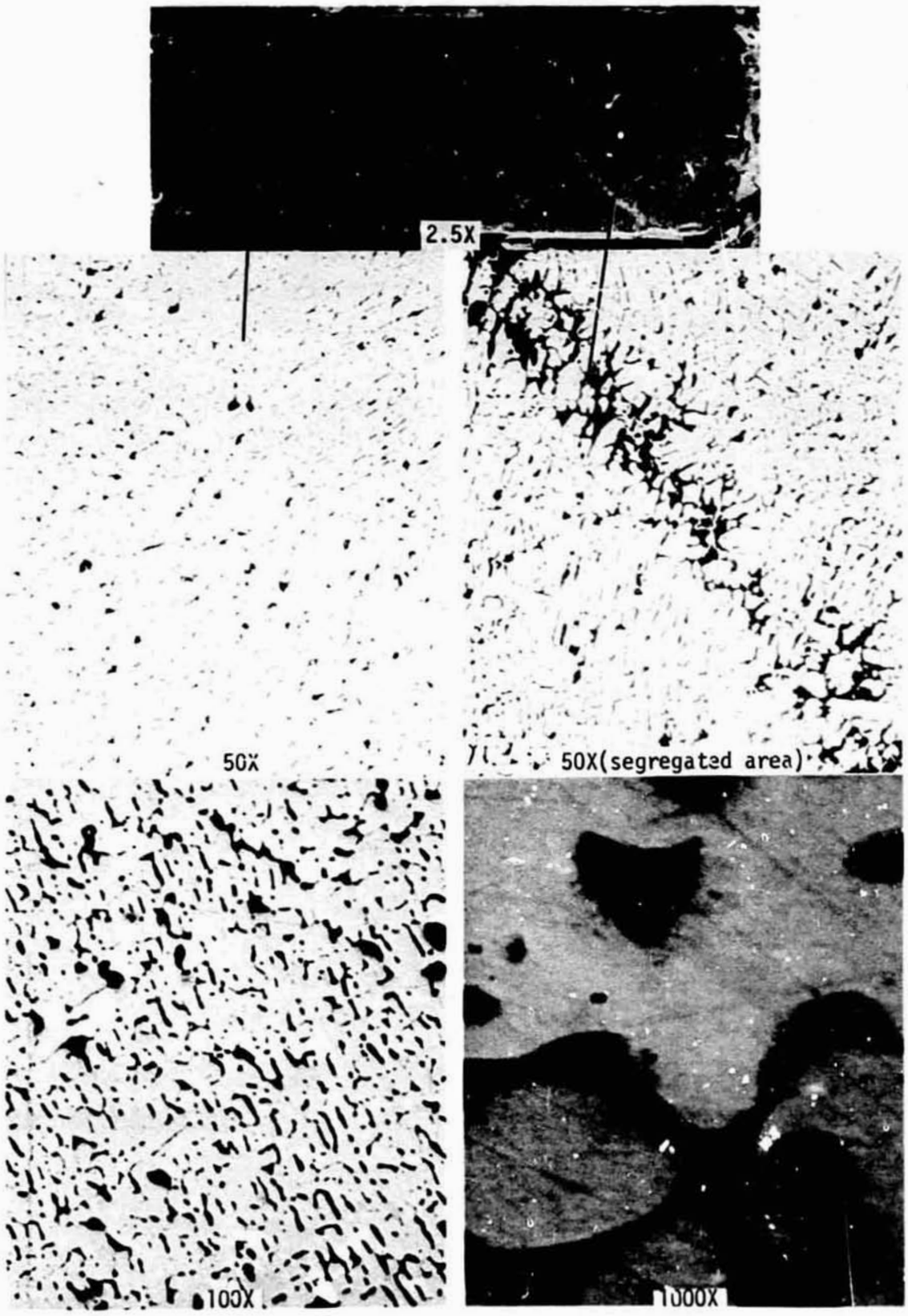

Figure 5-1. 80/20 w/o Cu/Pb with Additive at Various Magnifications

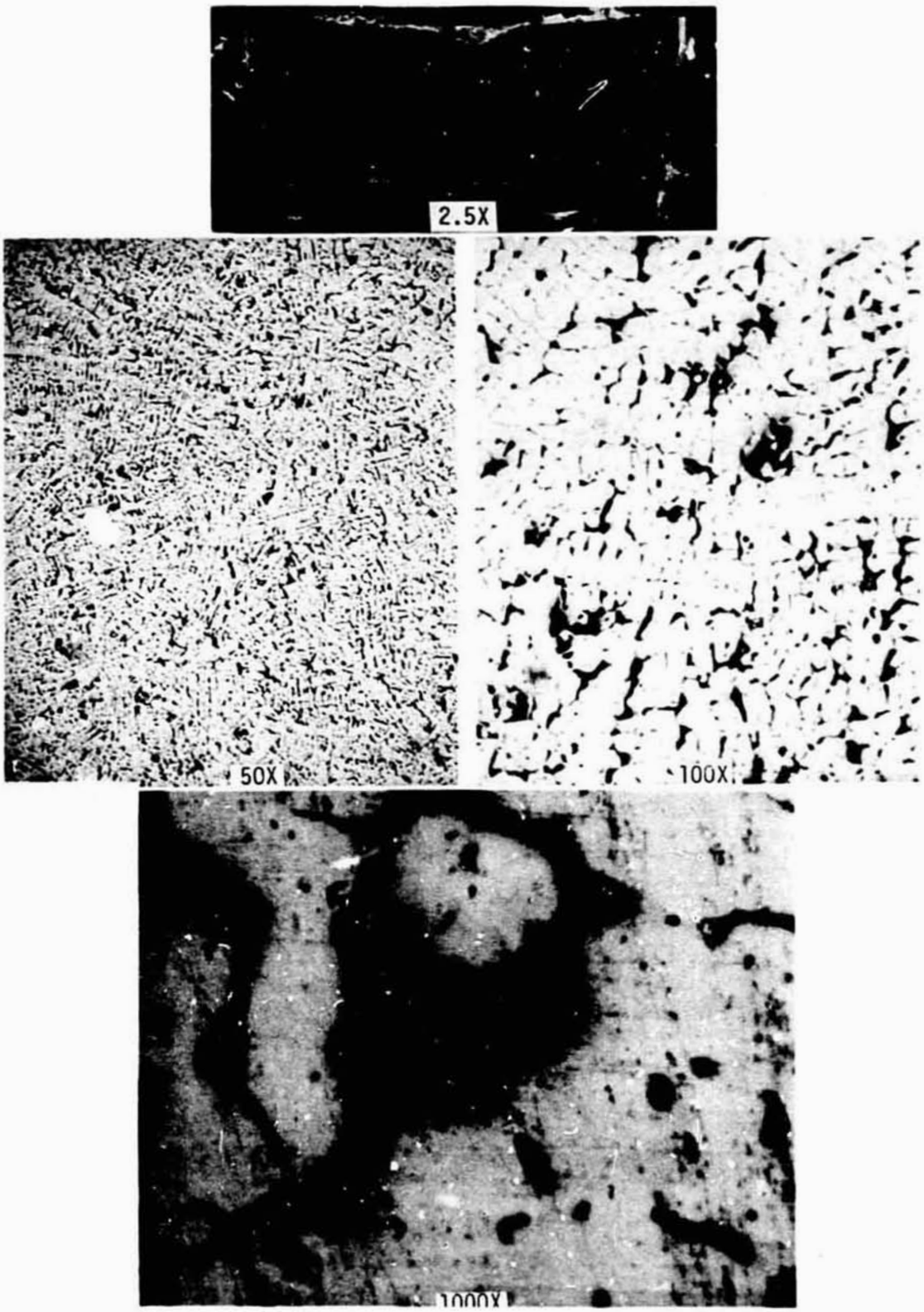

Figure 5-2. Remelted 80/20 w/o Cu/Pb with Additive at Various Magnifications

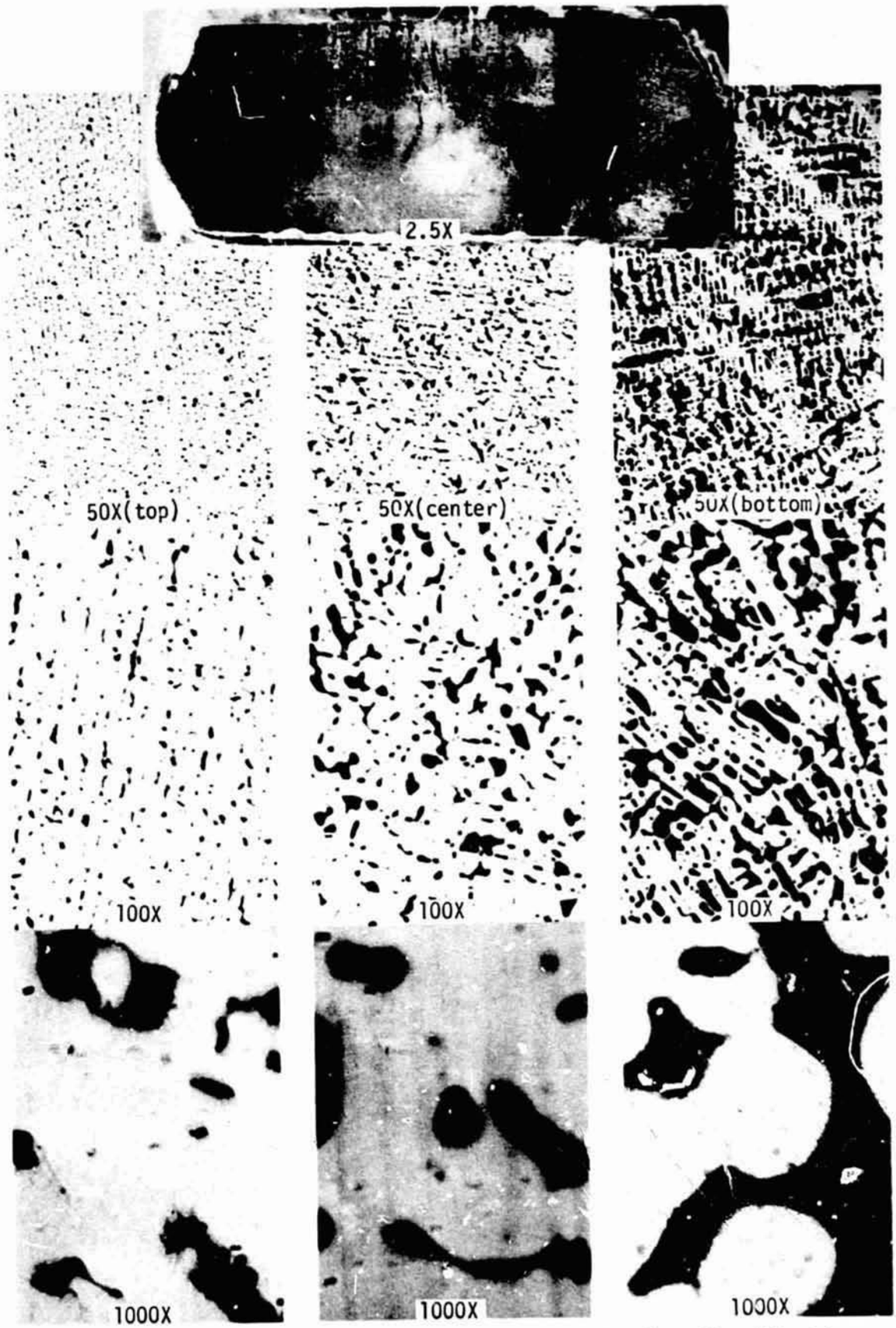

Figure 5-3. 80/20 w/o Cu/Pb without Additive at Various Magnifications

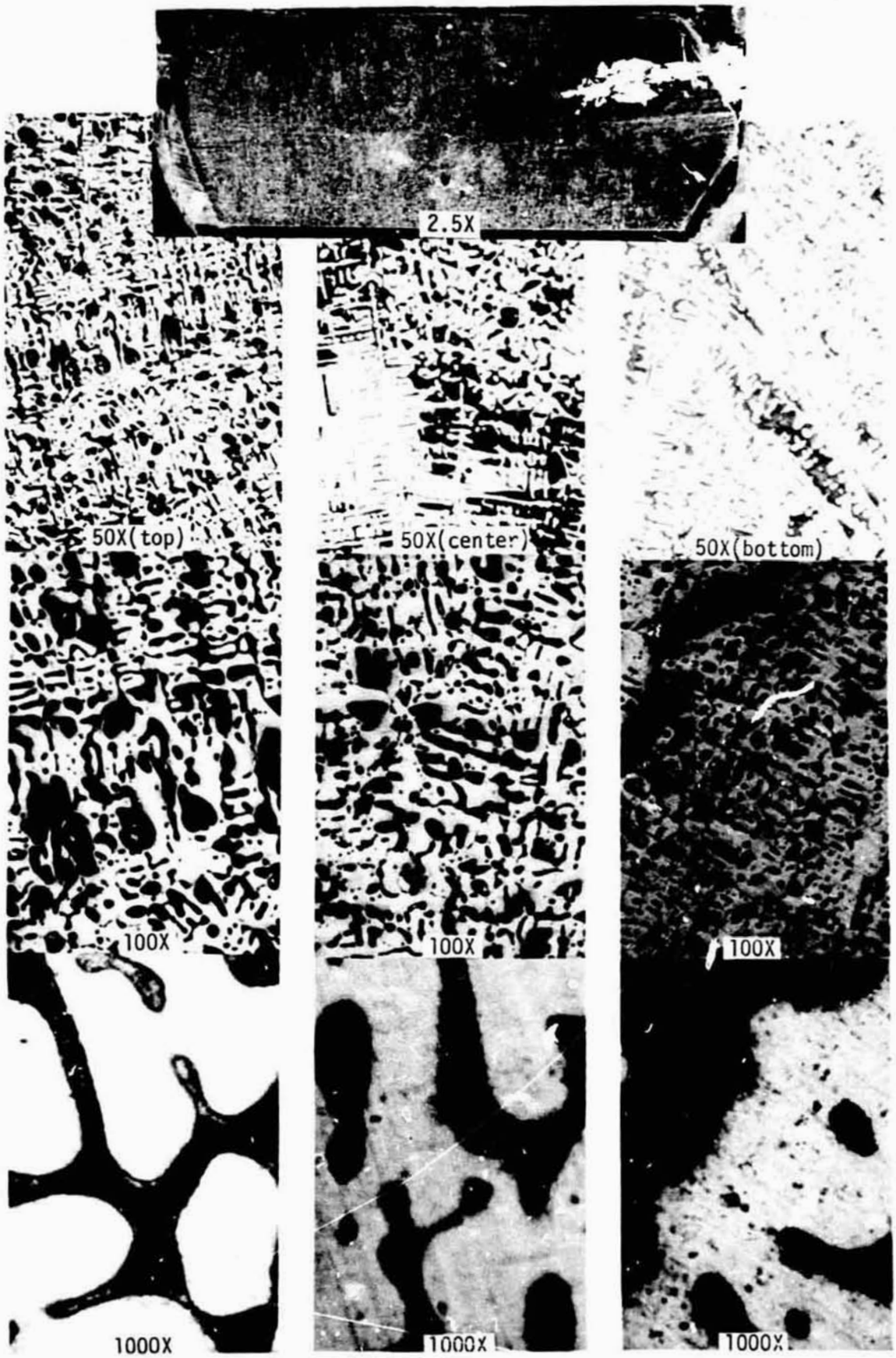

Figure 5-4. 70/30 w/o Cu/Pb with Additive at Various Magnifications

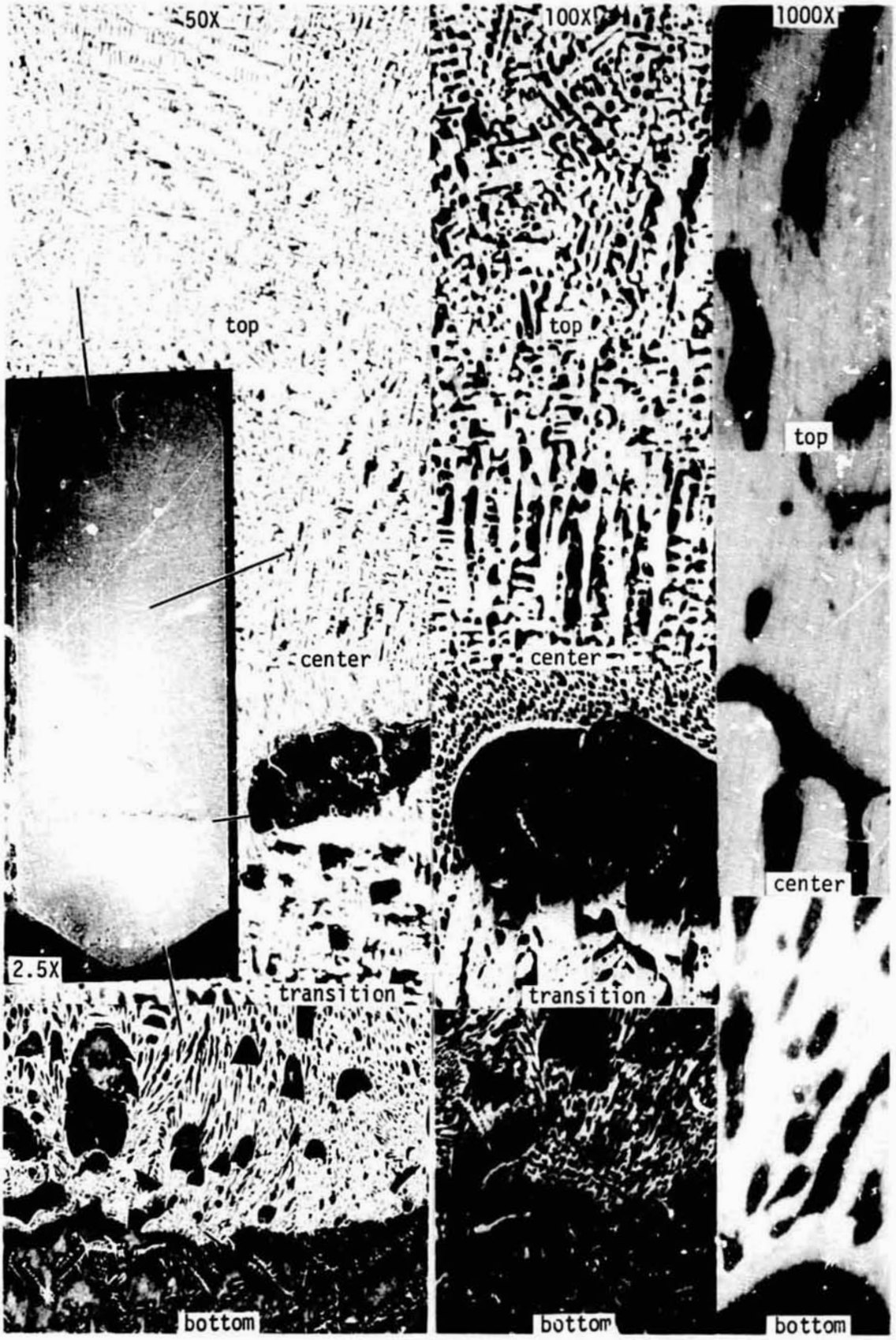

Figure 5-5. 70/30 w/o Cu/Pb without Additive at Various Magnifications

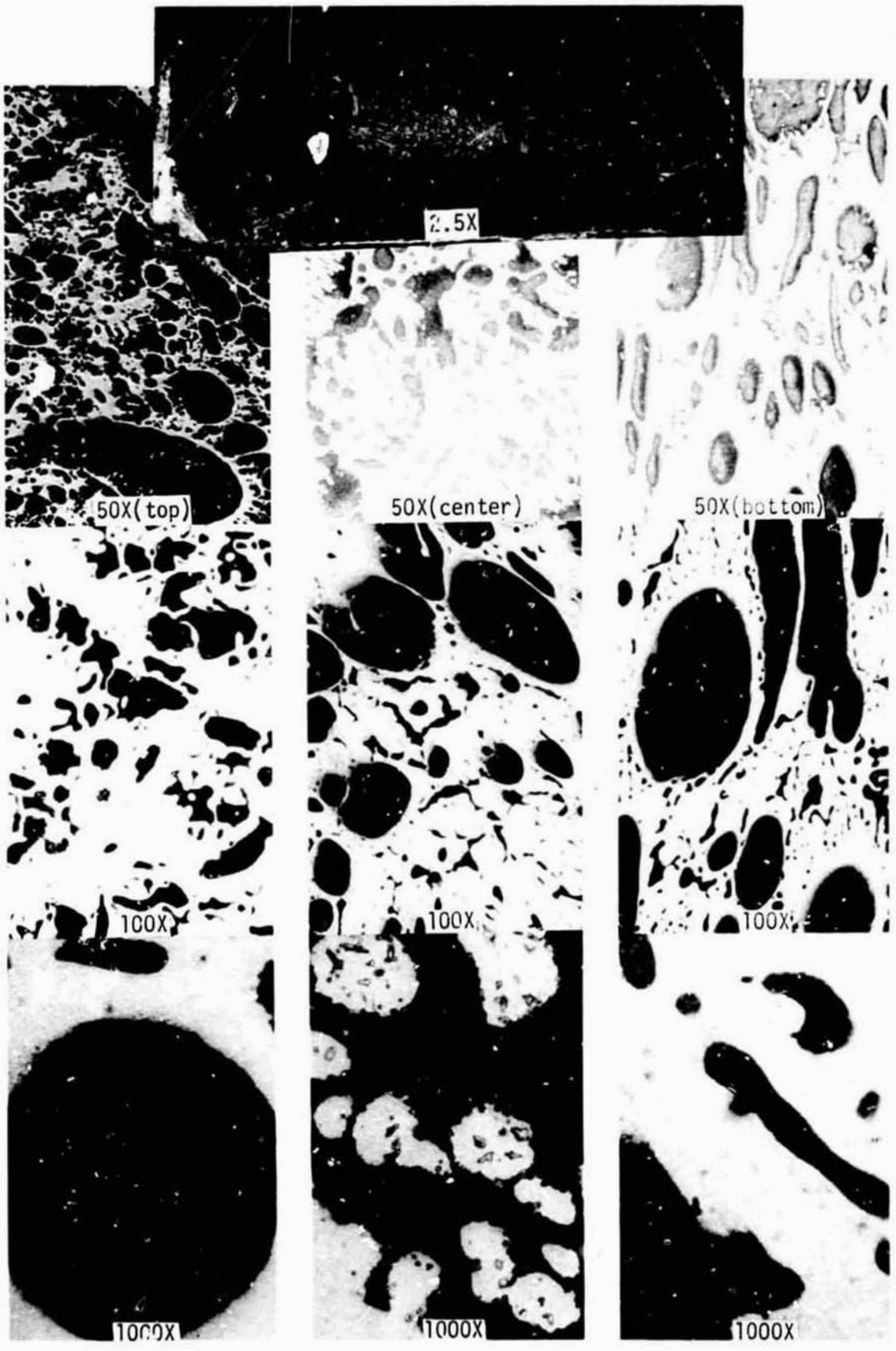

Figure 5-6. 60/40 w/o Cu/Pb with Additive of Various Magnifications

Figure 5-7. 60/40 w/o Cu/Pb without Additive at Various Magnifications

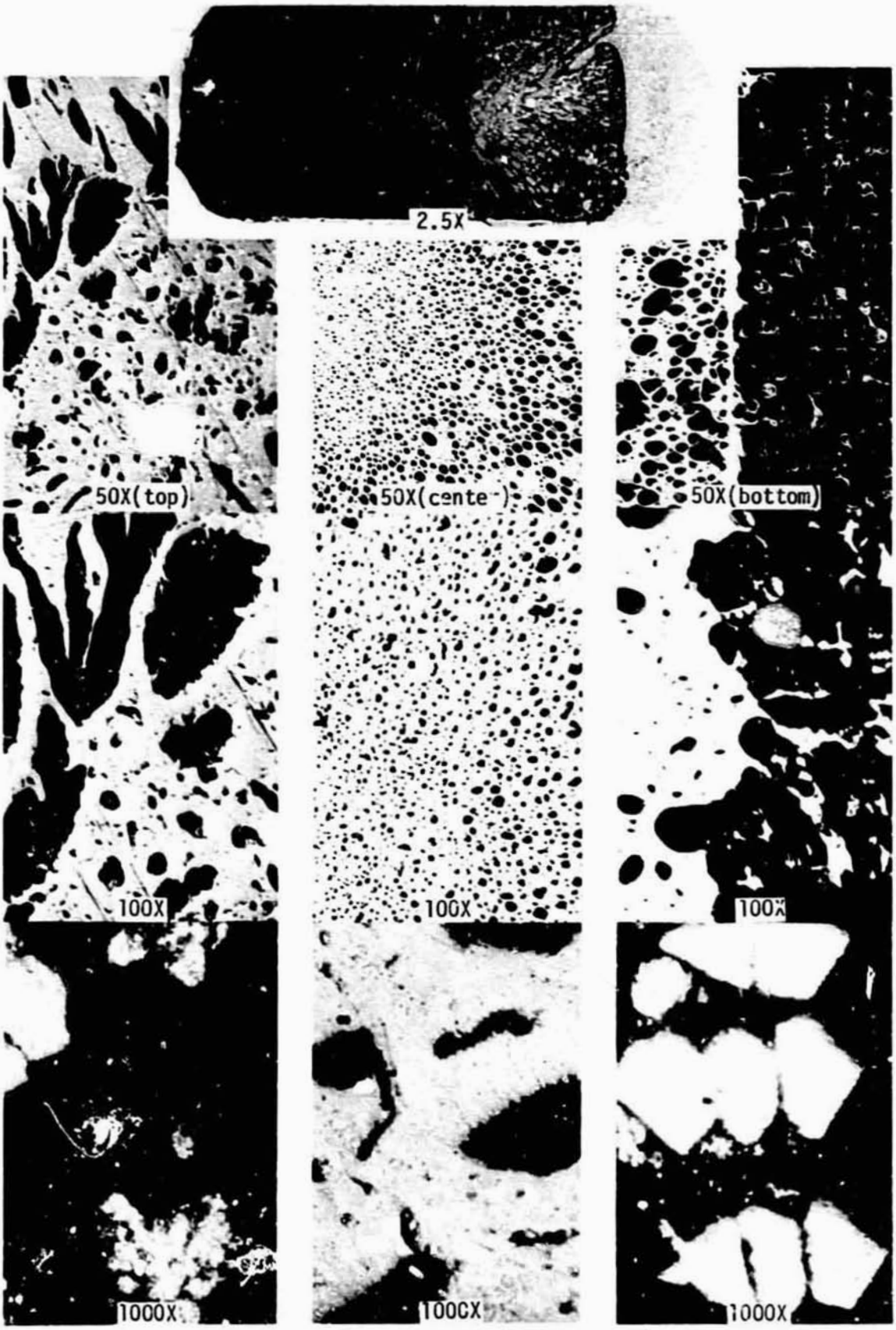

Figure 5-8. 50/50 w/o Cu/Pb with Additive at Various Magnifications

Magnification: 500X

Magnification: 600X

Figure 5-9. Photomicrographs of Duplex Dispersions in 50/50 w/o Cu/Pb with Additive

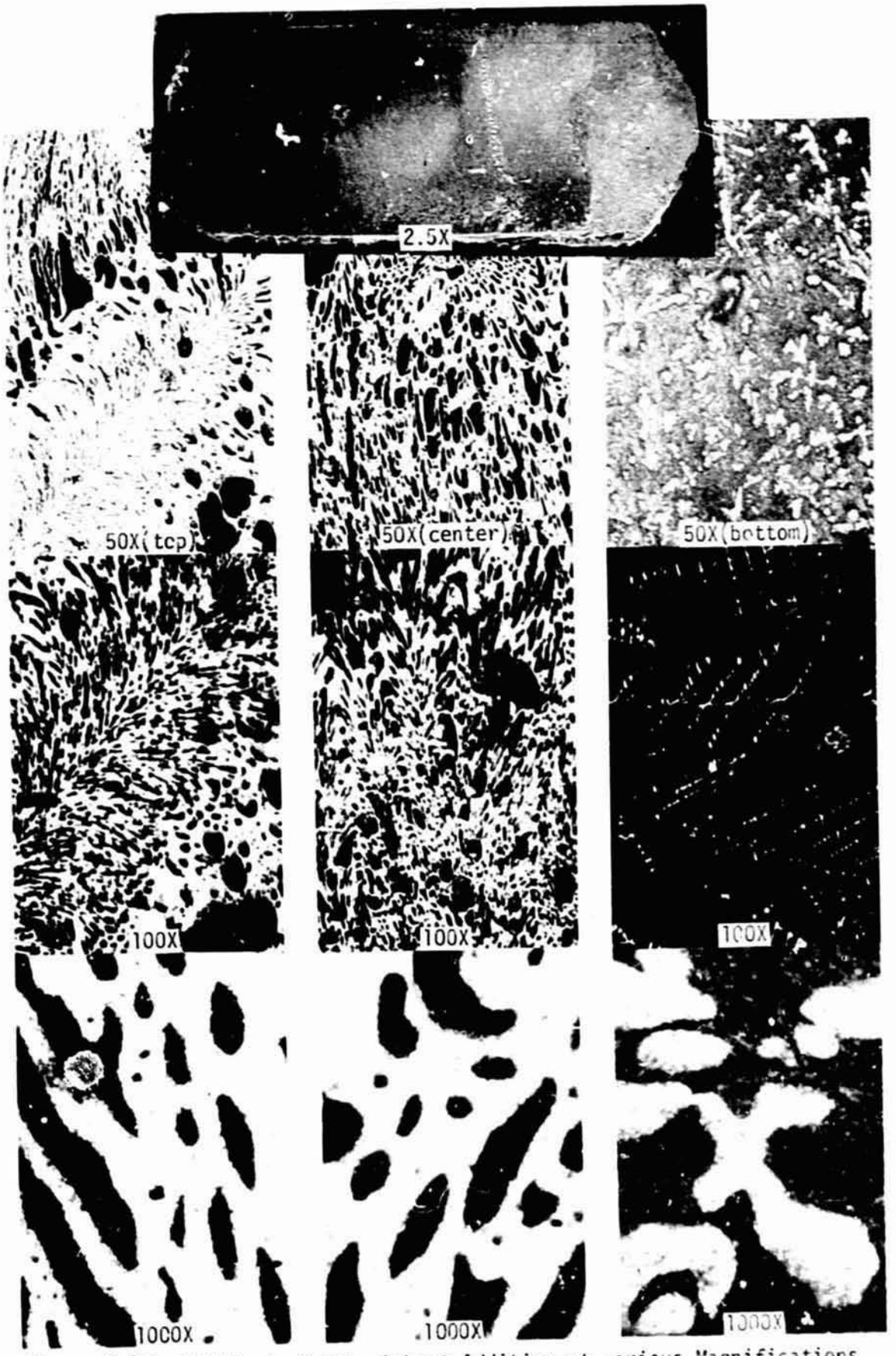

Figure 5-[illegible]. 50/50 w/o Cu/Pb without Additive at various Magnifications

a. Radial Section. Magnification: 3X

b. Axial Section. Magnification: 3X

Figure 5-11. Photomicrographs of NASA Supplied Cu/Pb Specimens with Additive

Magnification: 50X

Magnification: 100X

Magnification: 1000X

Figure 5-12. Select Area Photomicrographs of NASA Supplied Sample (Radial Section)

6.0 CONCLUSIONS AND RECOMMENDATIONS

From a previous survey of systems possessing an immiscibility gap, three systems (Ca-La, Cd-Ga and two compositions of Al-Bi) were processed and examined both metallurgically and for their superconducting behavior.

Metallurgical examination of the systems showed that the low gravity processed specimens demonstrated a more homogeneous distribution of the elements, with the exception of the cadmium-gallium system, where homogenization was also accomplished in the one gravity processed specimen. A wider particle distribution range was encountered in all the specimens as compared to specimens previously processed in the MSFC drop tower.

Both the calcium-lanthanum and the cadmium-gallium specimens showed enhanced superconducting transition temperatures, similar to some but not all immiscible systems with increased T_c. One couple, aluminum-bismuth, did not show any superconducting behavior to 3.0K. It is recommended that the fundamental quantum mechanical aspects of the superconducting transition enhancement effect be further studied on a theoretical aspect, although more experimentation is necessary for a broader data base and verification.

The above couples were processed by two different methods previously identified: Acoustic and electromagnetic. The aluminum-bismuth and calcium-lanthanum couples were processed acoustically and the cadmium-gallium system was processed with the electromagnetic mixer. Both mixing systems worked satisfactorily, although drawbacks were found in each type. The electromagnetic mixer has the drawback that the experimental cartridges are difficult to fabricate and the couple at the processing temperature must be electrically conducting. The fabrication difficulty can probably be circumvented by more advanced ceramic-metal (or conducting ceramics such as SiC) metallization techniques; in this case, processing temperatures exceeding 1500C may be achievable. The acoustic mixer has the drawback that both the thermal and acoustic coupling to the experimental cartridge must be carefully designed. Some of the results of the processed specimens are probably due to both this aspect and perhaps to a less than optimal processing sequence. Again, by using ceramic tips on the horn and other fabrication refinements, 1500C processing temperatures should

be achievable. Although the electromagnetic mixer appeared to process more efficiently, it is concluded that the acoustic mixer is the more versatile unit, since it is not limited to conducting materials. It is recommended that a more detailed analysis of acoustic coupling be undertaken; in particular, the development of a mixing frequency - specimen size - experiment cartridge dimension nomogram for sizing experiments for a single acoustic mixer unit.

The computer program successfully demonstrated that a cooling "envelope" can be computed in order to determine if the cooling temperature-materials process requirements can be met by the low gravity processing time available. The program is general enough to encompass any of the shorter time facilities (drop towers, rockets, etc.) with a variety of cooling techniques (e.g. radiation or convection coupled with liquid or gaseous cooling media).

The copper-lead couple was reasonably well homogenized in a one gravity environment by the use of the patented catalyst. This "emulsification" demonstration leads to the hypothesis of "surfactants" for the homogenization of immiscible systems and the recommendation that an investigation into this phenomena be undertaken in order to determine if a systematic (or empirical) approach would uncover other additives which would enhance the dispersion of immiscible systems with economic potential.

7.0 REFERENCES

1. "Test and Evaluation of Apollo 14 Composite Casting Demonstration Specimens 6, 9 and 12 - Phase I," Contract No. NAS 8-27085, 18677-6006-RO-00, September 1971.

2. "Experiment Development of Processes to Produce Homogenized Alloys of Immiscible Metals - Phase III," Contract No. NAS 8-27085, 19677-6019-RU-00, December 1972.

3. "Experiment No. M-557, Immiscible Alloy Compositions," Contract No. NAS 8-28309, 22457-6016-RU-00, April 1975

4. Liquid Metals Handbook, R.N. Lyon, ed., NAVEXOSP-733(Rev) Atomic Energy Commission and Department of Navy, U.S. Government Printing Office, Washington, D. C., 1952.

5. "Apollo Experiment Definition Study - Phase II, " Contract No. NAS 8-27085, 18677, 6008-RU-00, November 1971.

6. J. H. Westbrook, ed., Intermetallic Compounds, John Wiley and Sons, New York, New York, 1967 p. 581

7. C. G. Kuper, M.A. Jensen and D. C. Hamilton, Phys. Rev., 134, A 15 (1964)

8. D. C. Hamilton and M. A. Jensen, Phys. Rev. Lett., 11, 205 (1963)

9. J. T. Davies and E. K. Rideal, Interfacial Phenomena, 2nd ed., Academic Press, New York, New York, 1963.

10. M. F. Merriam and M. Von Herzen, Phys. Rev. 131, 637 (1963).

11. R. Ebhart, Heat Transfer, 2nd ed., McGraw-Hill, New York, New York, 1971, p.64 et.seq.

12. Carl E. Bazley, U.S. Patent No. 3, 544, 314, 'Homogeneous Copper Lead Metal and Method of Making", December 1, 1970, assigned to Colea Metals International, Ltd., Denver, Colorado.

13. V. K. Semenchenko, "Surface Phenomena in Metals and Alloys", Pergamon Press, N.Y., N.Y., 1962.

APPENDIX A

ACOUSTIC MIXER ASSEMBLY AND OPERATION

1.0 GENERAL

The assembled acoustic mixer assembly is shown pictorially in Figure 1 and the major components are shown in Figures 2 through 5. These major components are shown schematically in Figures 6 through 10 and Figure 11 shows the assembly details and voltage requirements. Each major subelement is described below.

1.1 DC TO AC CONVERTER

The converter is a Micronta Model 22-130 DC to AC power inverter, commercially available from Radio Shack, Tandy Corporation Co., Ft. Worth, Texas 76107. It produces a 115V, 60 HzAC square wave output with a power handling capability of 200 watts continuous, 225 watts intermittent. Input voltage can vary from 12 to 14 VDC, but 12V are recommended. Thus, the other subelements were designed and built for 12 volt operation.

This subelement serves as a source of high voltage AC power to the acoustic generator power supply, as well as a convenient 12V DC pick-off point for the frequency source of the acoustic driver. The interior of the convecter has been reworked and potted with silicone rubber (RTV 8111) for protection from the accelerative loads during drop.

1.2 ACOUSTIC GENERATOR POWER SUPPLY

The power supply is designed to provide 300 VDC, 0.7A to the high power driver portion of the acoustic generator. As with the converter, all components have been braced and potted to not only protect against accelerative loads but also against any shock hazard to drop tower personnel.

1.3 ACOUSTIC MIXER FREQUENCY CONVERTER AND HIGH POWER DRIVER

This unit consists of two functional assemblies: a DC to 27 kHz (nominal) frequency converter and a high power driver which increases the 27 kHz signal to a 27 kHz, 150 V p-p, 200 watt source for the piezoelectric transducers. Both fine and coarse adjustments are available to efficiently couple the piezoelectric transducers to the experimental capsule, as a function of large capsule weight or transducer variations.

APPENDIX A (CONT.)

1.4 ACOUSTIC MIXER AND HEATER/EXPERIMENTAL CAPSULE ASSEMBLY

The mixer assembly is a three quarter wave stepped horn with a quarter wave mixing stub and back-to-back strapped piezoelectric transducers. As mentioned previously, the design frequency is 27 kHz; however, tuning capabilities allow frequency variation to allow for piezoelectric manufacturer's tolerances and any large variations in capsule weight as may occur from experimental system to system.

The piezoelectric transducers are standard items obtainable from Vermitron Corporation (Piezoelectric Div.), 232 Forbed Rd., Bedford, Ohio 44146, Part No. 34250, PZT-4, dimensions 5.40 cm (2.125 inch) OD, 0.64 cm (0.25 inch) thick. Both sides of the disc have fired-on electrodes and have been polled. The positive going sides of each disc were placed together so that all external metal surfaces would be at fround potential to minimize any electrical shock hazard. The piezoelectric discs are clamped together by six bolts, torqued to 28 N.M (25 in-lbs) to give a total clamping force of 3 kN (700 pounds).

The heater container is a relatively standard revision of the previous heaters utilized for straight thermal processing and is designed to minimize heat loss to the main body of the transducer and provide a water seal during cooldown.

1.5 SAFETY RELAY

The safety relay is a Guardian Model IR-645-2C-12D DPDT all purpose relay with a 12 VDC coil. When energized, the connections between the high voltage power supply and the input to the power transistors and the connection between the power transistor output and the piezoelectric transducers are completed. When the coil is deenergized, the relay opens and shorts the transducers and discharges the high voltage power supply. This is done to protect the transistors from high voltage transients that may be generated when the drop package is decelerated.

2.0 MODE OF OPERATION

The acoustic mixer components are assembled except for the heater housing, experiment cartridge and electrical connections to the various components from the drop tower power supply. The following operational sequences have been tested and are recommended (it is assumed that the package has been

APPENDIX A (CONT.)

mounted in the drop package.)

1. Connect the 12 VDC inputs from the safety relay and the oscillator to the 12V DC input on the DC to AC power inverter.

2. Connect the 110 VAC power card from the power supply to the 110 V AC power output plug on the DC to AC power inverter.

3. Screw the experimental capsule into the mixer tip. Be careful of the thermocouple lead. Tighten to finger tight, then tighten 1/4-1/2 turn further with a pair of pliers. Bend the thermocouple wire to follow approximately the ti to the base, using needle-nose pliers between the bend and the cartridge to relieve any strain at the weld joint.

4. Attach the heater to the base plate as follows:

a. The three band straps seal the O-ring at the base of the mixer. These should be inserted through the heater flange and bolted down.

b. The three screws (4-40) clamp and seal the heater flange to the Teflon ring.

c. There is a notch in the heater flange for the thermocouple lead. Make sure the lead is positioned in the notch before thoroughly tightening the screws and bolts to make the water seal.

5. Attach the flexible hose to the outlet of the water quench and the inlet of the the heater package.

6. Attach the three water outlet leads to the base plate and clamp the copper outlet cup to the catch tank.

7. Connect the 12V DC line from the timer to the DC to AC power inverter inlet. Switch the inverter to ON, making sure the timer is off.

8. The processing sequence is as follows:

a. Heat the cartridge to the desired temperature. Hold the tempearture for ten (10) minutes to insure isothermalization.

b. Set the timer controlling the power to the inverter to perform the following sequence:

APPENDIX A (CONT.)

- No power to inverter until the cartridge is thermalized.
- Turn the power on and acoustically mix the cartridge for two (2) minute before drop.
- Turn the power off three (3) seconds after drop.
- Retain the same water quench sequence as before.

9. Remove cartridge after processing and repeat steps 3, 4 and 8 for next drop.

FIGURE 1. Assembled Acoustic Mixer

APPENDIX A (CONT.)

FIGURE 2. DC to AC Power Inverter

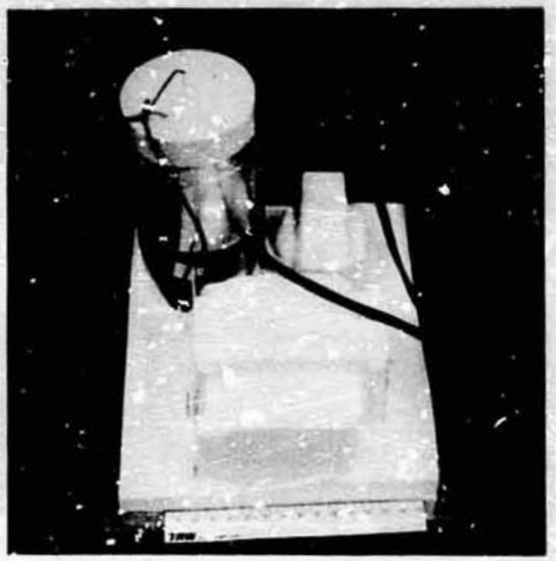

FIGURE 3. 300V DC Power Supply

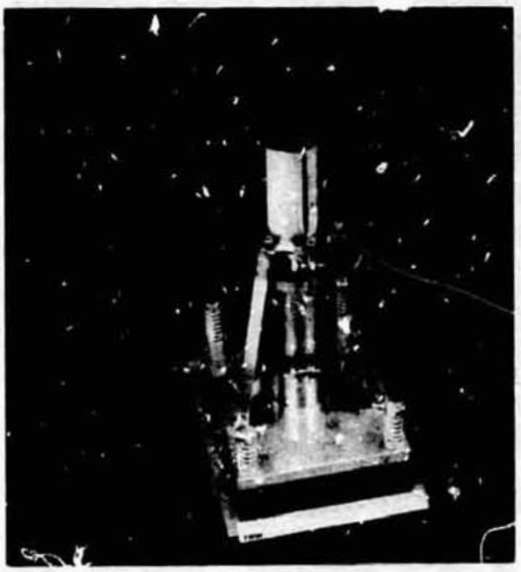

FIGURE 4. Acoustic Horn with Transducers

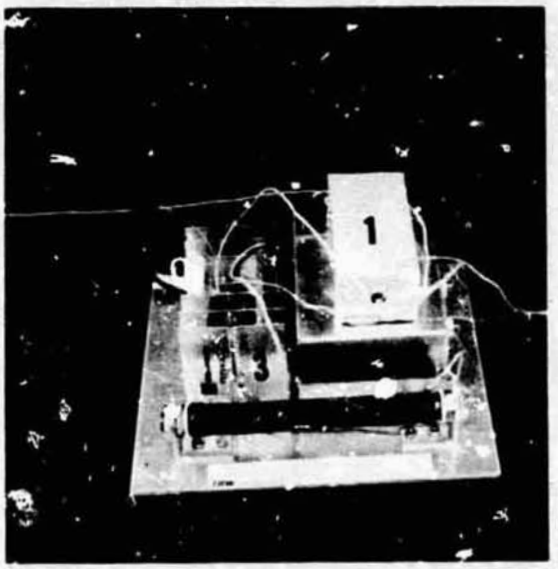

FIGURE 5. Acoustic Generator Showing:
(1) Safety Relay
(2) Frequency Generator
(3) Power Oscillator

APPENDIX A (CONT.)

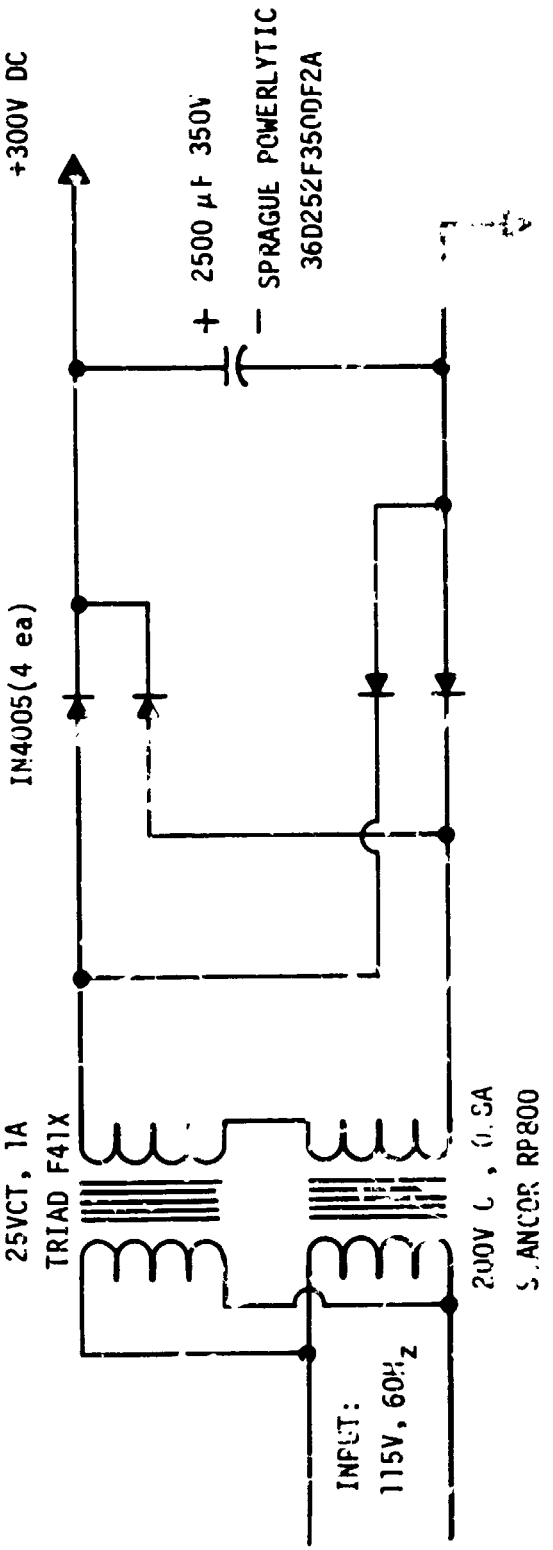

FIGURE 7. Schematic Diagram of 300V DC Power Supply

APPENDIX A (CONT.)

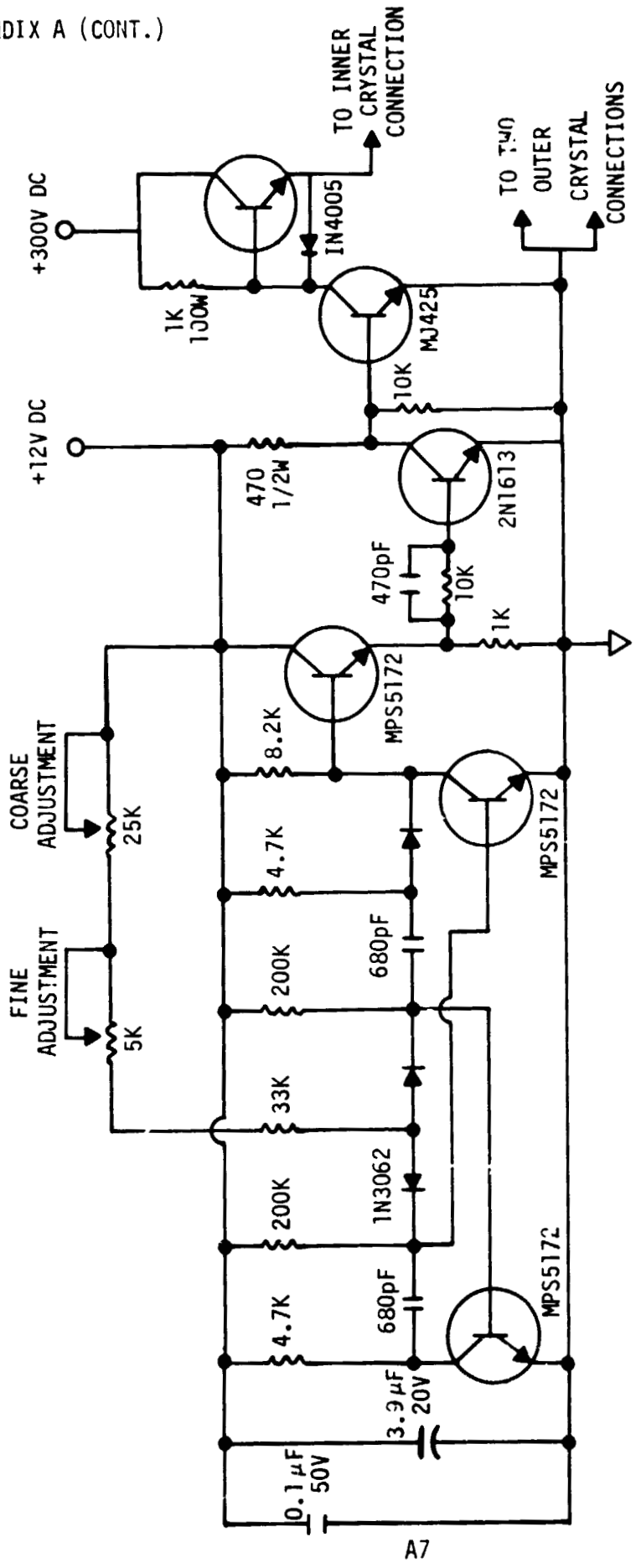

FIGURE 8. Schematic Diagram of Ultrasonic Generator and High Power Driver

APPENDIX A (CONT.)

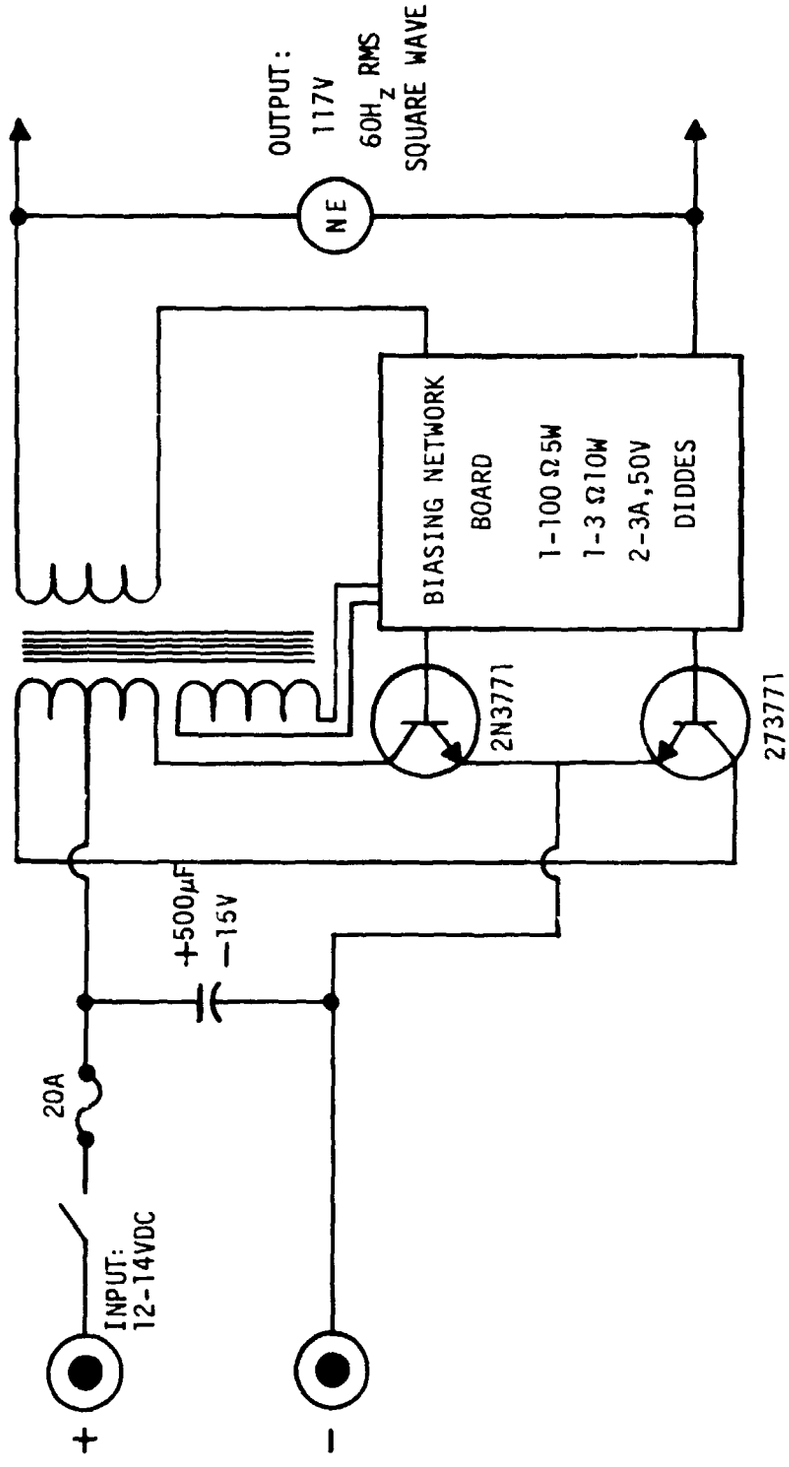

FIGURE 9. Schematic Diagram of Micronta Model 22-130 DC to AC Power Inverter

APPENDIX A (CONT.)

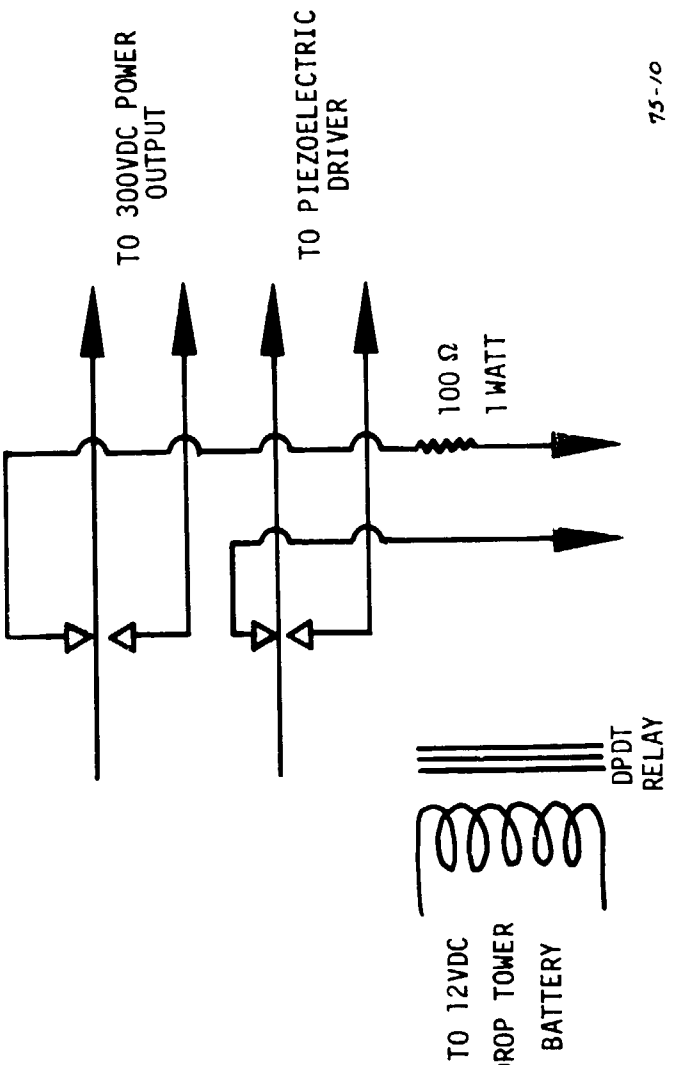

FIGURE 10. Safety Relay Schematic for Acoustic Mixer (Off Position)

APPENDIX A (CONT.)

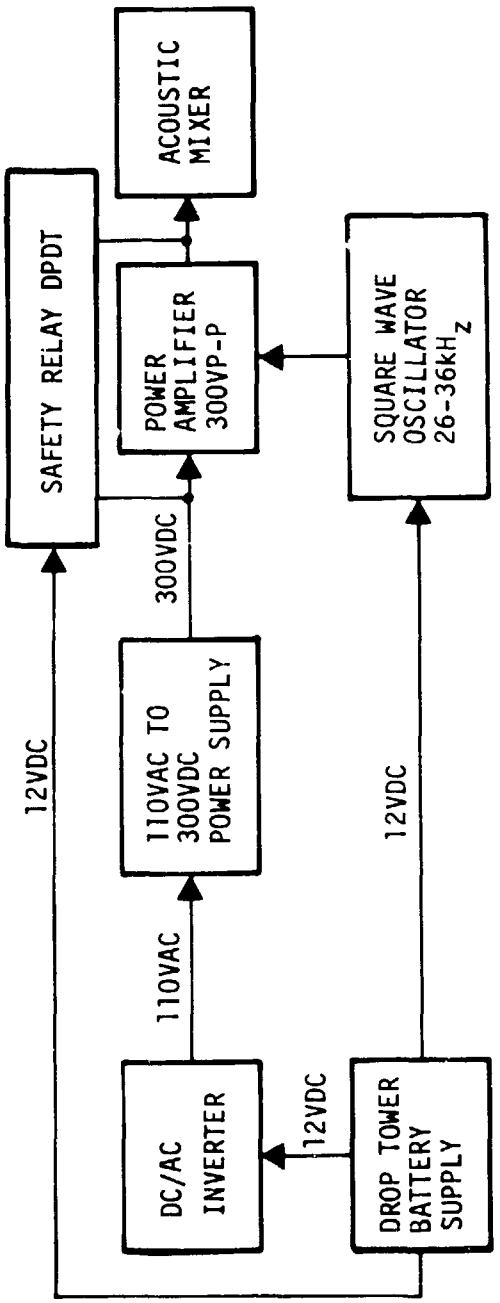

FIGURE 11. Schematic of Power Conversion Modules for Acoustic Mixer.

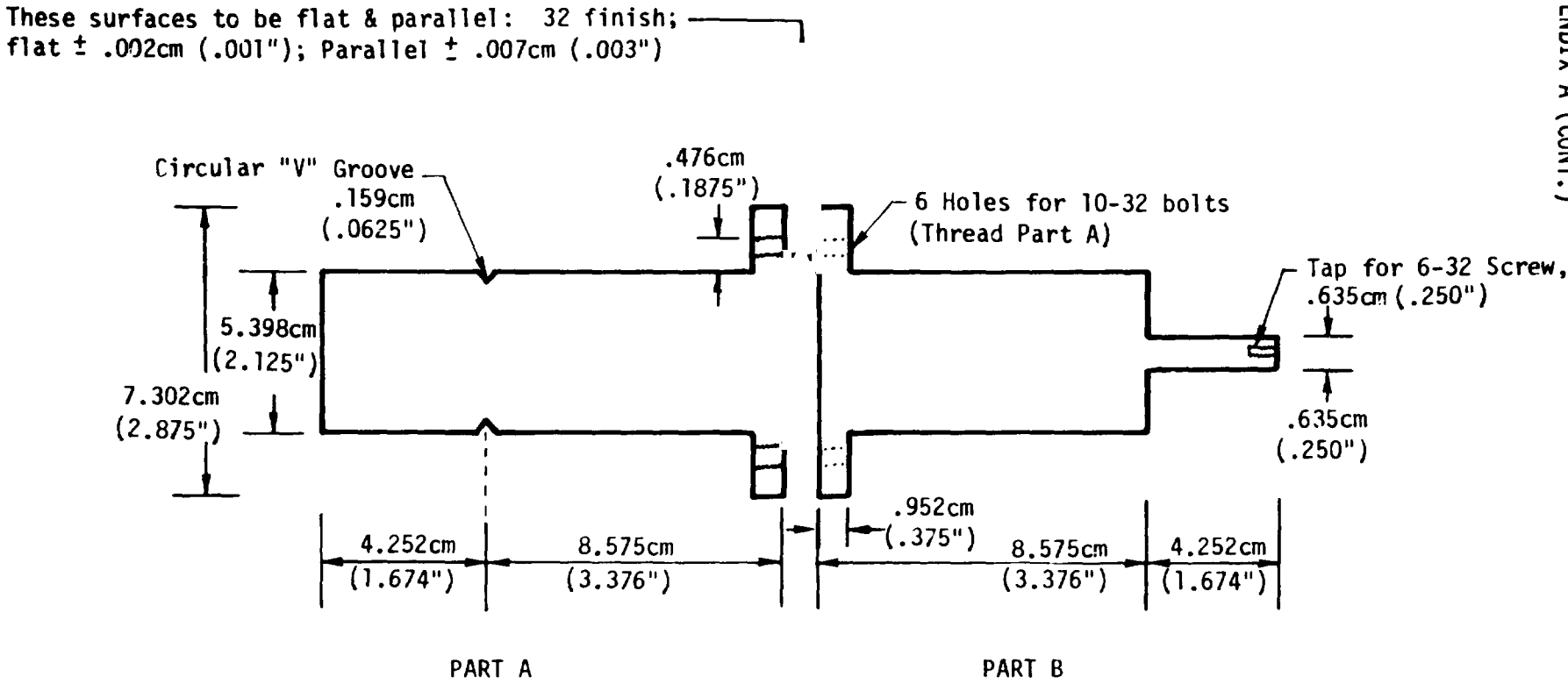

(All Dimensions are ± .002cm (.001") - Break all edges & corners
Material: Stainless 304)

FIGURE 6. Schematic Diagram of Acoustic Mixer

APPENDIX B

ELECTROMAGNETIC MIXER ASSEMBLY AND OPERATION

1.0 GENERAL

The various components of the electromagnetic mixer and the closeup views of the primary package are shown in Figures 1 through 5. Not shown is the Cutler-Hammer model BUL 6041H185, 120 A DC SPST relay with a 24 to 28 VDC energizing coil, or the heating coils.

1.1 PERMANENT MAGNET

The magnet is a surplus 2400 gauss field strength device used to supply the DC magnetic field for thyratrons. It contains the experiment housing, electrical leads and water inlet/exit parts as shown in Figures 1 and 2. The magnetic field per se is non-hazardous. However, all personnel working within approximately 30 to 50 cm (1-1.5 ft) of the magnet should remove wrist or pocket watches to prevent magnetization of their mechanisms. Also, steel tools will tend to become magnetized; this can be remedied by running them through a degausser or magnetic tape erasing head (bulk tape type) after use.

1.2 EXPERIMENT PACKAGE

Figures 3, 4 and 5 show the annular experiment package, the electrode clamps and the experiment positioner screwed to the bottom of the housing (Figure 3). The mixer electrical leads are connected to the experiment package by the fill tube, attached to the outer electrodes and the position clamp, which is attached to the inner electrode and serves both as an electrical and mechanical clamp. Either electrode can be positive or negative. The only constraint is that the experiment must face the magnet pole face protected by the asbestos (Figure 4). The heater coils are connected to the temperature controller.

1.3 ELECTRICAL WIRING

The wiring is extremely simple. The one major supplied item not shown is the relay, mentioned in Section 1.0. This relay should be connected in series with the positive DC battery cable. Thus, the wiring sequence would be the DC+ cable from experiment/magnet to relay terminal

APPENDIX B (CONT.)

A1, DC+ lead from relay terminal B1 to a 1/2-1 ohm resistor (to be supplied by NASA) then to main battery cable. Total current should be approximately 30 amperes. The resistor selection can be approximated closely by shorting the two current lugs inside the housing, since the initial experiment resistance will be nil.

The heating coil and electrical leads are connected in the same manner as with the acoustic mixer and the thermal housing.

All internal connections are standard hex nut or Allen wrench size. These may be changed if desired.

2.0 MODE OF OPERATION

The operational mode is simple: The heating coil heats the experiment cartridge until the metals are liquid; once liquid, the imposed current across the experiment interacts with the magnetic field to produce movement and concomitant mixing. After drop, the DC voltage is removed and the experiment package quenched. It is suggested that initial tests be done with shorted leads; the experiment packages are designed to work only once. The following operational sequence has been tested and is recommended:

1. Connect the main DC voltage supply to the DC- lug and through the power relay to the DC+ lug.
2. Connect the thermocouple leads to the drop package temperature controller.
3. Connect the temperature controller relay outlets to the main power relay coil terminals (X1 and X2).
4. Connect the experiment package to the holder and fasten the holder to the bottom housing by the two Phillip screws. Attach the two DC power lugs to the current tabs on the experiment package and connect heater coils. Make sure the housing is leak tight.
5. After all installation, etc., as is possible has been done in the drop shroud, initiate DC voltage to experiment package, using the temperature controller.

APPENDIX B (CONT.)

6. Heat the experiment package to the desired temperature.
7. As soon as possible after the temperature has been established, drop the package.
8. Sequence the DC power relay to provide maximum power from drop to start or water quench.
9. At start of water quench, cut off power to experiment package.
10. Retain the same water quench sequence as before.
11. Remove package as follows:
    - o Undo top housing
    - o Remove experiment from power clamps
12. Install new package in reverse sequence of Step 11.

Figure 1. Closeup Photograph of Experiment Housing of Electromagnetic Mixer

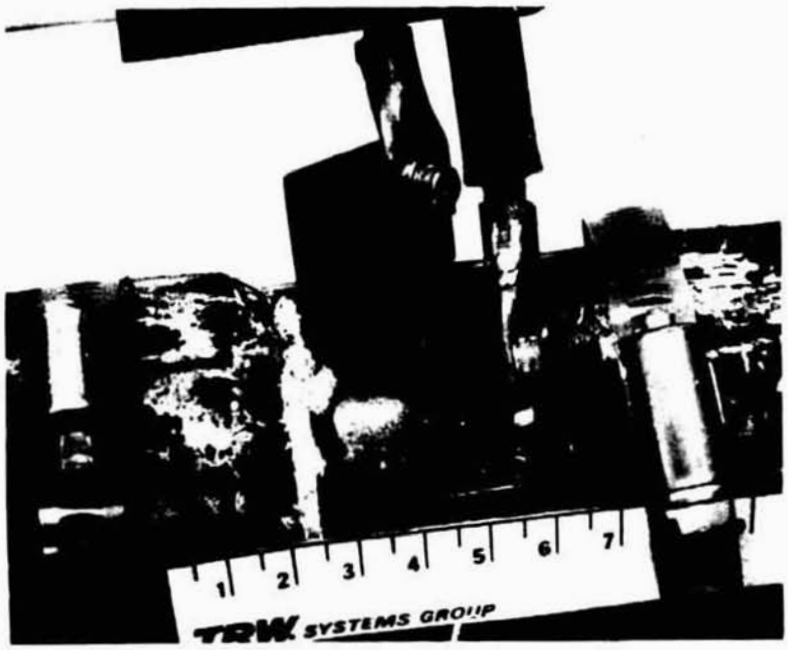

Figure 2. Overall View of Electromagnetic Mixer

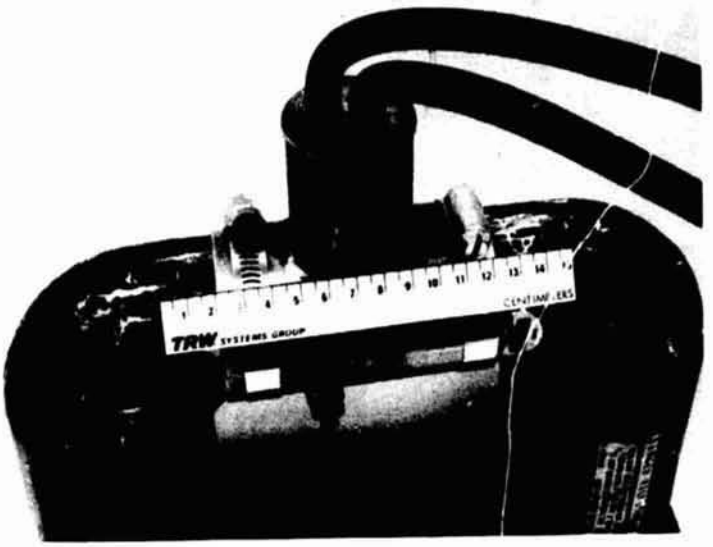

Figure 3. View of Disassembled Housing Showing Electrical and Mechanical Connections

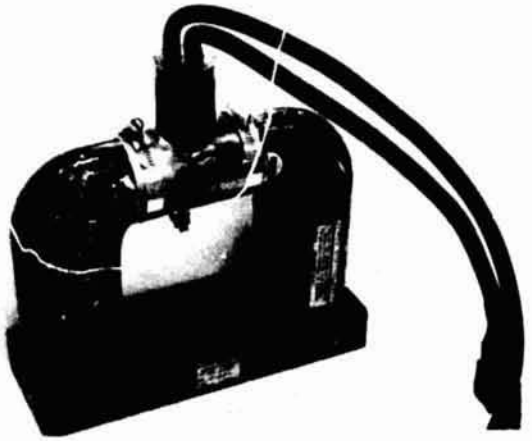

Figure 4. Closeup View of Experiment Showing Mechanical Connections and Location

Figure 5. Closeup View of Experiment Showing Electrical Connections

APPENDIX C

Appendix C consists of:

C-1 Listing of Computer Program

C-2 Required Input

C-3 Sample Solutions

APPENDIX C-1 - LISTING OF COMPUTER PROGRAM

```
100 PRINT " COOLING RATES FOR IMMISCIBLE MATERIALS IN ZERO GRAVITY"
110 REMARK: BASIC, REVISED(2-11-75)
120 PRINT
130 PRINT
140 X,R,P1=0
150 I1,I2,I3,I4=0
160 H1,H2,H3=0
170 A4=0
180 S5=5.67E-8                    !(JOULE/K4-M2-SEC)
190 R5=8.32                       !(JOULE/MOLE-K)
200 PRINT " GEOMETRY:          1 SPHERE"
210 PRINT "                    2 CYLINDER"
220 PRINT "                    3 PLATE"
230 PRINT "                    4 GENERAL"
240 PRINT
250 PRINT " TYPE GEOMETRY NO.":
260 INPUT G
270 ON G GOTO 280,340,400,460
280 PRINT "DIA(CM)":
290 INPUT S
300 S=S/2
310 A=4*PI*(S↑2)
320 V=(4/3)*PI*(S↑3)
330 GOTO 490
340 PRINT " DIA(CM), LENGTH(CM)":
350 INPUT S,L
360 S=S/2
370 A=(2*PI*S*L)+(2*P1*(S↑2))
380 V=PI*(S↑2)*L
390 GOTO 490
400 PRINT " LENGTH(CM), WIDTH(CM), THK(CM)":
410 INPUT L,W,S
420 S=S/2
430 A=2*(2*S*W)+2*(2*S*L)+2*(L*W)
440 V=2*S*L*W
450 GOTO 490
460 PRINT " SURFACE AREA(CM2), VOLUME(CM3)":
470 INPUT A,V
480 S=3*(V/A)
490 PRINT
500 PRINT "              SAMPLE PROPERTIES"
510 PRINT " K(WATT/CM-C)   DENS(GM/CM3)   SH(CAL/GM-C)":
520 INPUT K3,D3,S3
530 A9=0.2389*(K3/(D3*S3))              !(CM2/SEC)
540 PRINT
550 PRINT " TINIT(C)   TFINAL(C)    DT(C)    TSINK(C)":
560 INPUT T1,T9,T5,T0
570 T1=T1+273
580 T9=T9+273
590 T0=T0+273
600 T=T1-T5
```

APPENDIX C-1 (CONT.)

```
610 T4=T1-T5/2                          !AVG SAMPLE TEMP
620 T3=(T4+T0)/2                        !FILM TEMP
630 PRINT
640 PRINT
650 PRINT " COOLING MODES:        1 FORCED CONVECTION"
660 PRINT "                       2 RADIATION"
670 PRINT "                       3 CONDUCTION IN SUPPORTS"
680 PRINT
690 PRINT " TYPE NOS. FOR DESIRED COOLING MODES.  TYPE 0 FOR OTHERS."
700 PRINT " (EXAMPLE: 1,0,3)":
710 INPUT C1,C2,C3
720 PRINT
730 PRINT
740 REMARK: FORCED CONVECTION
750 IF C1=0 THEN 1090
760 PRINT " COOLANT VELOCITY(M/SEC)    COOLANT PRESSURE(ATM)":
770 INPUT U,P
780 PRINT
790 U=100*U                             !(CM/SEC)
800 P=(1.013E6)*P
810 GOSUB 10000                         !COOLANT
820 R=((D1*U*2*S)/V1)*100               !(V1 IN CP)
830 IF G=3 THEN R=((D1*U*W)/V1)*100     !(V1 IN CP)
840 P1=((V1/100)*(S1*4.186))/K1
850 ON G GOTO 860,900,1000,860
860 IF R<20 OR R>150000 THEN 1040
870 N=0.37*(R^0.6)*(P1^0.333)           !SPHERE OR GENERAL
880 H1=(N*K1)/(2*S)                     !(WATT/CM2-C)
890 GOTO 1090
900 IF R<40 OR R>250000 THEN 1040
910 IF R>4000 THEN 940
92  N=1.12*0.615*(R^0.466)*(P1^0.333)       !CYLINDER
930 GOTO 980
940 IF R>40000 THEN 970
950 N=1.12*0.1714*(R^0.618)*(P1^0.333)      !CYLINDER
960 GOTO 980
970 N=1.12*0.0239*(R^0.805)*(P1^0.333)   !CYLINDER
980 H1=(N*K1)/(2*S)                     !(WATT/CM2-C)
990 GOTO 1090
1000 IF R<100000 THEN N=0.648*(R^0.5)*(P1^0.333)        !FLAT PLATE(LAM)
1010 IF R>100000 THEN N=0.037*(R^0.8)*(P1^0.333)        !FLAT PLATE(TURB)
1020 H1=(N*K1)/W                        !(WATT/CM2-C)
1030 GOTO 1090
1040 PRINT " REYNOLDS NO.= ";R;" (OUT OF RANGE)"
1050 PRINT " TYPE CONV. HT COEFF.(WATTS/CM2-C)":
1060 INPUT H1
1070 PRINT
1080 REMARK: RADIATION
1090 IF C2=0 THEN 1180
1100 PRINT " ENCL AREA(  2)    EMIS1     EMIS2":
1110 INPUT A2,E1,E2.
1120 PRINT
```

ORIGINAL PAGE IS
OF POOR QUALITY

APPENDIX C-1 (CONT.)

```
1130 F1=1/E1+(A/A2)*((1/E2)-1)
1140 F1=1/F1
1150 H2=F1*S5*((T4↑4-T0↑4))/(T4-T0)
1160 H2=H2/10000                              !(WATT/CM2-C)
1170 REMARK: CONDUCTION IN SUPPORTS
1180 IF C3=0 THEN 1250
1190 IF I3=1 THEN 1250
1200 PRINT " SUPPORT LENGTH(CM)   CROSS-SECTION(CM2)   KS(WATTS/CM-C)":
1210 INPUT L4,A4,K4
1220 PRINT
1230 I3=1
1240 H3=K4/L4                                 !(WATT/CM2-C)
1250 H5=((H1*A)+(H2*A)+(H3*A4))/A
1260 B1=(H5*S)/K3
1270 IF I4=1 THEN 1550
1280 IF B1>0.05 THEN 1490
1290 Z1=T-T0
1300 Z2=T1-T0
1310 X0=-1*(LOG(Z1/Z2))
1320 X5=((S3*D3*V)/(H5*A))*X0*4.186            !(SEC)
1330 X=X+X5                                   !(SEC)
1340 PRINT "                        *******"
1350 PRINT " TEMP= ":T-273:" (C)";" TIME= ":X:" (SEC)"
1360 PRINT " RE= ":R;" BI= ":B1;" PR= ":P1
1370 PRINT " HR= ":H2:" (WATT/CM2-C)";" HK= ":H3:" (WATT/CM2-C)"
1380 PRINT " HC= ":H1:" (WATT/CM2-C)";" TFILM= ":T3-273:" (C)"
1390 PRINT " EQ H= ":H5:" (WATT/CM2-C)"
1400 PRINT "                        *******"
1410 PRINT
1420 IF I4=1 THEN 1630
1430 T1=T
1440 T=T-T5
1450 IF T<T9 THEN STOP
1460 T4=T1-T5/2
1470 T3=(T4+T0)/2
1480 GOTO 720
1490 PRINT " 1/BI= ":B1;" (HEISLER CHARTS REQUIRED.  CONSTANT AVERAGE"
1500 PRINT " HEAT TRANSFER COEFF. USED.)"
1510 T3=(((T1+T9)/2)+T0)/2
1520 T4=(T1+T9)/2
1530 I4=1
1540 GOTO 720
1550 Z1=T-T0
1560 Z2=T1-T0
1570 PRINT " 1/BI= ":1/B1;" (T-TS)/(TI-TS)= ":Z1/Z2
1580 PRINT " TYPE F0":
1590 INPUT F0
1600 PRINT
1610 X=((S↑2*F0)/A9)
1620 GOTO 1340
1630 T=T-T5
1640 IF T<T9 THEN STOP
```

ORIGINAL PAGE IS
OF POOR QUALITY

APPENDIX C-1 (CONT.)

```
1650 GOTO 1550
1660 END
10000 REMARK: S/R COOLANT, BASIC
10020 IF I1=1 THEN 10110
10030 PRINT " COOLANT              1 WATER(0C<T<320C)"
10040 PRINT "                      2 NITROGEN(-20C<T<820C)"
10050 PRINT "                      3 HELIUM(-20C<T<820C)"
10060 PRINT
10070 PRINT " TYPE COOLANT NO.":
10080 INPUT F
10090 I1=1
10100 PRINT
10110 ON F GOTO 10120,10200,10300
10120 REMARK: WATER
10130 M0=18.06
10140 D1=0.8225751+1.42435E-3*T3-2.8249E-6*T3↑2
10150 S1=-0.65575+1.441242E-2*T3-4.13337E-5*T3↑2+3.919158E-8*T3↑3
10160 V1=EXP(32.835499-0.26171538*T3+7.6722631E-4*T3↑2-1.0265253E-6*T3↑3
+ +5.1891037E-10*T3↑4)
10170 K1=-9.3765178E-3+9.2783242E-5*T3-1.5992952E-7*T3↑2+7.4795235E-11*T
+ 3↑3
10180 GOTO 10400
10200 REMARK: NITROGEN
10210 M0=28.013
10220 D1=(M0*P*1.0E-7)/(R5*T3)
10230 S1=0.24345498+6.1650323E-6*T3+2.8674466E-8*T3↑2
10240 V1=4.1519721E-3+5.0061395E-5*T3-1.4198016E-8*T3↑2
10250 K1=6.6187327E-5+6.5030676E-7*T3-3.5337747E-11*T3↑2
10260 GOTO 10400
10300 REMARK: HELIUM
10310 M0=4.003
10320 D1=(M0*P*1.0E-7)/(R5*T3)
10330 S1=1.24
10340 V1=6.3893368E-3+4.4760584E-5*T3-6.9527582E-9*T3↑2
10350 K1=0.46466604E-4+3.8136579E-6*T3-1.3524212E-9*T3↑2
10400 RETURN
$
```

APPENDIX C-2 - REQUIRED INPUT

PROGRAM MATS

I. REQUIRED INPUT

A. Geometry
   1. Sphere - dia. (cm)
   2. Cylinder - dia. (cm), length (cm)
   3. Plate - length (cm), width (cm), thickness (cm)
   4. General - surface area (cm^2), volume (cm^3)

B. Sample Properties
   1. Thermal conductivity (watts/cm-°C)
   2. Density (gm/cm^3)
   3. Specific heat (cal/gm-°C)

C. Temperatures
   1. Initial temperature (°C)
   2. Final temperature (°C)
   3. Temperature increment (°C)*
   4. Sink or coolant temperature (°C)

D. Cooling Modes
   1. Forced convection (requires subroutine)
      (a) Coolant
         (1) Water (liquid)
         (2) Nitrogen (gaseous)
         (3) Helium (gaseous)
      (b) Coolant velocity (m/sec)
      (c) Coolant pressure (atm)
   2. Radiation
      (a) Enclosure area (cm^2)
      (b) Emissivity of sample
      (c) Emissivity of enclosure
   3. Conduction in supports
      (a) Support length (cm)
      (b) Support cross-section area (cm^2)
      (c) Support thermal conductivity (watts/cm-°C)

*This program is a closed form solution, thus either the cooling curve or total time to cool to a given temperature can be obtained. C-3 is necessary only or obtaining cooling curves.

APPENDIX C-2 (CONT.)

4. Combined (any combination of the above) (requires subroutine)

II. ASSUMPTIONS

1. If Biot number (Bi) < 0.05, then sample cools uniformly. Program calculates cooling curve automatically.
2. If Biot number > 0.05 (high heat transfer coefficient), then Heisler** charts required to input the Fourier number (Fo) from the terminal. Heat transfer coefficient must be constant. An average value is computed for this case.
3. Cylinder is in cross-flow.
4. Plate width is parallel to flow (i.e., length > width).
5. General geometry treated as a sphere.

**B. Gebhart, Heat Transfer, 2nd Ed., McGraw-Hill Book Co., N. Y., N. Y., 1971, p. 64 et. seq. (or equivalent).

APPENDIX C-3 - SAMPLE SOLUTIONS

COOLING RATES FOR IMMISCIBLE MATERIALS IN ZERO GRAVITY

```
 GEOMETRY:          1 SPHERE
                    2 CYLINDER
                    3 PLATE
                    4 GENERAL

 TYPE GEOMETRY NO.
? 3
 LENGTH(CM), WIDTH(CM), THK(CM)
? 1.37          .74          .42

                SAMPLE PROPERTIES
 K(WATT/CM-C)   DENS(GM/CM3)   SH(CAL/GM-C)
? .114             8.41            .047

 TINIT(C)   TFINAL(C)    DT(C)    TSINK(C)
? 270         210         20         25


 COOLING MODES:         1 FORCED CONVECTION
                        2 RADIATION
                        3 CONDUCTION IN SUPPORTS

 TYPE NOS. FOR DESIRED COOLING MODES.  TYPE 0 FOR OTHERS.
 (EXAMPLE: 1,0,3)
? 1,0,0


 COOLANT VELOCITY(M/SEC)     COOLANT PRESSURE(ATM)
? 6                            1

 COOLANT.              1 WATER(0C<T<320C)
                       2 NITROGEN(-20C<T<320C)
                       3 HELIUM(-20C<T<820C)

 TYPE COOLANT NO.
? 1

 1/BI=  12.208662     (HEISLER CHARTS REQUIRED.  CONSTANT AVERAGE
 HEAT TRANSFER COEFF. USED.)


 COOLANT VELOCITY(M/SEC)     COOLANT PRESSURE(ATM)
? 6                                  1

 1/BI=  .84080251E-01     (T-TS)/(TI-TS)=  .91836735E+00
 TYPE FO
? .15
```

APPENDIX C-3 (CONT.)

```
                    ◆◆◆◆◆◆◆
 TEMP=  250 (C)     TIME=   .96006956E-01 (SEC)
 RE=  195730.74     BI=  11.893399     PR=  1.2873393
 HR=  0 (WATT/CM2-C)      HK=  0 (WATT/CM2-C)
 HC=  6.4564168 (WATT/CM2-C)   TFILM=  132.5 (C)
 EQ H=  6.4564168 (WATT/CM2-C)
                    ◆◆◆◆◆◆◆

 1/BI=  .84080251E-01     (T-TS)/(TI-TS)=  .83673469E+00
 TYPE FD
? .2

                    ◆◆◆◆◆◆◆
 TEMP=  230 (C)     TIME=   .12800927E+00 (SEC)
 RE=  195730.74     BI=  11.893399     PR=  1.2873393
 HR=  0 (WATT/CM2-C)      HK=  0 (WATT/CM2-C)
 HC=  6.4564168 (WATT/CM2-C)   TFILM=  132.5 (C)
 EQ H=  6.4564168 (WATT/CM2-C)
                    ◆◆◆◆◆◆◆

 1/BI=  .84080251E-01     (T-TS)/(TI-TS)=  .75510204E+00
 TYPE FD
? .25

                    ◆◆◆◆◆◆◆
 TEMP=  210 (C)     TIME=   .16001159E+00 (SEC)
 RE=  195730.74     BI=  11.893399     PR=  1.2873393
 HR=  0 (WATT/CM2-C)      HK=  0 (WATT/CM2-C)
 HC=  6.4564168 (WATT/CM2-C)   TFILM=  132.5 (C)
 EQ H=  6.4564168 (WATT/CM2-C)
                    ◆◆◆◆◆◆◆


LINE 01640
END
$ RUN
```

APPENDIX C-3 (CONT.)

```
 COOLING RATES FOR IMMISCIBLE MATERIALS IN ZERO GRAVITY


 GEOMETRY:          1 SPHERE
                    2 CYLINDER
                    3 PLATE
                    4 GENERAL

 TYPE GEOMETRY NO.
? 3
 LENGTH(CM), WIDTH(CM), THK(CM)
? 1.37          .74       .42

                SAMPLE PROPERTIES
 K(WATT/CM-C)    DENS(GM/CM3)    SH(CAL/GM-C)
? .114              8.41            .047

 TINIT(C)    TFINAL(C)     DT(C)     TSINK(C)
? 270           210         20          25


 COOLING MODES:          1 FORCED CONVECTION
                         2 RADIATION
                         3 CONDUCTION IN SUPPORTS

 TYPE NOS. FOR DESIRED COOLING MODES.  TYPE 0 FOR OTHERS.
 (EXAMPLE: 1,0,3)
? 1,0,0


 COOLANT VELOCITY(M/SEC)     COOLANT PRESSURE(ATM)
? 6                              1

 COOLANT             1 WATER(0C<T<320C)
                     2 NITROGEN(-20C<T<320C)
                     3 HELIUM(-20C<T<320C)

 TYPE COOLANT NO.
? 2

                     *******
 TEMP=  250 (C)     TIME=  1.5161715 (SEC)
 RE=  1619.7554     BI=  .19182343E-01    PR=  .7156973E+00
 HR=  0 (WATT/CM2-C)      HK=  0 (WATT/CM2-C)
 HC=  .10413272E-01 (WATT/CM2-C)      TFILM=  142.5 (C)
 EQ H=  .10413272E-01 (WATT/CM2-C)
                     *******
```

APPENDIX C-3 (CONT.)

```
 COOLANT VELOCITY(M/SEC)     COOLANT PRESSURE(ATM)
? 6                                 1

                    ◆◆◆◆◆◆◆
 TEMP=  230 (C)     TIME=  3.1702737 (SEC)
 RE=  1688.5194     BI=  .19220654E-01    PR=  .71512043E+00
 HR=  0 (WATT/CM2-C)      HK=  0 (WATT/CM2-C)
 HC=  .10434069E-01 (WATT/CM2-C)      TFILM=  132.5 (C)
 EQ H=  .10434069E-01 (WATT/CM2-C)
                    ◆◆◆◆◆◆◆


 COOLANT VELOCITY(M/SEC)     COOLANT PRESSURE(ATM)
? 6                                 1

                    ◆◆◆◆◆◆◆
 TEMP=  210 (C)     TIME=  4.9904512 (SEC)
 RE=  1762.0352     BI=  .19261426-01     PR=  .71652834E+00
 HR=  0 (WATT/CM2-C)      HK=  0 (WATT/CM2-C)
 HC=  .10456199E-01 (WATT/CM2-C)      TFILM=  122.5 (C)
 EQ H=  .10456199E-01 (WATT/CM2-C)
                    ◆◆◆◆◆◆◆


LINE 01450
END
$ RUN
```

APPENDIX C-3 (CONT.)

```
 COOLING RATES FOR IMMISCIBLE MATERIALS IN ZERO GRAVITY


 GEOMETRY:          1 SPHERE
                    2 CYLINDER
                    3 PLATE
                    4 GENERAL

 TYPE GEOMETRY NO.
? 3
 LENGTH(CM), WIDTH(CM), THK(CM)
? 1.37          .74          .42

                SAMPLE PROPERTIES
 K(WATT/CM-C)    DENS(GM/CM3)    SH(CAL/GM-C)
? .114              3.11            .047

 TINIT(C)    TFINAL(C)     DT(C)     TSINK(C)
? 270          210           20         25


 COOLING MODES:          1 FORCED CONVECTION
                         2 RADIATION
                         3 CONDUCTION IN SUPPORTS

 TYPE NOS. FOR DESIRED COOLING MODES.  TYPE 0 FOR OTHERS.
 (EXAMPLE: 1,0,3)
? 1,0,0


 COOLANT VELOCITY(M/SEC)     COOLANT PRESSURE(ATM)
? 6                                  1

 COOLANT             1 WATER(0C<T<320C)
                     2 NITROGEN(-20C<T<820C)
                     3 HELIUM(-20C<T<320C)

 TYPE COOLANT NO.
? 3

                    ◆◆◆◆◆◆◆
 TEMP=  250 (C)     TIME=  .90859171E+00 (SEC)
 RE=  213.9492      BI=  .32009671E-01    PP=  .88346837E+00
 HR=  0 (WATT/CM2-C)      HK=  0 (WATT/CM2-C)
 HC=  .17376678E-01 (WATT/CM2-C)      TFILM=  142.5 (C)
 EQ H=  .17376678E-01 (WATT/CM2-C)
                    ◆◆◆◆◆◆◆
```

APPENDIX C-3 (CONT.)

```
 COOLANT VELOCITY(M/SEC)     COOLANT PRESSURE(ATM)
? 6                                  1

                    ◆◆◆◆◆◆◆
 TEMP=  230 (C)     TIME=  1.8999183 (SEC)
 RE=  228.09341     BI=  .32071094E-01    PR=  .88610407E+00
 HR=  0 (WATT/CM2-C)      HK=  0 (WATT/CM2-C)
 HC=  .17410022E-01 (WATT/CM2-C)      TFILM=  132.5 (C)
 EQ H=  .17410022E-01 (WPTT/CM2-C)
                    ◆◆◆◆◆◆◆


 COOLANT VELOCITY(M/SEC)     COOLANT PRESSURE(ATM)
? 6                                  1

                    ◆◆◆◆◆◆◆
 TEMP=  210 (C)     TIME=  2.9910321 (SEC)
 RE=  237.84476     BI=  .32131573E-01    PR=  .88897109E+00
 HR=  0 (WATT/CM2-C)      HK=  0 (WATT/CM2-C)
 HC=  .17442854E-01 (WATT/CM2-C)      TFILM=  122.5 (C)
 EQ H=  .17442854E-01 (WATT/CM2-C)
                    ◆◆◆◆◆◆◆


LINE 01450
END
$ RUN
```

APPENDIX C-3 (CONT.)

```
 COOLING RATES FOR IMMISCIBLE MATERIALS IN ZERO GRAVITY


 GEOMETRY:          1 SPHERE
                    2 CYLINDER
                    3 PLATE
                    4 GENERAL

 TYPE GEOMETRY NO.
? 3
 LENGTH(CM), WIDTH(CM), THK(CM)
? 1.37          .74          .42

                SAMPLE PROPERTIES
 K(WATT/CM-C)    DENS(GM/CM3)    SH(CAL/GM-C)
? .114             8.41              .047

 TINIT(C)    TFINAL(C)     DT(C)     TSINK(C)
? 270          210           20        25


 COOLING MODES:          1 FORCED CONVECTION
                         2 RADIATION
                         3 CONDUCTION IN SUPPORTS

 TYPE NOS. FOR DESIRED COOLING MODES.  TYPE 0 FOR OTHERS.
 (EXAMPLE: 1,0,3)
? 0,2,0


 ENCL AREA(CM2)     EMIS1      EMIS2
? 1000               1            1

                    *******
 TEMP=  250 (C)     TIME=  8.9860167 (SEC)
 RE=  0    BI=  .32365533E-02    PR=  0
 HR=  .17569861E-02 (WATT/CM2-C)      HK=  0 (WATT/CM2-C)
 HC=  0 (WATT/CM2-C)      TFILM=  142.5 (C)
 EQ H=  .17569861E-02 (WATT/CM2-C)
                    *******
```

APPENDIX A-3 (CONT.)

```
 ENCL AREA(CM2)     EMIS1      EMIS2
? 1000                1          1

                    ◆◆◆◆◆◆◆
 TEMP=  230 (C)     TIME=  19.649591 (SEC)
 RE=  0    BI=  .29814512E-02    PR=  0
 HR=  .16185021E-02 (WATT/CM2-C)      HK=  0 (WATT/CM2-C)
 HC=  0 (WATT/CM2-C)      TFILM=  132.5 (C)
 EQ H=  .16185021E-02 (WATT/CM2-C)
                    ◆◆◆◆◆◆◆



 ENCL AREA(CM2)     EMIS1      EMIS2
? 1000                1          1

                    ◆◆◆◆◆◆◆
 TEMP=  210 (C)     TIME=  32.436992 (SEC)
 RE=  0    BI=  .27416987E-02    PR=  0
 HR=  .14883507E-02 (WATT/CM2-C)      HK=  0 (WATT/CM2-C)
 HC=  0 (WATT/CM2-C)      TFILM=  122.5 (C)
 EQ H=  .14883507E-02 (WATT/CM2-C)
                    ◆◆◆◆◆◆◆


LINE 01450
END
$ RUN
```

APPENDIX C-3 (CONT.)

```
 COOLING RATES FOR IMMISCIBLE MATERIALS IN ZERO GRAVITY


 GEOMETRY:          1 SPHERE
                    2 CYLINDER
                    3 PLATE
                    4 GENERAL

 TYPE GEOMETRY NO.
? 3
 LENGTH(CM), WIDTH(CM), THK(CM)
? 1.37          .74        .42

                SAMPLE PROPERTIES
 K(WATT/CM-C)    DENS(GM/CM3)    SH(CAL/GM-C)
? .114             8.41             .047

 TINIT(C)    TFINAL(C)     DT(C)     TSINK(C)
? 270          210          20          3*25


 COOLING MODES:          1 FORCED CONVECTION
                         2 RADIATION
                         3 CONDUCTION IN SUPPORTS

 TYPE NOS. FOR DESIRED COOLING MODES.  TYPE 0 FOR OTHERS.
 (EXAMPLE: 1,0,3)
? 1,2,0


 COOLANT VELOCITY(M/SEC)     COOLANT PRESSURE(ATM)
? 6                              1

 COOLANT             1 WATER(0C<T<320C)
                     2 NITROGEN(-20C<T<820C)
                     3 HELIUM(-20C<T<820C)

 TYPE COOLANT NO.
? 3

 ENCL AREA(CM2)     EMIS1      EMIS2
? 1000               1             1
```

APPENDIX C-3 (CONT.)

```
                    ◆◆◆◆◆◆◆
 TEMP=  250 (C)     TIME=  .8851585E+00 (SEC)
 RE=  218.9492      BI=  .35846224E-01   PR=  .33346837E+00
 HR=  .17569861E-02 (WATT/CM2-C)      HK=  0 (WATT/CM2-C)
 HC=  .17376678E-01 (WATT/CM2-C)      TFILM=  142.5 (C)
 EQ H=  .19133664E-01 (WATT/CM2-C)
                    ◆◆◆◆◆◆◆


 COOLANT VELOCITY(M/SEC)     COOLANT PRESSURE(ATM)
? 6                            1

 ENCL AREA(CM2)     EMIS1      EMIS2
? 1000               1          1

                    ◆◆◆◆◆◆◆
 TEMP=  230 (C)     TIME=  1.7321662 (SEC)
 RE=  228.09341     BI=  .35052545E-01   PR=  .33610407E+00
 HR=  .16185021E-02 (WATT/CM2-C)      HK=  0 (WATT/CM2-C)
 HC=  .17410022E-01 (WATT/CM2-C)      TFILM=  132.5 (C)
 EQ H=  .19028524E-01 (WATT/CM2-C)
                    ◆◆◆◆◆◆◆


 COOLANT VELOCITY(M/SEC)     COOLANT PRESSURE(ATM)
? 6                            1

 ENCL AREA(CM2)     EMIS1      EMIS2
? 1000               1          1

                    ◆◆◆◆◆◆◆
 TEMP=  210 (C)     TIME=  2.7374978 (SEC)
 RE=  237.84476     BI=  .34873271E-01   PR=  .33897109E+00
 HR=  .14883507E-02 (WATT/CM2-C)      HK=  0 (WATT/CM2-C)
 HC=  .17442854E-01 (WATT/CM2-C)      TFILM=  122.5 (C)
 EQ H=  .18931204E-01 (WATT/CM2-C)
                    ◆◆◆◆◆◆◆


LINE 01450
END
```